MAYRA ALEJANDRA TORO HERRERA

SOURCE-SINK PATTERNS ON COFFEE TREES RELATED TO ANNUAL CLIMATE VARIABILITY: AN APPROACH THROUGH ISOTOPES, CARBOHYDRATES, AND SPECTRAL ANALYSIS

LAVRAS – MG
2022

MAYRA ALEJANDRA TORO HERRERA

SOURCE-SINK PATTERNS ON COFFEE TREES RELATED TO ANNUAL CLIMATE VARIABILITY: AN APPROACH THROUGH ISOTOPES, CARBOHYDRATES, AND SPECTRAL ANALYSIS

Thesis presented to the Federal University of Lavras, as part of the requirements of the Postgraduate Program in Agronomy / Plant Physiology, area of concentration in Plant Ecophysiology, to obtain the title of Doctor.

Prof. Dr. João Paulo Rodrigues Alves Delfino Barbosa

Advisor

LAVRAS- MG

2022

Ficha catalográfica elaborada pelo Sistema de Geração de Ficha Catalográfica da Biblioteca Universitária da UFLA, com dados informados pelo(a) próprio(a) autor(a).

Toro-Herrera, Mayra Alejandra.

Source-sink patterns on coffee trees related to annual climate variability: an approach through isotopes, carbohydrates, and spectral analysis / Mayra Alejandra Toro-Herrera. - 2022.

164 p. : il.

Orientador(a): João Paulo Rodrigues Alves Delfino Barbosa.

Tese (doutorado) - Universidade Federal de Lavras, 2022.

Bibliografia.

1. Coffea arabica. 2. Carbon / nitrogen allocation. 3. Metabolic flux vision. I. Delfino Barbosa, João Paulo Rodrigues Alves. II. Título.

MAYRA ALEJANDRA TORO HERRERA

SOURCE-SINK PATTERNS ON COFFEE TREES RELATED TO ANNUAL CLIMATE VARIABILITY: AN APPROACH THROUGH ISOTOPES, CARBOHYDRATES, AND SPECTRAL ANALYSIS

PADRÕES FONTE-DRENO EM CAFEEIROS RELACIONADOS À VARIABILIDADE CLIMÁTICA ANUAL: UMA ABORDAGEM ATRAVÉS DE ISOTOPOS, CARBOIDRATOS E ANÁLISE ESPECTRAL

Thesis presented to the Federal University of Lavras, as part of the requirements of the Postgraduate Program in Agronomy / Plant Physiology, area of concentration in Plant Ecophysiology, to obtain the title of Doctor.

APPROVED on February 24, 2022.
Dr. Daniel Gerardo Cayon Salinas UN
Dr. Vladimir Eliodoro Costa UNESP
Dr. José Donizeti Alves UFLA
Dr. Paulo Eduardo Ribeiro Marchiori UFLA

Prof. Dr. João Paulo Rodrigues Alves Delfino Barbosa
Advisor

LAVRAS- MG
2022

A mis padres y hermano a quienes debo lo que soy

Dedico

ACKNOWLEDGEMENTS

To God, for allowing the conclusion of another stage of my academic life.

To my family: thank you for always supporting me in each of my dreams and for always being by my side, even from a distance. Every achievement in my life is because of you and for you.

Dawyson: thank you for becoming my family and my support in Brazil. For the patience, the encouragement, and the support in all the moments of this way. This achievement is ours

To my advisor, Professor João Paulo Rodrigues Delfino Alves Barbosa: I wish to show my appreciation for your guidance, your patience, your willingness to always help me and for the teachings during my master's and doctorate. Thank you so much for helping me to grow professionally and personally.

I wish to extend my special thanks to professors Paulo Eduardo Ribeiro Marchiori, Vladimir Eliodoro Costa, and Paulo Hein for providing the spaces, infrastructure, and materials in their laboratories to carry out the biochemical, isotopic, and spectral analyzes of the thesis.

I would like to thank the postdoctoral fellows of the laboratory Ane Marcela das Chagas Mendonça and João Paulo Pennacchi for the time dedicated to each stage of my doctorate. Thank you Pennacchi for always being available to solve my doubts and for teaching me about statistical analysis.

I would like to thank the thesis examining committee, for accepting to participate in the defense of the thesis, contributing to the improvement of the final document.

To my foreign friends: I thank you for being my family in Lavras, for the moments of study, friendship, and leisure. It was a blessing to coincide in this place all together.

To colleagues and friends in the laboratory and in the Plant Physiology sector: thank you for the moments of study, friendship, for the long hours of physiological analyses, for the coffee after lunch, for the conversations, for sharing dreams. I always felt very welcomed in Brazil thanks to you. I always carry you in my heart and I look forward to seeing you in Colombia.

To the Federal University of Lavras and the Plant Physiology Sector, for the opportunity to carry out my master's and doctorate.

To the professors of the Plant Physiology Sector, for the teachings in my academic formation process.

To the Consortium Pesquisa Café and the Procafé Foundation for their support during the development of the project.

To Lissa Vasconcellos Vilas Boas and Cássio Honda Pereira for providing the samples. Thank you Lissa for teaching me how to carry out the biochemical analyses.

This study was financed in part by the Coordenação de Aperfeiçoamento de Pessoal de Nível Superior – Brasil (CAPES) – Finance Code 001.

Thank you all!

ABSTRACT

The coffee tree is subject throughout the year to adversities resulting from climatic events that can affect the development and productivity of the crop. One of the processes highly influenced by climate is the allocation and partitioning of carbon, with changes in the export/import of resources between source and sink tissues. Thus, unraveling the mechanisms of differential allocation as well as the source-sink relationship under different climatic conditions is of great relevance for management, agroecological and socioeconomic issues. A quick and straightforward approach to assessing a plant's carbon status is to measure the size of its overall non-structural carbon (NSC) stock in periods of variable demand. However, long-term studies with this approach are scarce, making it difficult to understand the physiological processes and controls involved. Thus, this thesis proposes the use of three analytical methods to address the spatio-temporal variation in source-sink relationship in coffee plants in field conditions: growth analysis, stable isotope analysis and carbohydrate profile analysis validated by near infrared spectroscopy (NIRS). The growth analysis involves and integrates the form and function of the plant in a holistic way and allowed us to know the main patterns of vegetative and reproductive growth depending on the phenology and climate of the region, as well as confirming the bienniality patterns linked to the negative correlation that exists between growth and reproduction. Stable isotopic analysis constitutes a useful tool to identify the processes that control the dynamics of carbon (C) and nitrogen (N) flux in the plant and led us to identify the null variation of the C isotopic ratio over time, as well as the isotopic differences between heterotrophic and autotrophic tissues and the isotopic differences within the tree canopy between the established thirds. Carbohydrate profile analysis is a tool that allows us to determine the stock of the main non-structural compounds (NSC) in plant organs, leading us to quantify the stocks of protein, amino acids, reducing sugars, total soluble sugars, sucrose, and starch throughout of time and in the different portions of the tree canopy. The values quantified in the laboratory were validated through near-infrared spectroscopy, which is a quick and easy technique to evaluate the composition of NSC in different tissues and plant organs. After obtaining the raw spectral information, several predictive models were used to scale the spectra in NSC content measurements, using measured values as a reference. These methods were used to achieve a "metabolic flux" vision allowing us to understand the carbon and nitrogen flows/allocation in response to the plant's phenology (alternating between vegetative / reproductive cycles) and especially in response to the climate.

Keywords: *Coffea arabica* L. Carbon/ nitrogen allocation. Spatio-temporal variation. Metabolic flux vision. Climate variability.

RESUMO

O cafeeiro está sujeito durante todo ano a adversidades decorrentes de eventos climáticos que podem prejudicar o desenvolvimento e a produtividade da cultura. Um dos processos altamente influenciados pelo clima é a alocação e partição de carbono, com mudanças na exportação/importação de recursos entre tecidos fonte e dreno. Assim, desvendar os mecanismos da alocação diferencial bem como da relação fonte-dreno sob diferentes condições climáticas é de grande relevância para questões de manejo, agroecológicas e socioeconômicas. Uma abordagem rápida e direta para avaliar o status de carbono da planta é medir o tamanho de seu estoque geral de carbono não estrutural (NSC) em períodos de demanda variável. No entanto, estudos de longo prazo com essa abordagem são escassos, dificultando o entendimento dos processos fisiológicos e controles envolvidos. Assim, nesse contexto, esta tese propõe o uso de três métodos analíticos para abordar a variação espaço-temporal na relação fonte-dreno em cafeeiros em condições de campo: análise de crescimento, análise isotópica estável e análise de perfil de carboidratos validada através de análise por espectroscopia no infravermelho próximo (NIRS). A análise de crescimento envolve e integra a forma e a função da planta numa forma holística e nos permitiu chegar aos principais padrões de crescimento vegetativo e reprodutivo em função da fenologia e do clima da região, bem como confirmar os padrões de bienalidade ligados à correlação negativa que existe entre crescimento e reprodução. A análise isotópica estável constitui uma ferramenta útil para identificar os processos que controlam a dinâmica do fluxo de carbono (C) e nitrogênio (N) na planta e nos levou a identificar a variação nula da razão isotópica do C ao longo do tempo, bem como as diferenças isotópicas entre tecidos heterotróficos e autotróficos e as diferenças isotópicas dentro da copa da árvore entre os terços estabelecidos. A análise de perfil de carboidratos é uma ferramenta que permite determinar o estoque dos principais compostos não estruturais (NSC) nos órgãos da planta, nos levando à quantificação dos estoques de proteína, aminoácidos, açucares redutores, açúcares solúveis totais, sacarose e amido ao longo do tempo e nas diferentes porções da copa da árvore. Os valores quantificados em laboratório foram validados através de análise espectral no infravermelho próximo que se constitui como uma técnica rápida e fácil para avaliar a composição de NSC em diversos tecidos e órgãos vegetais. Após a obtenção das informações espectrais brutas, vários modelos preditivos foram usados para dimensionar os espectros em medidas de conteúdo NSC, a partir de valores medidos como referência. Esses métodos foram usados para alcançar uma visão de "fluxo metabólico" que nos permitiu entender os fluxos/alocação de carbono e nitrogênio em resposta à fenologia da planta (alternando entre ciclos vegetativos / reprodutivos) e principalmente em resposta ao clima.

Palavras-chave: *Coffea arabica* L. Alocação de carbono/nitrogênio. Variação espaço-temporal. Visão do fluxo metabólico. Variabilidade climática.

LIST OF FIGURES

LIST OF TABLES

LIST OF ACRONYMS / SYMBOLS

%C	Carbon percentage
%N	Nitrogen percentage
‰	Delta (Notation to express isotopic ratios)
A	Net photosynthetic rate (μmol m^{-2} s^{-1})
AA	Amino acids
BDM	Branch dry matter (g)
BM	Bud maturation
BrT	Branch temperature (ºC)
C	Carbon
Cherry	Cherry (Fruit development stage)
D	Distal section of plagiotropic branch
DM	Dry matter
E	Transpiration rate (mmol H_2O $m^{-2}.s^{-1}$)
ETo	Evapotranspiration
Evap	Evaporation
Exp	Expansion (Fruit development stage)
FDM	Fruits dry matter (g)
FFM	Fruit formation and filling
GC	Green-cane (Fruit development stage)
Green	Green (Fruit development stage)
gs	Stomatal conductance (mol H_2O $m^{-2}.s^{-1}$)
H	Holes
I	Intermediate section of plagiotropic branch
LA	Leaves area (cm^2)
LDM	Leaves dry matter (g)
LN	Leaves number
LT	Lower third of the tree
LeT	Leaf temperature (ºC)
MaxTAv	The average maximum annual temperature
MaxTY	Maximum temperature of the year
MinTAv	The average minimum annual temperature
MinTY	Minimum temperature of the year
MT	Middle third of the tree
N	Nitrogen
NIRS	Near infrared spectroscopy
NPB	Number of plagiotropic branches
NSC	Non-structural carbohydrates
P	Proximal section of plagiotropic branch

PBL	Plagiotropic branch length (cm)
PCA	Principal component analysis
PCR	Principal components regression
PH	Plant height (cm)
PLSR	Partial least squares regression
Prec	Precipitation
PS	Phenological stages
O	Organs
QP	Quiescent phase
R^2	Coefficient of determination
RFR	Random Forest regression
RH	Relative humidity
RMSE	Root mean square error
RS	Reducing sugars
S	Sampling
Se	Sections
SED	Standard error of the difference between two treatment means
SL	Sunlight hours
SR	Spectral range
T	Current climate
T-1	Climate of the previous year
T-1D	Dry season for the climate of the previous year
T-1W	Wet season for the climate of the previous year
TD	Dry season for the current climate
Th	Thirds
Ti	Tissues
Tmax	Maximum temperature
Tmin	Minimum temperature
TNF	Total number of fruits
TSS	Total soluble sugars
TW	Wet season for the current climate
Un	Unripe (Fruit development stage)
UT	Upper third of the tree
VS/BF	Vegetative stage and bud formation
WB	Water balance
WS	Wind speed
$\delta^{13}C$	Carbon isotopic ratio
$\delta^{15}N$	Nitrogen isotopic ratio

SUMMARY

CHAPTER 1: THEORETICAL BASIS AND BIBLIOGRAPHIC REVIEW

ABSTRACT

The coffee tree is subject throughout the year to adversities resulting from climatic events that can affect the development and productivity of the crop. One of the processes highly influenced by climate is the allocation and partitioning of carbon, with changes in the export/import of resources between source and sink tissues/organs. Thus, unraveling the mechanisms of differential allocation as well as the source-sink relationship under different climatic conditions is fundamental. For this purpose, several analytical methods are proposed in this thesis, in order to approach and study the source-sink relationship in coffee trees in production. However, before proceeding to the understanding of the methods, it is vital to deepen the knowledge about the source-sink relationship in plants. Thus, the aim of chapter 1 is to present a short review with the main concepts associated with the term "source-sink relationship", starting with the basic identification of source and sink organs in the plant, how the process is regulated and what is the influence of the climate in it. Additionally, the main research questions that gave rise to our hypothesis and aims are presented, as well as a schematic representation with the proposed structure to approach the research. The structure comprises a brief presentation of the three proposed methods, with a chapter in the thesis being assigned to each one. Furthermore, methodological issues that are transversal to all chapters are presented, such as the plant material and study site, systematic sampling, the climatic dataset used and the statistical approach. Finally, a brief closing is presented with some of the key points to guide the understanding and reading of the next chapters.

Keywords: Theoretical review. Research framework. Methodological issues. Carbon allocation. Source-sink relationship.

1 INTRODUCTION

Coffee, a product of great global importance, is grown in more than 80 countries, reaching a production of 176 million bags in the 20220/2021 season and an estimated 167 million bags for the 2021/2022 season (USDA Foreign Agricultural Service, 2021). Brazil, is the largest producer and exporter of coffee in the world, being considered one of the most important agricultural crops in the country, with Arabica (*Coffee arabica* L.) and Robusta (*Coffee canephora* Pierre ex A. Froehner) coffee plantations in several producing states. Among them, the state of Minas Gerais, predominantly the South of Minas, concentrates the largest production of coffee, corresponding to approximately 50% of the national production (Companhia Nacional de Abastecimento - CONAB, 2022).

Most fluctuations in coffee production are associated with site characteristics, so that favorable edaphoclimatic conditions throughout the vegetative and reproductive cycle are determinants of the good development, productivity, and quality of the final product. Based on that, coffee cultivation areas must meet some climatic requirements especially in relation to air temperature and water availability (Tavares et al., 2018). For arabica coffee, the ideal annual range of average temperature and average precipitation are 18–21 °C and 1200–1800 mm, respectively (DaMatta et al., 2007). Outside these ranges, there may be negative effects on coffee trees resulting on yield reduction (Craparo et al., 2015; Tavares et al., 2018), reduction in beverage quality (de Camargo, 2010; Ovalle-Rivera et al., 2015), changes in the cycles of the main coffee pests and diseases (Ghini, Bettiol, and Hamada, 2011; Jaramillo et al., 2011) and even reduction of areas considered suitable for cultivation (Bunn et al., 2015; Ovalle-Rivera et al., 2015; Schroth et al., 2015).

Since coffee development patterns are highly influenced by the environment, the export/ import of resources in the source and sink tissues/organs changes due to environmental fluctuations causing modifications in the investment of resources by the plant, according to their availability (Freschet, Swart, and Cornelissen, 2015). In the most producing areas in Brazil, the vegetative and the reproductive stages co-occur, in time scale, in different parts of plagiotropic branches and, therefore, the growth and reproductive sinks compete for carbon. Thus, the plant tends to balance the partition of photoassimilates, changing the existing source-sink relationship between fruits, stems, and leaves (Barros, Maestri and Rena, 1999). Such phenomenon is complex and emerges from climate variability, cropping practices and plant physiological status and is well known among coffee growers and coffee traders as the biennial yield cycle. The understanding of this balance and the differentiated carbon

allocation is then an important factor to identify the periods of greatest demand for photoassimilates, allowing to maximize production in the most critical stages (Laviola et al., 2007). In this context, research that addresses the source-sink relationships allows us to predict the consequences of changes in the supply or demand for resources (light, water, temperature, carbon) in plants, in response to the climate variability.

In coffee trees, unraveling the mechanisms of differential carbon investment in different organs and under different environmental conditions is of great relevance for management, agroecological and socioeconomic issues. However, long-term studies in this area are scarce, making it difficult to understand the physiological processes and controls involved. Thus, this thesis proposes the use of three analytical methods to address the source-sink relationship in coffee plants in field conditions: stable isotopic analysis, carbohydrate profile analysis and near infrared spectroscopy (NIRS) analysis. These methods were used to achieve a "metabolic flux" vision that would allow us to understand the carbon and nitrogen flows/allocation in response to the plant's phenology (alternating between vegetative / reproductive cycles) and especially in response to the climate in a 17 months samples.

These methods allowed us to answer the main question of the research in which we hypothesized that the inter and intra annual climatic variability, interfere in the source-sink patterns and in turn in the process of allocation of biomass of coffee trees on both scales - temporal and spatial. From this general hypothesis, some questions were raised. For example, in years with less water availability and / or higher temperature:

- Is there a greater allocation of biomass to stems, with less investment in leaves and fruit production due to the modification of the source-sink relationship between the plant's organs?
- Are there variations in the isotopic composition of carbon ($\delta^{13}C$) and nitrogen ($\delta^{15}N$) in the coffee organs (autotrophic vs. heterotrophic), reflecting the differential use of atmospheric C and N assimilated from the soil, versus C and N relocated from other parts of the plant?
- Are there changes in the pool of NSC, amino acids and proteins in plant organs as a function of phenology and climatic variation? Do these changes reflect source-sink patterns in the plant?
- Are changes in the NSC profile accompanied / reflected by changes in the spectra of the samples for each organ?

Thus, using these three proposed analytical methods, the aim was to identify, in detail, the temporal / spatial patterns of the source-sink relationships and the allocation of biomass in different organs of coffee plants under field conditions, in response to climate.

2 THEORETICAL FRAMEWORK

2.1 Source- sink relationship

2.1.1 General basis

As sessile, self-sufficient, and resilient organisms, plants require the dynamic coordination of their metabolism and various signal transduction pathways to regulate their growth and development and to cope with changing environments. As part of this process, changes in supply and demand of carbon (C) follow the development of the plant, regulating the partitioning/ allocation of C in different organs under different environmental conditions (Wardlaw, 1990).

In early stages, plants develop from an embryo, which depends on the metabolism of nutrients transported from storage organs, such as seeds. Later during growth and development, plants rely on the energy obtained from fixing CO_2 into carbohydrates (via photosynthesis) by source organs, and the translocation to sinks for their use. Finally, in the reproductive phase, sugars and other nutrients are remobilized from mature leaves to developing fruits/seeds. Thus, the life cycle of the plant is characterized by the transition between sources and sinks (Yu, Lo, and Ho, 2015). This transition is regulated by direct and indirect factors: directly, through photosynthetic rate (source activity) and carbon utilization rate (sink activity); indirectly, through hormonal metabolism, nutritional status, vascular restrictions that can favor the growth of one organ over another, and the buffer effect of C storage in different places in the plant (Wardlaw, 1990).

Source tissues are exporters of elementary resources necessary for plant growth (such as C or N), which they acquire from the external environment, although the remobilization of stored resources can also transform a sink into an internal source. Sink tissues are importers responsible for assimilating resources from source tissues. Although all tissues/organs have some sink activity, in general, the leaves are N deposits transported from the root system, and the roots are liquid sinks of sucrose exported from the leaves (White et al., 2016). Mature

leaves are liquid sources of C fixed in photosynthesis while roots, tubers, reproductive structures, and young leaves represent the main sink tissues.

Thus, the "source strength" is determined by the net absorption rate (mol s^{-1}) for a specific resource in the external environment.

$$\text{Source strength} = \text{source size} \times \text{source activity} \qquad (1)$$

Where size refers to the total biomass of the source tissue (g), and the activity at the specific absorption rate of the resource (mol g^{-1} s^{-1}). In turn, the "sink strength" is determined by the net absorption rate (mol s^{-1}) for a specific resource by a tissue defined within the plant.

$$\text{Sink strength} = \text{sink size} \times \text{sink activity} \qquad (2)$$

Where the sink size is the total biomass of the sink tissue (g) and the sink activity refers to the specific absorption rate of the resource (mol g^{-1} s^{-1}) (White et al., 2016). The competitive advantage in terms of controlling the carbon partition that a sink has is due to the size of the surface area (membrane) through which the metabolites are transferred, the efficiency of the carbon transfer (rate per unit area) from the vascular system to the sink organ and the spatial or biochemical isolation of assimilates into growth / storage organs as they leave the vascular system. Thus, the basis for the sink strength (assuming a translocation pressure flow mechanism) would be in the ability to decrease the concentration of photoassimilates in the sieved elements and thus establish the favorable concentration gradient between the source and the sink (Wardlaw, 1990).

The source-sink relationship modulates C assimilation and partition during growth and development, determining the pattern of carbohydrate allocation throughout the plant, thereby determining crop productivity. Consequently, studies in this area increase the capacity of predicting the consequences of changes in C supply or demand, allowing a better understanding of the regulation of their allocation and partition in plants.

2.1.2 Regulation of source-sink relationship

Carbon partitioning in plants is controlled by several factors including the rate of photosynthesis, the rate of carbon utilization, the number and size of competing sinks and their location in the plant, vascular connections, and the potential for temporary storage. When several factors share control of the growth rate, the developing plant can reduce or increase the allocation for those who exercise a high degree of control. Thus, there is a

dynamic process that balances fluctuations in the availability / supply of external resources with ontogenic changes in the demand for them. This regulation allows the plant to maintain an appropriate growth rate for a given availability of resources (White et al., 2016).

A complex molecular network, including signals and phytohormones derived from carbon and nitrogen, has evolved to integrate the capture, assimilation, and allocation of resources; allowing both sources and sinks to modify their own activity and regulate the activity of other tissues (Nunes-Nesi, Fernie, and Stitt, 2010; Ruan, 2014). Thus, the levels of carbon and nitrogen are key components of the regulation of the source-sink relationship, with the crosstalk points between the signaling pathways a fundamental part of the regulation (Bihmidine et al., 2013).

Another important factor to consider in the regulation process is the storage of metabolites in the leaves and tissues along the translocation path between the source and the sink. Storage can act as a temporary buffer against short-term changes in resource availability. Thus, an excessive supply of photoassimilates leads to storage, with the possibility of remobilization of these resources when photosynthesis is low or when demand is increased (Wardlaw, 1990).

2.1.3 Effect of climate on the source-sink relationship

The export / import of resources in the source and sink tissues/organs changes due to fluctuations in the external environment and the plant reacts to these variations in the availability of resources by modifying its investment (Freschet et al., 2015). These resources capable of influencing the source-sink relationship are light, CO_2, temperature, water available in the soil and the nutritional status of the plant. The differential sensitivity of the activities of both tissues to the controls that exert these environmental factors can lead to an imbalance between the C provided by photosynthesis and the C used for growth and respiration. This could create a long-term surplus or shortage of the assimilated carbon.

With water limitations, cambial and leaf growth is affected earlier and more intensely than photosynthesis. Plants that are under water deficit in the soil often continue to assimilate C while sink activity (tissue growth) is inhibited, leading to the accumulation of non-structural carbohydrates and reduced growth. Prioritizing storage over growth would maintain the integrity of the plant's hydraulic system (Hartmann et al., 2013; Woodruff and Meinzer, 2011). On the other hand, plants limited by temperature are typically limited by the activity of

the sinks earlier than by the activity of the source, due to the influence of temperature on the potential growth rate of the organs in the absence of other growth limiting factors (Körner, 2013). Thus, changes in temperature generally result in the accumulation of starch and soluble carbohydrates, due to the storage of C resulting from low demand and slow growth, instead of a direct effect of temperature on leaf function (Wardlaw, 1990).

The limitation of nutrients exerts negative feedback on photosynthesis, limiting the number of fundamental enzymes necessary for the assimilation of C that can be produced. It can also limit tissue growth by affecting sink activity. In the case of light and CO_2, they can indirectly affect the growth activity through the activity of the sources, especially in young seedlings and understory seedlings or in individual leaves in dense canopies that are almost always operating below the light saturation or the CO_2 absorption (Fatichi, Leuzinger, and Körner, 2014; Lloyd and Farquhar, 2008).

Thus, in summary, several abiotic factors modify the source-sink relationships that influence plant growth, consequently affecting crop productivity. This reduction in yield may respond to the decrease in the number and size of sink organs, due to the inability of source organs to maintain the supply of assimilates necessary to support the processes of vegetative growth and filling of reproductive structures (Albacete, Martínez-Andújar, and Pérez-Alfocea, 2014).In turn, the excess of assimilates caused by the inhibition of the activity of the sinks or by a slow export, can lead to an accumulation of sugars that affects photosynthesis through negative feedback.

3 RESEARCH FRAMEWORK

Considering our hypothesis that intra-annual and inter-annual climatic variability changes the C and N flows between plants and the atmosphere, affecting growth and maintenance processes; we propose a “tripod” approach to test the hypothesis and achieve our aim. In this approach, each of the "feet" or "axes" corresponds to one of the methods proposed to assess the spatial (canopy) and temporal source-sink patterns and in turn the process of allocation of biomass in coffee trees in field condition. The schematic representation of the proposed approach is shown in Figure 1. So, we associated growth analysis with Biochemical and Isotopic quantifications in different coffee tree parts and along two producing years in a systematic sampling. We associated those results with climatic variability.

Figure 1 - Research framework proposed to test the hypothesis and achieve the research aims

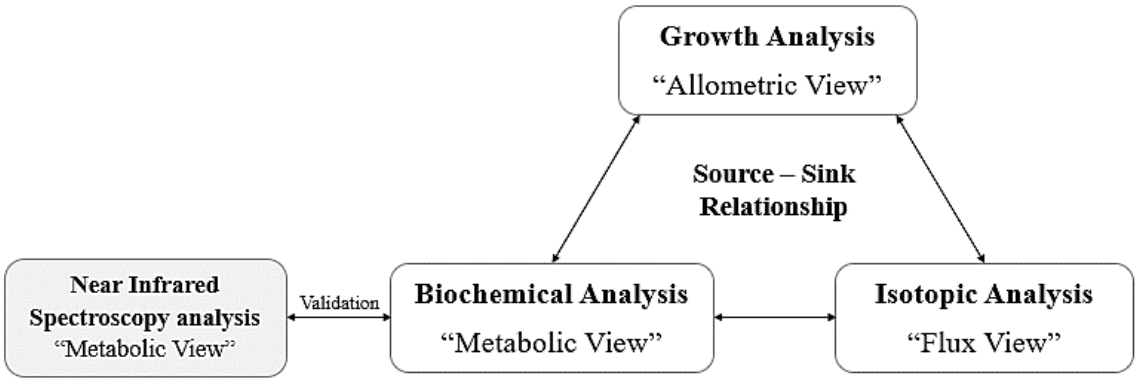

Source: From the author (2022)

Now, methodological issues that are transversal to all chapters are presented:

3.1 Location and plant material

Samples of *Coffea arabica* L. cv. Arara with five to seven years old of age were collected in the southern Minas Gerais State, in Varginha municipality (21º 34 '00" S; 45º 24' 22" W; 940 m). The experimental area belongs to the Procafé Foundation Experimental Farm which according to the Köppen climate classification map for Brazil (Alvares et al., 2013; Beck et al., 2018; Kottek et al., 2006), is classified as Cwa, showing a climatic seasonality where the winter is cold and dry and summer is hot and humid and with an annual mean temperature of 19.3 °C. The farm has an area of 60 ha and soil with sandy clay texture, granular structure, and good depth.

The seedlings were grown from seeds, starting in July 2012, and were kept in the seedling nursery for 8 months until being transplanted to the final location, in the field, in March 2013. They were disposed in a north-south direction, with spacing of 3.5m between rows and 0.5m between plants. The cultivar is characterized by high yield, high vegetative vigor, compact and large canopy with thick and bifurcated branches and late fruit ripening, which are yellow and with oblong-shaped seeds.

3.2 Systematic Sampling

The plants were collected in 17 months distributed between 2016 and 2018, as follows: December 2016; January, February, March, April, June, September, October,

November, and December 2017, and January, February, March, April, May, June, and October 2018. In each month, four plants were destructively sampled and separated in stems, leaves, and fruits, aiming to determine the carbon allocation to each of the organs. The samples were taken into a forced air circulation oven at 70 °C until constant weight to determine the dry mass. Later they were ground in a hammer mill (MA-090CF, Marconi, Piracicaba- SP, Brazil) with a sieve until reaching a particle size of less than 1mm. The powder obtained from the mill was passed through a sieve of 250 µm (NBR NM 3310-1, SoloTest, São Paulo- SP, Brazil) to further reduce the particle size.

The sampled plants were divided into different portions that were collected separately to perform the biochemical and spectral analyses as described below. Thus, sampling was carried out following a pattern of division vertically (orthotropic axis - from the apex to the base of the plant) and horizontally (plagiotropic axis - from the end of the branches to their insertion in the principal stem). Vertically, the plant was divided into three thirds: the upper third (UT), the middle third (MT) and the lower third (LT) (Figure 2a). Horizontally, each plagiotropic branch was divided into three sections: The proximal section (P) closest to the orthotropic branch, the intermediate section (I) and the distal section (D) farthest from the orthotropic branch (Figure 2b). In addition, the plant was divided into branches opposite the planting line (branch 1 or south and branch 2 or north) and branches parallel to it (branch 3 or west and branch 4 or east) (Figure 2c).

Thus, considering the three thirds, the three sections on the horizontal axis and the four branches, a maximum amount of up to 36 parts of each plant was collected and analyzed. Based on this information, in Box 1 the maximum possible samples that could be collected in the experimental period from this division scheme are explained, considering that depending on the part of the plant and the time of year, fewer samples were obtained.

Box 1

3 thirds x 3 sections x 4 branches = 36 sampled parts per plant

36 parts/plant x 4 replicates = 144 samples per sampling

144 samples x 3 organs = 432 samples per sampling

432 samples x 17 samplings = 7344 samples in total

For primary growth analyzes, all plant portions were considered. For secondary growth analyzes, the basal portion of the orthotropic branch was considered, as well as several diameters along the total height of the plant in its three thirds (Figure 2d). For isotopic analyzes, just the distal portion of the three thirds was selected for being considered the youngest region with the most sinks in the plant, allowing the assessment of C and N flows. For spectral analyzes, the collected samples were split in two main groups: training/testing of models and prediction. Samples in the first group were evaluated for spectral reflectance and biochemical analysis; 75% of these samples were randomly chosen for training the models and the other 25% were used for the testing of the models. The samples of the second group were evaluated only for spectral reflectance; the biochemical characteristics were predicted from the defined models. The variation in the predicted values was them correlated to the climatic conditions and growth stages of the plant, along the crop cycle.

Figure 2 - Coffee tree division pattern for sampling (a) Division of the tree on the vertical axis into upper (UT), middle (MT) and lower (IT) thirds. (b) Division of the plagiotropic branches of the tree along the horizontal axis into the proximal (P), intermediate (I) and distal (D) sections. (c) Division of the tree symmetry in the South-North and East-West directions. (d) Sections of the orthotropic branch of the tree selected for measuring branch volume and for obtaining samples for dendrochronological analyses.

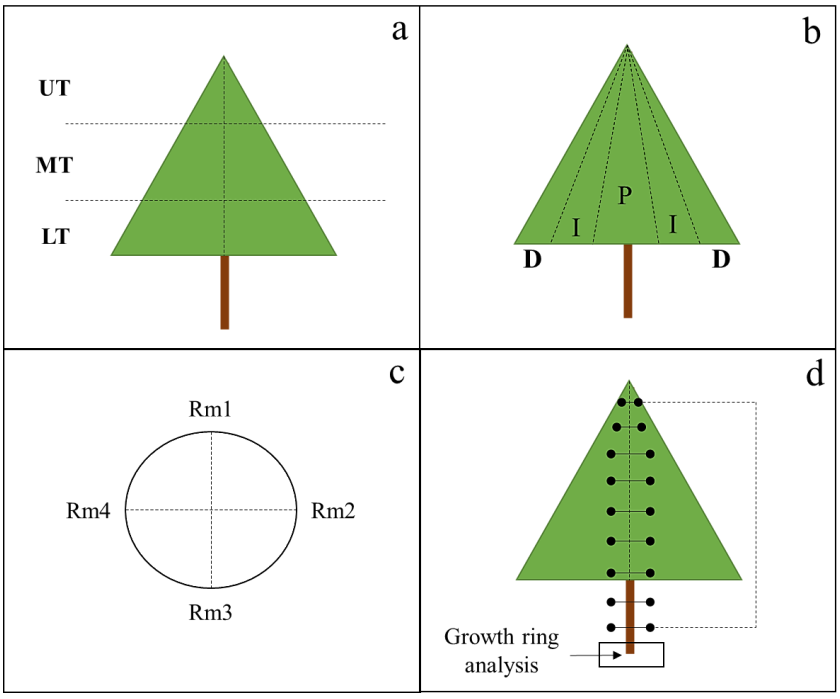

Source: From the author (2022)

The sampling scheme was defined based on the coffee phenology proposed by Camargo and Camargo (2001) and can be found in Figure 3. The experimental period started in December 2016 and ended in October 2018, with 17 months sampled (all shaded in the figure) and among these, six chosen for the calibration/validation process of the NIRS and biochemical analyzes (boxes in dark gray). In the two main years evaluated (2017 and 2018) were selected: (1) January; summertime, when maximum temperatures are reached and precipitation is above evapotranspiration, (2) June/May; wintertime, when minimum temperatures and lowest precipitation values are reached, with evapotranspiration being greater than precipitation (predominantly negative water balance), and (3) October; when the coffee quiescent phase normally ends, separating one phenological year from another.

Figure 3 - Proposed sampling scheme based on the phenological stages of the coffee tree. Months not sampled (○ - white circles), months sampled for spectral and biochemical traits and used for training/testing of the models (hatched circles), and months sampled for prediction (dark gray circles).

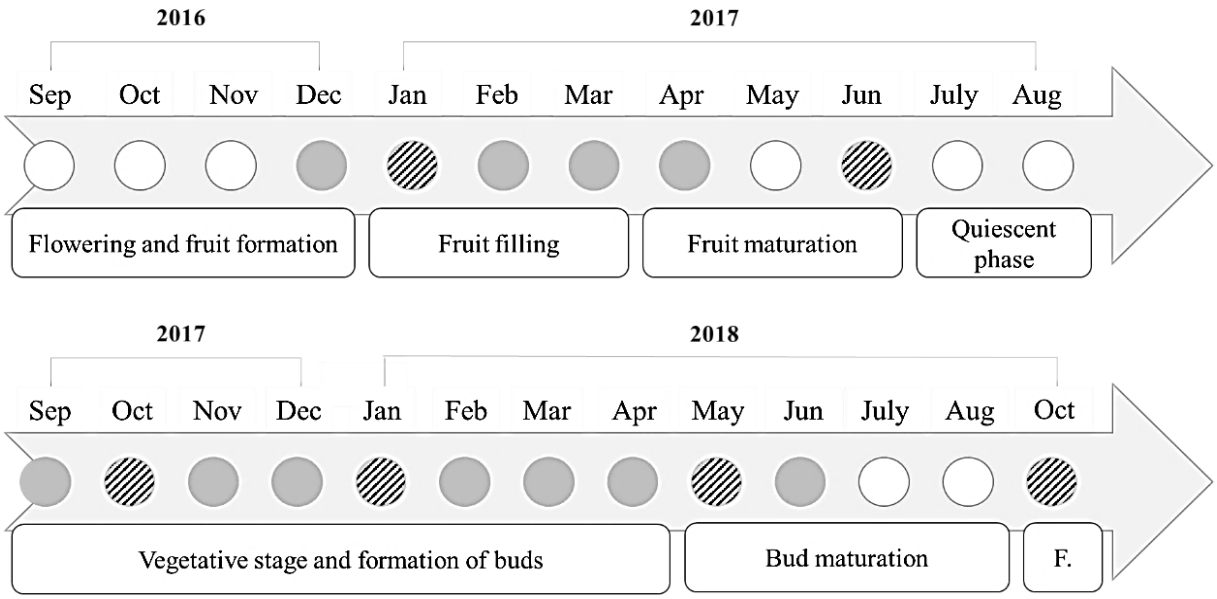

Source: Adapted from Camargo and Camargo (2001)

Considering only these six samples, the new quantity to be analyzed in the laboratory reduces (Box 2). On the other hand, a pool of samples from branches one and two (south-north) and from branches three and four (east-west) was made, which generated the final number of

analyzed samples with a maximum possible of 1296 samples. This pool was carried out based on the results reported by Vasconcellos (2019), who evaluated a series of growth and physiological variables in the canopy of the same coffee trees, not finding significant differences between the branches of each of these faces. More details about the selected portions and sampling scheme can be found in this document and in the dissertation by Pereira (2018), as they worked with the same set of plants.

Box 2

432 samples x 6 samplings = 2592 samples in total
2592 samples / 2 groups of branches = 1296 samples for laboratory analysis

3.3 Climate Data

The climatic data of the experimental area during the study period (October 2011 to September 2018), was calculated as a combination of three agrometeorological stations near the Varginha-MG region: Lavras-MG (station 83687, 60 linear km from the experimental area), Machado-MG (station 83683, 50 linear km from the experimental area) and São Lourenço-MG (station 83736, 70 linear km from the experimental area). The daily data for the three stations was downloaded from the meteorological database of the National Institute of Meteorology (INMET, 2019). The meteorological data were submitted to a quality control process to verify the occurrence of inconsistent data, following the methodology proposed by Baba, Vaz, and Costa (2014). As a basic validation, for each agrometeorological station, each climatic variable was restricted within a limit of possible values. Therefore, logical rules were established to restrict inconsistent data (for example, Tmin <Tmed <Tmax). As spatial validation, using a Pearson correlation (r), the spatial distribution pattern between the three stations was evaluated, based on the average temperature variable. The correlation coefficient obtained was r = 0.80. Additionally, the monthly meteorological data for the same variable provided by the Procafé Foundation (https://www.fundacaoprocafe.com.br/estacao-de-avisos-sul-de-minas) were also correlated with INMET stations. In this case, the correlation was r = 0.82. In addition to quality control, meteorological data was organized according to the coffee agricultural year, which is conditioned by the plant's phenology. Thus, in our study period each agricultural year begins in October and ends in September (for example, the 2012 agricultural year begins in October 2012 and ends in September 2013 and so for other years).

The following parameters were calculated monthly as a combination of the daily data for each location: precipitation (Prec, in mm), evaporation (Evap, in mm) and sunlight hours (SL, in hours) calculated as the sum of daily values and minimum temperature (Tmin, in °C), maximum temperature (Tmax, in °C), relative humidity (RH, in %) and wind speed (WS, in mps) as the average of daily values. The above-mentioned parameters were estimated for the experimental area as a weighted average of the three locations where the weight was inversely proportional to the distances from the location to the experimental area. Tmin, Tmax, RH and WindS, in addition to geolocation, were used to calculate evapotranspiration (ETo, in mm) for each month according to FAO Penman-Monteith equation through the ETo Calculator software developed by the FAO Land and Water Division (Allen et al., 1998; FAO, 2019). Finally, the water balance of the growing period (WB), as well as the months of sampling, was calculated as the subtraction between Prec and ETo, monthly.

Additionally, the following variables were calculated from the monthly data: the average maximum and minimum annual temperature (MaxTAv and MinTAv, in°C), calculated as the average of the maximum and minimum temperature of all months, respectively; the maximum temperature of the year (MaxTY, in °C), or the highest maximum monthly temperature of the year and the minimum temperature of the year (MinTY, in °C), or the lowest minimum monthly temperature value of the year.

The database with the climatic information obtained after the data quality control process and after the determination of the calculated variables can be found in the Supplementary material (SM Table 1).

3.4 General methodology

All statistical analyzes were conducted using the RStudio statistical software (Version 1.2.5033 © 2009-2019 RStudio, Inc.). In general, the data collected for all chapters (except for growth ring analysis) was analyzed in the same way/trend in a three-step process:

1. Considering the large volume of information collected due to tree portions and sampling over time, initially, the data were organized to perform an analysis of variance (ANOVA). Thus, the variation factors evaluated were samplings – S, thirds - Th, sections – Se and Organs – O, when the analysis involved different organs of the plant. Tables of averages were also built considering all analyzed variables.
2. Then a principal component analysis (PCA) was performed. Considering that many variables presented statistically significant differences between the evaluated factors, as

well as between their interaction, this analysis was performed in order to reduce the dimensionality of datasets, improving the analysis capacity. Also allowing to observe trends, clusters, and outliers in the data. For this analysis, biplots were made showing the samples, loadings, and confidence ellipses (95%) grouping data according to variation factors.

3. Finally, the variables were correlated with the climatic characteristics of the region, using a Pearson statistical correlation analysis ($p < 0.05$ for statistical significance and $p < 0.1$ as indicative), in order to find the relationships that best explain the growth-climate interaction and the source-sink relationship in response to climate. Therefore, for each variable response, a correlation was made with the climatic data on an intra-annual/monthly scale.

   The climatic data of each month were correlated with the response variables obtained, being the month in which each sampling was carried out the indicator of the values to be correlated. For example, sampling 2 was carried out in January 2017, so every January between 2012 and 2018 - years in which the tree grew - was correlated with the results obtained in that sampling. So successively for the other samplings.

   Subsequently, with the same way of correlating, the data were divided separately into thirds and sections, in order to assess the influence of climatic variables in space/in different portions of the tree. Each of these results was plotted on separate graphs. Additionally, for this analysis a PCA was also performed.

4 CONCLUDING REMARKS

Based on the literature review on carbon allocation and source-sink relationship, as well as the basic structure of the thesis, then, each of the methods used and the results obtained will be discussed in more detail. In general, chapter 2 focuses on the “Allometric View” and will be addressed through basic growth analysis in which changes in weight, shape, and number over time and space were considered. In addition, the variation in secondary growth was also determined through the analysis of tree growth rings. In turn, chapter 3 focuses on the “Flow View” and will be addressed through the determination of the isotopic ratios of carbon ($\delta^{13}C$) and nitrogen ($\delta^{15}N$) in the organs of coffee plants in order to try to understand the flow of C and N between the portions of the plant over time. Finally, chapter 4 focuses on the “Metabolic View” and will be addressed through the quantification of a profile of carbohydrates, amino acids, and proteins, in order to determine the temporal

and spatial variation in the content of these compounds, allowing to infer the C and N dynamics of the coffee plant.

REFERENCES

ALBACETE, A. A.; MARTÍNEZ-ANDÚJAR, C.; PÉREZ-ALFOCEA, F. Hormonal and metabolic regulation of source-sink relations under salinity and drought: From plant survival to crop yield stability. **Biotechnology Advances**, v. 32, n. 1, p. 12–30, 2014.

ALLEN, R. G. et al. FAO Irrigation and Drainage Paper No. 56 - Crop Evapotranspiration. **Journal of Hydrology**, p. 1–327, 1998.

ALVARES, C. A. et al. Köppen's climate classification map for Brazil. **Meteorologische Zeitschrift**, v. 22, n. 6, p. 711–728, 2013.

BABA, R. K.; VAZ, M. S. M. G.; COSTA, J. DA. Correção de dados agrometeorológicos utilizando métodos estatísticos. **Revista brasileira de Meteorologia**, v. 29, n. 4, p. 515–526, 2014.

BARROS, R.S., MAESTRI, M., RENA, A. B. Physiology of growth and production of the coffee tree - a review. **J. Coffee Res**, v. 27, p. 1-54. 1999

BECK, H. E. et al. Data Descriptor: Present and future Köppen-Geiger climate classification maps at 1-km resolution Background & Summary. **Nature Publishing Group**, v. 5, p. 0–12, 2018.

BIHMIDINE, S. et al. Regulation of assimilate import into sink organs: Update on molecular drivers of sink strength. **Frontiers in Plant Science**, v. 4, n. JUN, p. 1–15, 2013.

BUNN, C. et al. A bitter cup: climate change profile of global production of Arabica and Robusta coffee. **Climatic Change**, v. 129, n. 1–2, p. 89–101, 2015.

CAMARGO, A. P.; CAMARGO, B. P. Definição e Esquematização das Fases Fenológicas do Cafeeiro Arábica nas Condições Tropicais do Brasil. **Bragantia**, v. 60, n. 1, p. 65–68, 2001.

COMPANHIA NACIONAL DE ABASTECIMENTO - CONAB. Acompanhamento da Safra Brasileira. Café. 1° Levantamento 2022. v. 9, n. 1, p. 1–61, 2022.

CRAPARO, A. C. W. et al. Coffea arabica yields decline in Tanzania due to climate change: Global implications. **Agricultural and Forest Meteorology**, v. 207, p. 1–10, 2015.

DAMATTA, F. M. et al. Ecophysiology of coffee growth and production. **Brazilian Journal of Plant Physiology**, v. 19, n. 4, p. 485–510, 2007.

DE CAMARGO, M. B. P. The impact of climatic variability and climate change on Arabic coffee crop in Brazil. **Bragantia**, v. 69, n. 1, p. 239–247, 2010.

FATICHI, S.; LEUZINGER, S.; KÖRNER, C. Moving beyond photosynthesis: From carbon source to sink-driven vegetation modeling. **New Phytologist**, v. 201, n. 4, p. 1086–1095, 2014.

FOOD AND AGRICULTURE ORGANIZATION OF THE UNITED NATIONS - FAO. ETo Calculator. Retrieved from http://www.fao.org/land-water/ databases-and-software/eto-calculator/es/. 2019.

FRESCHET, G. T.; SWART, E. M.; CORNELISSEN, J. H. C. Integrated plant phenotypic responses to contrasting above- and below-ground resources: Key roles of specific leaf area and root mass fraction. **New Phytologist**, v. 206, n. 4, p. 1247–1260, 2015.

GHINI, R.; BETTIOL, W.; HAMADA, E. Diseases in tropical and plantation crops as affected by climate changes: Current knowledge and perspectives. **Plant Pathology**, v. 60, n. 1, p. 122–132, 2011.

HARTMANN, H. et al. Thirst beats hunger - declining hydration during drought prevents carbon starvation in Norway spruce saplings. **New Phytologist**, v. 200, n. 2, p. 340–349, 2013.

INSTITUTO NACIONAL DE METEOROLOGIA - INMET. BDMEP—Banco de Dados Meteorológicos para Ensino e Pesquisa. Retrieved from http://www.inmet.gov.br/portal/index.php?r=bdmep/bdmep. 2019.

JARAMILLO, J. et al. Some like it hot: The influence and implications of climate change on coffee berry borer (Hypothenemus hampei) and coffee production in East Africa. **PLoS ONE**, v. 6, n. 9, 2011.

KÖRNER, C. Growth controls photosynthesis - mostly. **Nova Acta Leopoldina. N.F.**, v. Vol. 114, n. 391, p. 273–283, 2013.

KOTTEK, M. et al. World map of the Köppen-Geiger climate classification updated. **Meteorologische Zeitschrift**, v. 15, n. 3, p. 259–263, 2006.

LAVIOLA, B. G. et al. Alocação de fotoassimilados em folhas e frutos de cafeeiro cultivado em duas altitudes. **Pesquisa Agropecuária Brasileira**, v. 42, n. 11, p. 1521–1530, 2007.

LLOYD, J.; FARQUHAR, G. D. Effects of rising temperatures and [CO2] on the physiology of tropical forest trees. **Philosophical Transactions of the Royal Society B: Biological Sciences**, v. 363, n. 1498, p. 1811–1817, 2008.

NUNES-NESI, A.; FERNIE, A. R.; STITT, M. Metabolic and signaling aspects underpinning the regulation of plant carbon nitrogen interactions. **Molecular Plant**, v. 3, n. 6, p. 973–996, 2010.

OVALLE-RIVERA, O. et al. Projected shifts in Coffea arabica suitability among major global producing regions due to climate change. **PLoS ONE**, v. 10, n. 4, p. 1–13, 2015.

PEREIRA, Cássio Honda Filho. **Dinâmica do crescimento vegetativo e reprodutivo do cafeeiro.** 2018. Dissertação (Mestrado em Fisiologia Vegetal) – Universidade Federal de Lavras, Lavras, 2018.

RUAN, Y. L. Sucrose metabolism: Gateway to diverse carbon use and sugar signaling. **Annual Review of Plant Biology**, v. 65, p. 33–67, 2014.

SCHROTH, G. et al. Winner or loser of climate change? A modeling study of current and future climatic suitability of Arabica coffee in Indonesia. **Regional Environmental Change**, v. 15, n. 7, p. 1473–1482, 2015.

TAVARES, P. DA S. et al. Climate change impact on the potential yield of Arabica coffee in southeast Brazil. **Regional Environmental Change**, v. 18, n. 3, p. 873–883, 2018.

USDA FOREIGN AGRICULTURAL SERVICE. Coffee: World Markets and Trade. **Coffee: World Markets and Trade**, n. December, p. 1–9, 2021.

VASCONCELLOS, Lissa Vilas Boas. **Mapeamento fisiológico e do crescimento da copa de coffea arabica cv. Arara.** 2019. Tese (Doutorado em Fisiologia Vegetal) – Universidade Federal de Lavras, Lavras, 2019.

WARDLAW, I. F. Tansley Review No. 27 The control of carbon partitioning in plants. **New Phytologist**, v. 116, n. 3, p. 341–381, 1990.

WHITE, A. C. et al. How can we make plants grow faster? A source-sink perspective on growth rate. **Journal of Experimental Botany**, v. 67, n. 1, p. 31–45, 2016.

WOODRUFF, D. R.; MEINZER, F. C. Water stress, shoot growth and storage of non-structural carbohydrates along a tree height gradient in a tall conifer. **Plant, Cell and Environment**, v. 34, n. 11, p. 1920–1930, 2011.

YU, S. M.; LO, S. F.; HO, T. H. D. Source-Sink Communication: Regulated by Hormone, Nutrient, and Stress Cross-Signaling. **Trends in Plant Science**, v. 20, n. 12, p. 844–857, 2015.

CHAPTER 2: GROWTH ANALYSIS AND GAS EXCHANGE – ALLOMETRIC VIEW

ABSTRACT

Plant growth comprises the coordinated distribution of C to structural components and storage compounds, in order to supply two fundamental processes: growth and reproduction. Understanding the source-sink relationship and differential C allocation dynamics in response to climate for these two processes can be approached through growth analysis that involves and integrates plant form and function in a holistic way. Thus, the aim of the chapter was to evaluate the source-sink patterns of coffee trees under field conditions over time and in different portions of the plant in response to climatic conditions through growth analysis and gas exchange. For this purpose, in each of the samplings and in the portions established in the trees, several variables of primary and secondary growth were destructively measured. In terms of primary growth, plant height, number of leaves, leaf area, number of plagiotropic branches, number of fruits and dry mass of leaves, fruits and branches were evaluated. In turn, in terms of secondary growth, the analysis of the structure of the plant growth rings was used through dendrochronological methods, to determine the annual radial growth rates of the trees. Gas exchange was measured using an infrared gas analyzer on fully expanded leaves for each portion of the plant, and the measurement was made on the same plant throughout the experimental period. The results obtained for each variable were correlated with the climatic characteristics of the region, using Pearson's statistical correlation analysis. All primary growth and gas exchange variables, except for stomatal conductance, were significantly influenced ($p<0.05$) by all variation factors. The variation in time showed that growth and reproduction follow the phenology reported for the coffee tree, in addition to presenting a negative correlation dynamic that results in a biennial pattern of production. The variation in space demonstrated that reproductive structures have a high capacity to import carbohydrates, constituting strong sinks that compete with vegetative structures for resources. The variation in annual radial growth rates showed an annual pattern of growth rings formation, whose dimensions can be correlated and modeled as a function of climate and biomass allocation to describe tree growth. In general, the main climatic determinants of the primary and secondary growth of coffee trees were the water balance conditioned by its components – Prec, Evap and ETo- and the wind speed. From the results obtained, the importance of growth analysis and analysis of growth rings can be highlighted to improve the understanding of the allocation of C for the growth and/or reproduction of coffee trees, both in time and in space.

Keywords: Primary growth. Secondary growth. Reproduction. Tree growth rings. Biennial pattern.

1 INTRODUCTION

Growth, in the context of the individual plant, represents an irreversible change over time: this change occurs mainly in size, often in shape and, occasionally, in number (Hunt, 1990). In turn, the term “plant growth analysis” refers to a set of quantitative methods that describe and interpret the performance of whole plants and its environmental constraints. This type of analysis integrates the form and function of the plant in an explanatory and holistic way (Thomas and Ougham, 2017).

The analysis mainly uses two types of measurements: the dry weight of the plant and the size of the assimilatory system, usually composed by leaf area. Although other simple primary data such as height, volumes, protein content, chlorophyll content, among others, can also be used (Hunt et al., 2002). Generally, these data are collected by sampling the plants in a destructive way, which is why homogeneous groups of plants or plots are needed (Beadle, 1985). The primary information obtained from these measurements allows the calculation of absolute and relative growth rates and simple ratios between two quantities or variables (Thomas and Ougham, 2017).

Another type of analysis is the analysis of growth rings. It is a technique greatly applied for the evaluation of the vegetative growth of trees, however, studies using this type of analysis on trees such as coffee have not been reported, despite their socioeconomic importance. Growth rings formation is the result of the cambial activity of the tree between the vegetative period and the quiescent phase. These rings are, then, a response of the plant in ecosystems with seasonally variable environments, which produce cyclical plant growth. This happens due to a period of seasonal stress that induces cambial meristem dormancy, interrupting the growth of the diameter and inducing the formation of growth rings (Alves and Angyalossy-Alfonso, 2000; Nath et al., 2016; dos Santos Silva et al., 2017; Worbes, 2002).

The growth ring analysis allows the indirect, but long-term, evaluation of biomass allocation for secondary growth, which can be used as a proxy, relating the characteristics and rates of annual growth and production with the characteristics of climate seasonality (Babst et al., 2014). Thus, carbon allocation modeling through growth ring analysis allows the indirect evaluation of carbon allocation in different parts of the plant (Sevanto and Dickman, 2015). This improves the understanding of how different environmental factors produce different patterns of carbon allocation and, therefore, how different climatic signs are expressed in tree rings (Gea-Izquierdo et al., 2015). These signals represent a valuable file of variability that

annually results in biomass and stem growth, allowing the reconstruction of the history and growth trajectory of trees on interannual to centennial scales (Babst et al., 2014; Mbow et al., 2013).

Considering these two forms of growth analysis, we hypothesized that there is a change in the source-sink relationship in coffee trees in response to climate, with changes in the patterns of biomass allocation between organs. To test the hypothesis, specifically, (1) we verified biennial patterns of coffee production in the region that imply a negative correlation between growth and reproduction (2) we verified the carbohydrate import capacity of each of the coffee organs over time and space (3) we used dimensional parameters of tree growth rings to indirectly assess biomass allocation in plant organs in response to climate

2 METHODOLOGY

For the primary growth analyzes, plant height, length of each fraction of the orthotropic branch, number of plagiotropic branches and length of each fraction of the plagiotropic branch were evaluated. In each portion of the plagiotropic branch, the number of leaves, leaf area, number of rosettes and number of fruits at each stage of development were evaluated based on the phenological scale proposed by Pezzopane et al., (2003). To determine the leaf area, a sampling of 10% of the total number of leaves of each part of the branches was collected. The leaf area was calculated by measuring the length and width of the leaf using a ruler and multiplied by the coffee correction factor (Righi, 2005). After obtaining the dry mass of these leaves, a relationship between leaf area and dry mass was established. Thus, the estimate of the total leaf area was performed based on the weight and leaf area of the sampled leaves using a simple proportion.

For the secondary growth analyzes, in the lower third of each tree, the basal part with the largest diameter of the orthotropic stem was selected (Figure 4a). This basal section was divided into cross-sections that were processed according to standard dendrochronological procedures (Stokes and Smiley, 1968), as following: (i) initially surface preparation was carried out to increase the visibility of growing zones as much as possible by sanding methods using sandpapers with progressively finer grids (80 - 600 grit); (ii) subsequently, each section was divided into three axes/repetitions to circumferentially verify the boundaries between the rings (Figure 4b); (iii) detection of ring boundaries was performed using a stereomicroscopic magnifying glass and ring width was measured with a digital measuring device (LINTAB,

Rinntech, Heidelberg, Germany) supported by the software TSAP-Win (Rinntech, Heidelberg, Germany). In addition, ring area was determined by scanning each cross-section at a resolution of 600 dpi with a scanner MUSTEK model SE A3. The resulting images were processed in the *ImageJ* image analysis software. The area considered as a standard for measuring the area of the tree rings was a regulated ruler that was scanned along with the stems. This rule allowed the calibration of the image analysis software. In the software, considering the three radii of each stem section, each ring was independently contoured to determine its area. The different color of the cell layers between one ring and another helped to identify the limits between the rings in areas without radii demarcation.

In order to correlate the values of secondary growth with another variables, the volume of the orthotropic stem was estimated by adjusting a curve between the values of diameter and height in 10 points in different sections of the coffee stem (Figure 4a), to determine the area under that curve and the polynomial model whose mathematical expression represents the shape of the stem from the base to the apex of the tree.

Figure 4 - (a) Coffee tree showing sampling sections for tree-ring analysis (b) Cross-sections from the base after surface preparation revealing tree rings

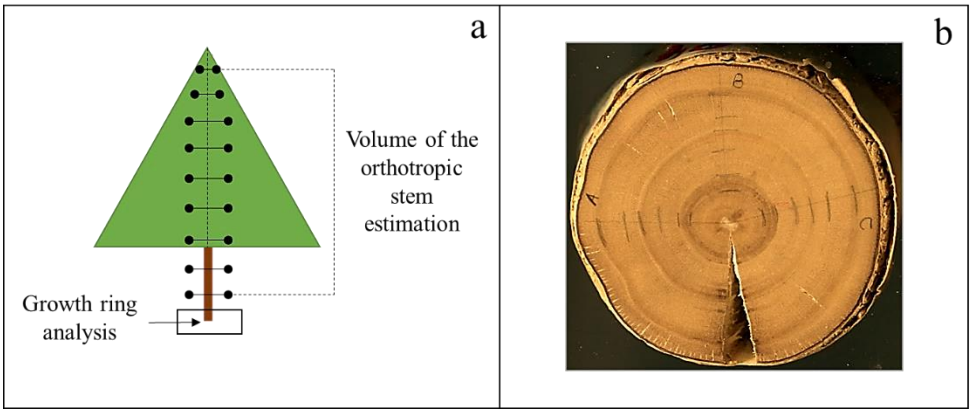

Source: From the author (2022)

The time series obtained from the growth ring area were submitted to a normalization/filtering process through two methodologies: the first differences and the normalization by the relative growth of the plant. The first difference was tested in order to evaluate the stationarity of the time series of the growth ring area. Thus, we evaluated changes in the response variable from one period to the next. For this, each ring area value was

subtracted from the previous year's value. For example, from the value of the 2013 ring area, was subtracted the 2012 ring value, and so for all subsequent years. This resulted in a shorter time series (number of years/rings 1). In turn, the second methodology was tested in order to eliminate the effect of the difference between plants. In this case, the value of the area of each ring was divided by the value of the area of the first ring formed for each plant individually. With that, a notion of the proportion of growth per plant was obtained, eliminating the effect of the repetitions being different plants.

From the cross-sectional growth ring area data after normalization process, the annual radial growth rate of each tree was determined. These rates were correlated with the climatic characteristics of the region, using a Pearson statistical correlation analysis ($p < 0.05$ for statistical significance and $p < 0.1$ as indicative), on an annual scale. Thus, each annual growth rate was correlated with the climatic data for that year and the previous year ('time lag' correlation), in order to assess the influence of the current climate (T) on the current growing season, and the influence of the climate of the previous year (T-1) on the growth season of the current year (T). Also, each annual growth rate was correlated with the climatic data for the dry season and the wet season both for the current climate (TD and TW, respectively) and for the climate of the previous year (T-1D and T1W, respectively). The dry season was considered between the months of April–September and the wet season was considered between the months of October–March. Additionally, the annual growth rates were correlated with the primary tree growth data, and subsequently, linear models were fit, demonstrating which interactions influence the secondary growth and describe them through growth curves and mathematical models.

For the gas exchanges analysis, it was used an infrared gas analyzer (IRGA - LI-6400XT Portable Photosynthesis System, LI-COR, Lincoln, USA), in fully expanded leaves, in the respective plant portions, in the same plant throughout of the entire experimental period. The evaluations performed were net photosynthetic rate (A), stomatal conductance (gs), transpiration rate (E), leaf temperature (LeT) and branch temperature (BrT). The evaluations were carried out considering the PAR incident on each leaf, and the temperature, humidity, and concentration of CO_2 in the air. The measurements were carried out on the same day as the destructive samplings, however, always on the same plant marked since the beginning of the experiment. Measurements were taken in all samplings except the first and last (S1 and S17, respectively) due to lack of equipment.

3 RESULTS

3.1 Primary growth

Nine primary growth variables were analyzed. Seven considering all variation factors (samplings – S, thirds - Th, sections – Se) and two which vary only in the vertical axis (without considering Se). For all, the interaction between the factors was considered (Table 1). For the first group of 7 variables, in general, the length of the plagiotropic branches, the leaf area, the total number of fruits, and the dry matter of leaves and fruits were significantly influenced ($p < 0.05$, F-test) by the variation factors individually, as well as by their triple interaction. The number of leaves and branch dry matter were significantly influenced ($p < 0.05$, F-test) by the variation factors individually, but not by their interaction.

Considering the temporal variation (between the samplings), in general, most variables had the lowest values between samplings 7 and 8, which represent the period of September and October of the year 2017, quiescent phase that separates a phenological year from another. Comparing the two years evaluated, in 2017 there was a greater harvest, which is why among samplings 5 and 6 representing the months of April and June 2017 (traditional harvest season), the highest values of the total number of fruits (TNF) and the dry matter of fruits (FDM) were presented. In turn, after harvest, with the resting or quiescent phase, the lowest TNF and FDM values were presented in samplings 7 and 8 (Table 2, Table 3).

In sequence, after a big harvest, there is a vegetative period in which new branches and leaves grow that will later give rise to new fruits. Thus, between samplings 12 and 16, the highest values of number and dry matter of leaves, leaf area, and number, length and dry matter of branches were presented. In contrast to other variables, the number of plagiotropic branches and their dry matter had the lowest values between samplings 2 and 3, from January to February 2017, which makes sense considering that at this time the plant may be allocating all the resources in the growth of fruits, and there may be less investment in vegetative structures.

Considering the spatial variation (between the thirds and between the sections of the tree), there was a clear and increasing trend for most of the variables, with the highest values in the lower third of the tree and the smallest in the upper third (Table 2, Table 3). The total number of fruits and their dry matter had a different behavior, with the highest values found in the middle third of the tree, traditionally considered the most productive third. Regarding the sampled sections of the plagiotropic branches, although there was not such a clear trend, the

total number of fruits and their dry matter showed the highest values in the middle section of the branch, which is also traditionally considered as the most productive section of the branches. The number, area and dry matter of leaves were higher in the proximal section, the youngest of the tree, which has a predominance of vegetative growth (Table 2, Table 3).

In addition to the total number of fruits, their stage of development over time and space is a great indicator to consider. Thus, Figure 5 shows the proportion of fruits harvested at each stage of development in each sampling, third or section of the tree. As shown in Figure 3, between January and June the period of filling and maturation of the fruits is presented, and it is possible to visualize this process with the change in the proportion of fruits between the unripe and cherry stages from samplings 2 to 6 (Jan to Jun 2017) and 11 to 16 (Jan to Jun 2018).

In the thirds, the predominant stages that were harvested were unripe, expansion and green, which may indicate that the transition between these stages takes longer than the transition between the green cane to cherry stages. Also, the third in which more cherry fruits were harvested was in the middle third as shown in Table 2. In the sections of the plagiotropic branches, the unripe, expansion and green stages also predominated, and the fruits in the green-cane and cherry stages were located in the proximal and intermediate sections, which may indicate the direction of fruit maturation within the branches (proximal to distal). The number of plagiotropic branches and plant height were significantly influenced ($p < 0.05$, F-test) by the variation factors individually, as well as by their double interaction (since for these variables the sections on the horizontal axis were not considered) (Table 1).

Figure 5 - Proportion of each of the stages of development of the coffee fruits harvested in 17 samples over time and sampled in 36 regions distributed in thirds and sections along the tree

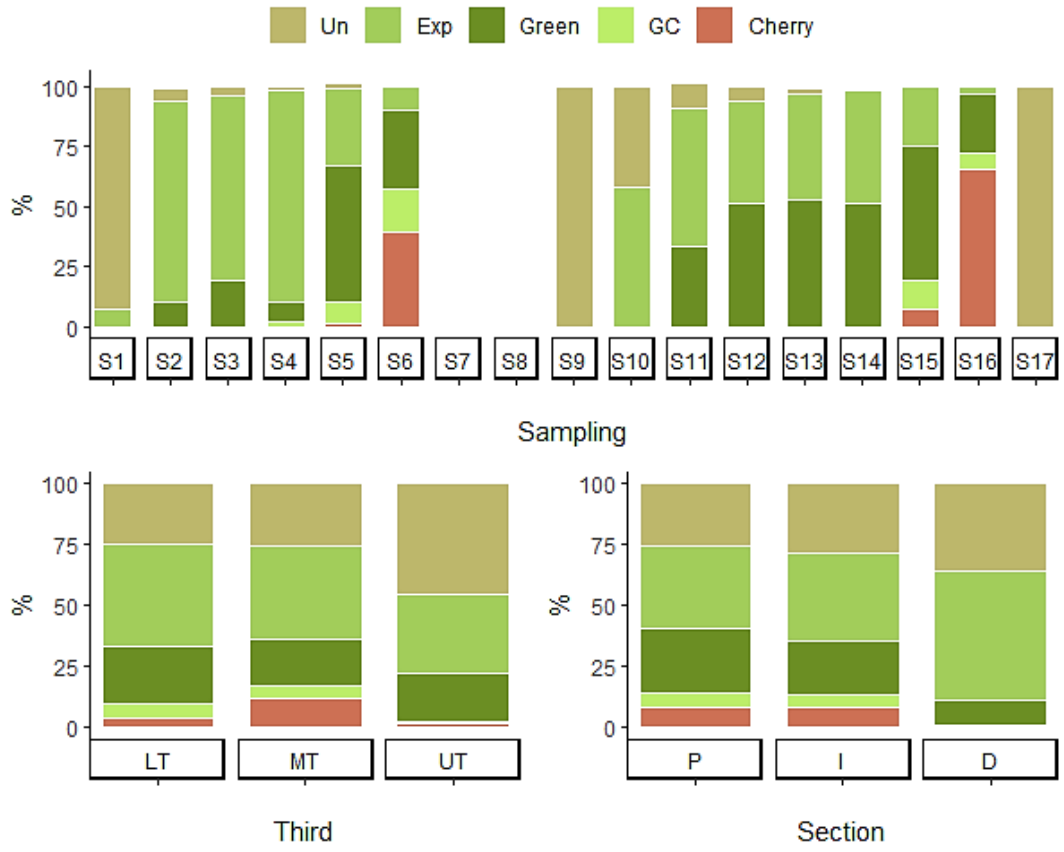

Note. Un, unripe; Exp, expansion; GC, green cane. LT, lower third; MT, middle third; UT, upper third. P, proximal; I, intermediate; D, distal. Source: From the author (2022).

Table 1 - F-values and significance levels in three-way/two-way ANOVA of primary growth variables from coffee plants in production evaluated in 17 samplings over time and sampled in 36 regions distributed in thirds and sections along the tree.

Factor	PBL	LN	LA	TNF	BDM	LDM	FDM	NPB	PH
Sampling (S)	6.536 ***	4.842 ***	10.169 ***	43.064 ***	3.695 ***	9.736 ***	83.712 ***	7.127 ***	7.631 ***
Third (Th)	395.138 ***	63.517 ***	51.792 ***	36.158 ***	110.543 ***	23.461 ***	64.752 ***	22.703 ***	526.754 ***
Section (Se)	1742.451 ***	7.988 ***	16.141 ***	130.159 ***	130.581 ***	50.349 ***	141.440 ***	---	---
S x Th	1.760 **	1.707 *	1.727 **	7.450 ***	1.016 ns	1.500 *	18.766 ***	4.475 ***	7.795 ***
S x Se	24.110 ***	1.190 ns	1.581 *	15.496 ***	1.485 *	1.753 **	29.058 ***	---	---
Th x Se	465.150 ***	70.244 ***	70.187 ***	12.375 ***	52.703 ***	84.006 ***	18.830 ***	---	---
S x Th X Se	3.321 ***	1.265 “	1.806 ***	2.098 ***	0.740 ns	1.997 ***	6.366 ***	---	---

Note. PBL, plagiotropic branch length (cm); LN, leaves number; LA, leaves area (cm^2); TNF, total number of fruits; BDM, branch dry matter (g); LDM, leaves dry matter (g); FDM, fruits dry matter (g); NPB, number of plagiotropic branches; PH, plant height (cm). Significance levels are: *** ($p < 0.001$), ** ($p < 0.01$), * ($p < 0.05$), “ ($p < 0.1$), ns, not significant. Source: From the author (2022)

Table 2 - Primary growth variables from coffee plants evaluated in 17 samplings over time and sampled in 36 regions distributed in thirds and sections along the tree. Values reported as the means of the plant portions evaluated.

Factor	PBL	LN	LA	TNF	BDM	LDM	FDM	NPB	PH
Sampling (S)									
S1	---	223.81±32.597	0.19±0.027	157.34±27.476	50.10±9.844	58.85±7.478	3.87±0.760	5.35±0.313	57.67±2.988
S2	22.47±2.228	259.31±43.526	0.85±0.143	100.09±14.807	69.56±14.171	64.78±10.955	11.46±1.815	5.56±0.273	56.42±3.669
S3	21.30±2.049	159.94±28.070	0.57±0.102	96.35±14.689	45.71±8.912	41.53±7.584	15.72±2.466	4.77±0.320	50.17±4.011
S4	22.50±2.188	223.53±44.508	0.69±0.134	97.39±18.523	64.29±15.002	51.26±9.554	22.16±4.191	5.33±0.373	52.04±5.088
S5	24.29±2.258	261.75±51.164	0.86±0.148	111.44±23.943	81.87±18.685	63.95±11.229	34.60±7.409	6.00±0.336	51.38±4.505
S6	22.56±1.958	240.39±38.942	0.94±0.157	142.94±31.132	67.03±13.527	77.35±11.389	54.37±11.661	6.04±0.377	52.58±5.031
S7	23.00±2.365	104.11±15.725	0.33±0.049	0.00±0.000	85.66±16.117	29.22±4.633	0.00±0.000	6.98±0.316	54.96±4.561

S8	20.86±2.431	97.43±19.258	0.19±0.041	0.00±0.000	68.48±12.668	19.05±4.447	0.00±0.000	6.33±0.348	53.29±2.390
S9	24.31±2.508	155.66±25.719	0.40±0.063	31.49±7.409	68.44±11.443	33.24±5.272	0.14±0.028	6.35±0.248	55.42±2.408
S10	23.13±2.609	179.33±30.026	0.48±0.073	5.35±1.232	69.89±13.128	37.77±5.653	0.07±0.017	6.75±0.283	57.83±3.470
S11	24.36±2.049	249.64±34.768	0.77±0.113	22.81±4.282	78.63±12.566	63.80±8.914	2.18±0.442	6.92±0.305	56.65±2.964
S12	26.00±2.109	306.75±46.539	1.05±0.163	18.83±3.652	91.67±17.641	86.87±13.276	3.39±0.697	7.31±0.344	59.17±1.456
S13	23.88±2.277	256.72±51.057	0.91±0.193	9.15±2.167	84.20±19.315	71.48±13.755	2.22±0.534	6.75±0.369	57.75±3.725
S14	23.19±1.947	302.64±64.459	1.11±0.209	15.15±2.978	92.35±21.502	86.47±15.937	4.42±0.888	7.06±0.388	59.58±4.813
S15	25.84±2.214	238.58±34.732	0.92±0.134	9.17±2.209	92.84±15.402	79.77±11.740	3.41±0.836	7.06±0.280	61.75±3.215
S16	25.44±2.184	287.36±40.165	1.14±0.169	2.79±0.727	108.71±20.975	97.3±13.357	1.36±0.376	7.48±0.326	61.42±2.601
S17	25.33±2.130	304.69±47.123	1.00±0.172	61.9±11.759	133.84±24.597	90.05±14.224	0.34±0.066	7.08±0.279	62.75±5.227
SED	8.906	164.979	0.553	57.627	66.667	43.577	14.866	1.338	15.706
Third (Th)									
LT	27.75±1.082	340.06±22.997	1.06±0.080	52.87±7.452	127.83±9.720	78.97±5.682	9.60±1.757	7.10±0.179	71.69±0.909
MT	25.40±0.900	189.39±10.285	0.63±0.038	72.13±8.438	80.56±4.613	57.18±3.452	14.83±2.499	6.14±0.116	48.16±1.143
UT	17.78±0.703	149.97±12.431	0.49±0.044	30.54±3.262	30.43±1.552	49.56±4.351	3.76±0.458	6.01±0.116	49.70±0.665
SED	1.573	28.092	0.099	11.720	10.870	7.945	3.089	0.242	1.605
Section (Se)									
D	17.36±0.558	198.65±21.558	0.68±0.080	31.84±3.947	110.42±9.303	49.08±5.672	7.00±1.190	---	---
I	36.31±0.833	214.37±17.280	0.59±0.048	97.4±10.086	109.92±5.150	48.89±3.637	18.51±2.766	---	---
P	17.27±0.703	266.4±10.612	0.91±0.040	26.30±2.986	18.47±0.919	87.74±3.885	2.68±0.342	---	---
SED	1.225	29.597	0.102	11.235	10.673	7.778	3.031	---	---

Note. PBL, plagiotropic branch length (cm); LN, leaves number; LA, leaves area (cm^2); TNF, total number of fruits; BDM, branch dry matter (g); LDM, leaves dry matter (g); FDM, fruits dry matter (g); NPB, number of plagiotropic branches; PH, plant height (cm). Residual degrees of freedom = 432 for PBL, 765 for NPB and 459 for the rest of variables. SED, standard error of the difference between two treatment means. **Values are reported as the means ± standard error** (n=36 for S, n=204 for Th, n=204 for Se). Source: From the author (2022).

Table 3 - Primary growth variables from coffee plants evaluated in 17 samplings over time and sampled in 36 regions distributed in thirds and sections along the tree. Values reported as the sum of the plant portions evaluated.

Factor	LN	TNF	BDM	LDM	FDM	NPB	PH
Sampling (S)							
S1	8057	5664	1803.61	2118.53	139.23	257	173.00
S2	9335	3603	2504.09	2331.90	412.62	267	169.25
S3	5758	3469	1645.49	1495.14	565.85	229	150.50
S4	8047	3506	2314.36	1845.21	797.80	256	156.13
S5	9423	4012	2947.17	2302.24	1245.44	288	154.13
S6	8654	5146	2412.92	2784.77	1957.27	290	157.75
S7	3748	0	3083.65	1051.83	0.00	335	164.88
S8	3605	0	2533.74	704.95	0.00	304	159.88
S9	5448	1102	2395.30	1163.50	4.91	305	166.25
S10	6456	193	2516.19	1359.83	2.57	324	173.50
S11	8987	821	2830.56	2296.62	78.32	332	169.95
S12	11043	678	3300.19	3127.35	122.02	351	177.50
S13	9242	329	3031.30	2573.41	80.05	324	173.25
S14	10895	545	3324.56	3113.00	159.23	339	178.75
S15	8589	330	3342.21	2871.67	122.58	339	185.25
S16	10345	101	3913.52	3502.78	48.86	359	184.25
S17	10969	2229	4818.24	3241.97	12.25	340	188.25
Third (Th)							
LT	69372	10786	26076.43	16110.07	1957.61	1636	71.69
MT	38635	14715	16433.87	11664.04	3024.36	1671	48.16
UT	30594	6231	6206.80	10110.59	767.08	1932	49.70

Section (Se)							
D	54345	5365	3767.77	17898.72	546.35	--	--
I	43731	19870	22423.37	9972.80	3775.03	--	--
P	40525	6496	22525.96	10013.18	1427.67	--	--

Note. LN, leaves number; TNF, total number of fruits; BDM, branch dry matter (g); LDM, leaves dry matter (g); FDM, fruits dry matter (g); NPB, number of plagiotropic branches; PH, plant height (cm). **Values are reported as the sum of the plant portions** (n=36 for S, n=204 for Th, n=204 for Se). Source: From the author (2022).

To visualize the distribution and grouping of data more clearly, the PCA performed is shown in Figure 18. Between the first two components the 76% of the data variation is explained. The evaluation of loads in the biplot helps to characterize each component in terms of the variables. Thus, variables related to vegetative structures such as LN, LA, LDM, PBL and BDM have large positive loadings on component 1, so this component primarily measures the vegetative development of trees.

On the other hand, variables related to reproductive structures such as TNF and FDM have large negative loadings on component 2, therefore, this component primarily measures reproductive development of trees. From these loads, we can also observe that, due to the proximity of the vectors, there is a positive correlation between three groups of variables: the vectors that represent the leaf variables (LN, LA and LDM), the vectors that represent the branch variables (PBL and BDM) and the vectors that represent the fruit variables (TNF and FDM). Also, given a smaller proximity and an angle close to 90° between the vectors of the variables of vegetative and reproductive structures, there is an indication of uncorrelated variables. Considering the scores in the biplot, it is not easily recognized a grouping of data in the graph that might indicate two or more separate distributions in the data. In general, both the points and the confidence ellipses are superimposed on each other.

For the second group of 2 variables, both were significantly influenced ($p < 0.05$, F-test) by the variation factors individually, as well as by their double interaction. The number of plagiotropic branches tended to increase between samplings, with the lowest values close to 5 in the first samplings and reaching values of 7 in the last ones. Among the thirds, the largest number of branches was concentrated in the lower third, followed by the middle and upper thirds. These results could indicate the tendency or direction of aging of the tree on the vertical axis. However, it is important to consider that although LT has more plagiotropic branches, it is not necessarily the most productive third considering the age of the structures.

In turn, the height of the plant evaluated from the length of the orthotropic branch in each third showed a small but significant difference between the samplings, with the last ones (S15, S16 and S17) showing the highest values of length with values close to 61 cm per third. Among the thirds, the lower third had a greater length on average of +21 cm compared with the other

thirds (Table 2). Adding the length of the three thirds, in general the height of the plant ranged from 150 to 180 cm.

Figure 6 - Biplot with confidence ellipses (95%) as a result of the Principal Component Analysis – PCA - of primary growth variables evaluated in a three-way ANOVA from coffee plants in production evaluated in 17 samplings over time and sampled in 36 regions distributed in thirds and sections along the tree. (a) PCA grouped by tree thirds (b) PCA grouped by sections of plagiotropic branches (c) PCA grouped by samplings (d) PCA grouped by phenological stages: FFM, Fruit formation and filling; VS/BF, Vegetative stage, and bud formation; BM, Bud maturation; QP, Quiescent phase.

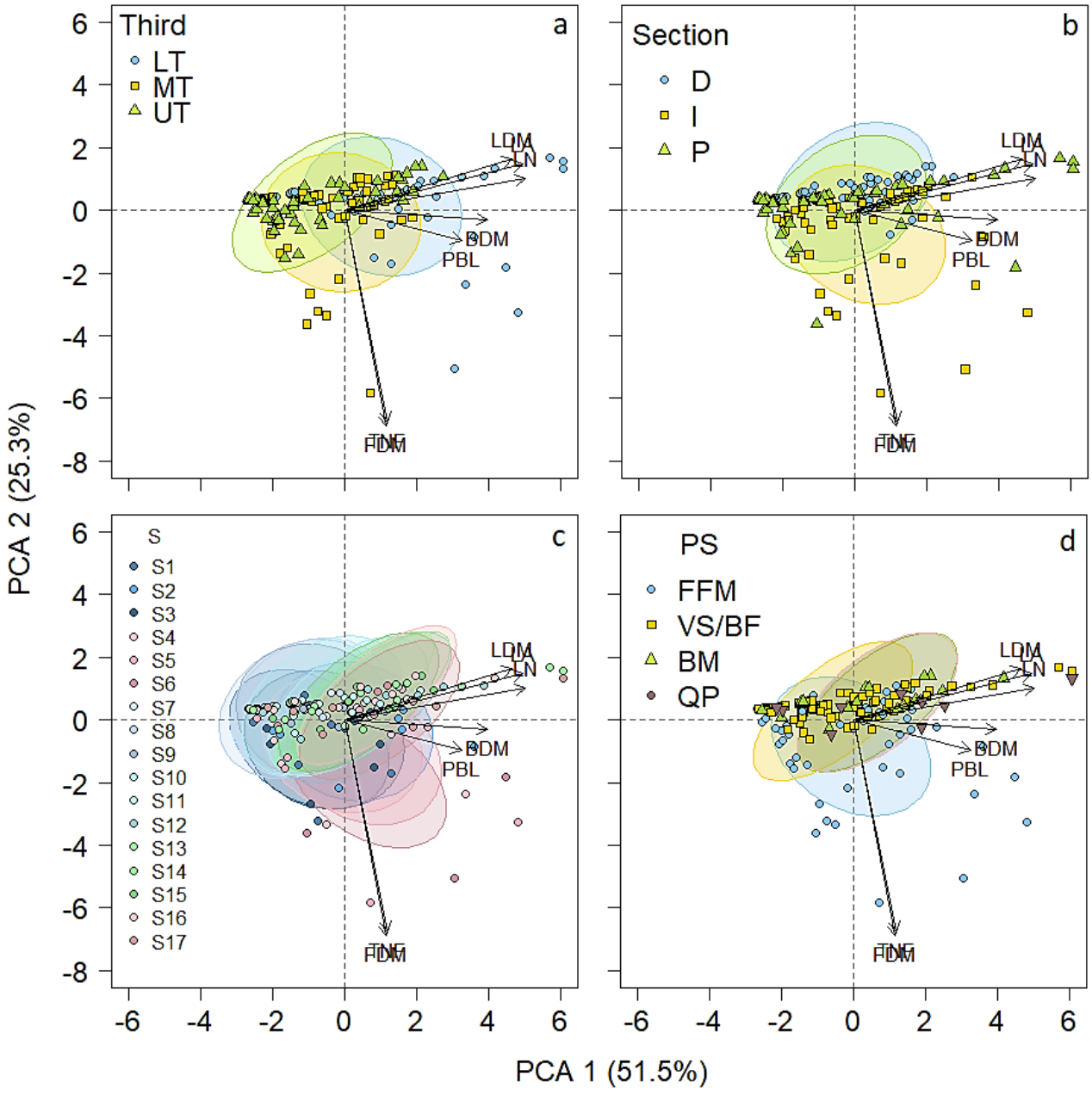

To visualize the distribution and grouping of data more clearly, the PCA performed for these variables is shown in Figure 7. The first two components explain the 100% of the data variation. PH have large negative loadings on component 1, so this component is mainly related to this variable. NPB have large positive loadings on component 2, so this component is mainly related with this variable. From the distance and angle between the vectors, it is possible to infer that the variables are not correlated. Considering the scores in the biplot, it is easily recognized a grouping of data in the graph that indicate three separate distributions by the thirds (Figure 7a). These findings are supported by the confidence ellipses, which allow the visualization of differential behavior in these three groups. In the case of phenological stages, a grouping is not easily visualized.

Figure 7 - Biplot with confidence ellipses (95%) as a result of the Principal Component Analysis – PCA - of primary growth variables evaluated in a two-way ANOVA from coffee plants in production evaluated in 17 samplings over time and sampled in 36 regions distributed in thirds and sections along the tree. (a) PCA grouped by tree thirds (b) PCA grouped by phenological stages -PS. FFM, Fruit formation and filling; VS/BF, Vegetative stage, and bud formation; BM, Bud maturation; QP, Quiescent phase.

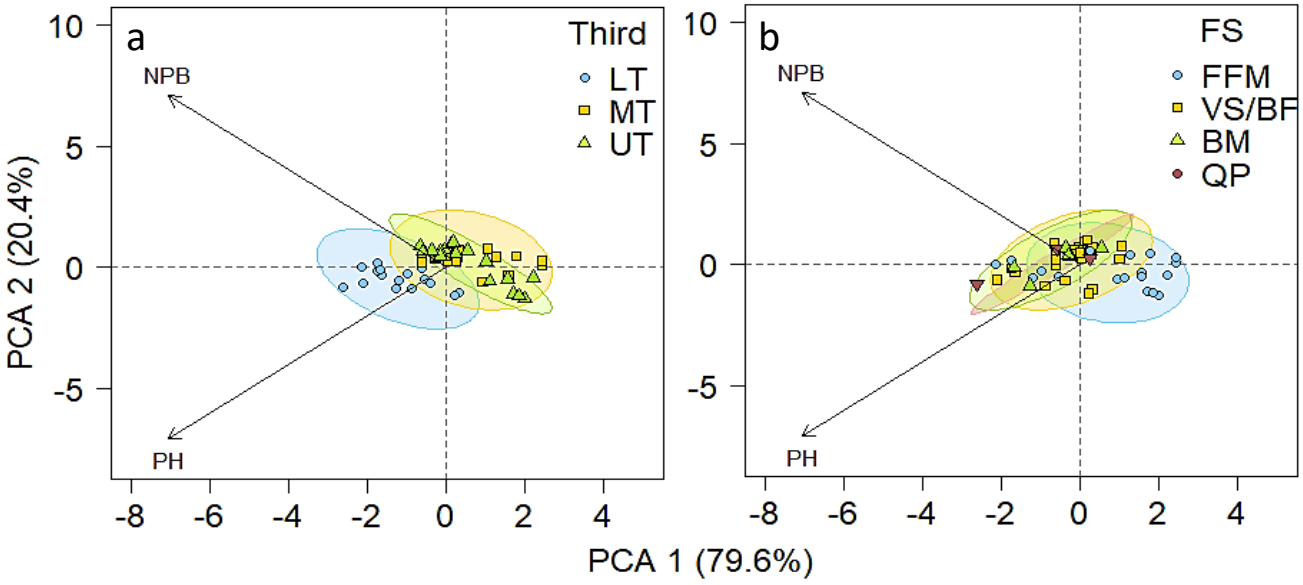

Source: From the author (2022).

Regarding annual climate variability, considering all the temporal variation (S1 to S17), the results of Pearson's correlation between the primary growth data and the evaluated climatic variables showed that medium temperature, evaporation, and wind speed were negatively correlated to LA, FDM and LDM. Additionally, LN correlated negatively and positively with evaporation and wind speed, respectively. The minimum temperature correlated negatively to FDM and evapotranspiration negatively with FDM, LA and LDM. In turn, PBL and BDM did not significantly correlate with any of the climatic variables (Figure 8a).

When data is analyzed in a PCA (Figure 8b), it is possible to observe that the first two components explain just the 56% of the data variation. There is a separation of loads between the quadrants, with the climatic variables on the left side and the growth variables on the right side (in relation to component 1). Considering the scores in the biplot, it is easily recognized a grouping of data supported by the confidence ellipse between the phenological stage. The PCA clearly shows the division between the samplings conditioned by climatic conditions. The vectors that point to the blue group that shows the stage of formation and filling of fruits (S1 to S6) corroborate that the main climatic components that influence this stage are the temperature and the components of the water balance - Prec and ETo. Most of these vectors are at angles close to 90° with the growth variables, which indicates that they are not correlated, or the correlation is weak.

The yellow group that shows the vegetative stage and bud formation is also pointed out by some of the temperature and ETo vectors, but the greatest influence is given by evaporation and the wind speed, which must have been higher in these months. From the position of the vectors in relation to the growth variables, negative correlations can be inferred between them. Most of the evaluated climatic variables are not related to the green and purple groups that show the bud maturation stage and the quiescent phase. This makes sense since these months have the lowest temperatures, rainfall and a negative water balance prevails. However, the explanatory level of the first two components is not so high to explain the variation in the data.

On the other hand, when the spatial variation between the thirds is considered, the results of the Pearson correlation show, in general, that the main growth variables influenced by the climate in the evaluated period were leaf variables such as LA, LN and LDM, and variables related to fruits such as TNF and FDM. Among the variables evaluated, maximum temperature,

sunlight hours and precipitation were the ones that showed the least significant correlations, while evaporation, water balance and wind speed were the ones that most correlated with growth in the thirds. More detailed results can be seen in Figure 9.

In the case of sections of plagiotropic branches, the results of the Pearson correlation show in general that the influence of climate variables in the study period reached more growth variables, with significant results also for others such as PBL, especially in the distal section. Following the same trend, maximum temperature, sunlight hours and precipitation were the ones that showed the least significant correlations, while evaporation, evapotranspiration and wind speed were the ones that most correlated with growth in the sections. More detailed results are found in Figure 10.

The most influenced regions are the middle and lower thirds, as well as sections I and D. The two middle regions (MT and I) comprise the most physiologically active regions, while the LT and D section comprise the oldest and new area from the tree, respectively. This pattern may be related to several processes that regulate the carbon allocation, modulating the source-sink relationship.

Figure 8 - Analysis between the primary growth data and the evaluated climatic variables (a) Pearson's correlation analysis. Positive significant correlations (blue squares), negative significant correlations (red squares) and no correlation (white squares). Significant correlation: p<0.05. (b) Principal component analysis—PCA with confidence ellipses (95%) grouped by phenological stage.

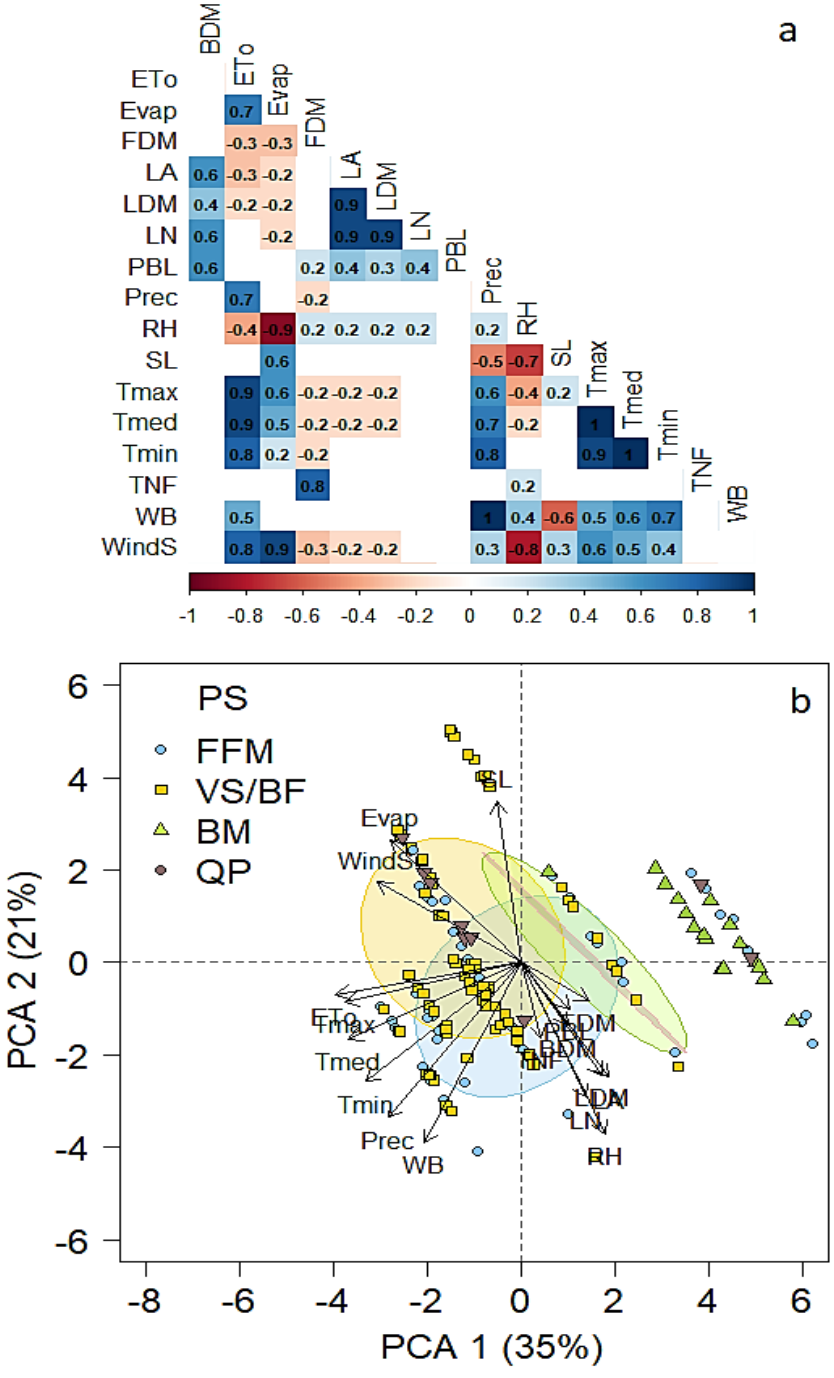

Source: From the author (2022).

Figure 9 - Pearson's correlation analysis between the growth data separated between the thirds and the evaluated climate variables**.** The bars show only the significant correlations obtained ($p<0.05$).

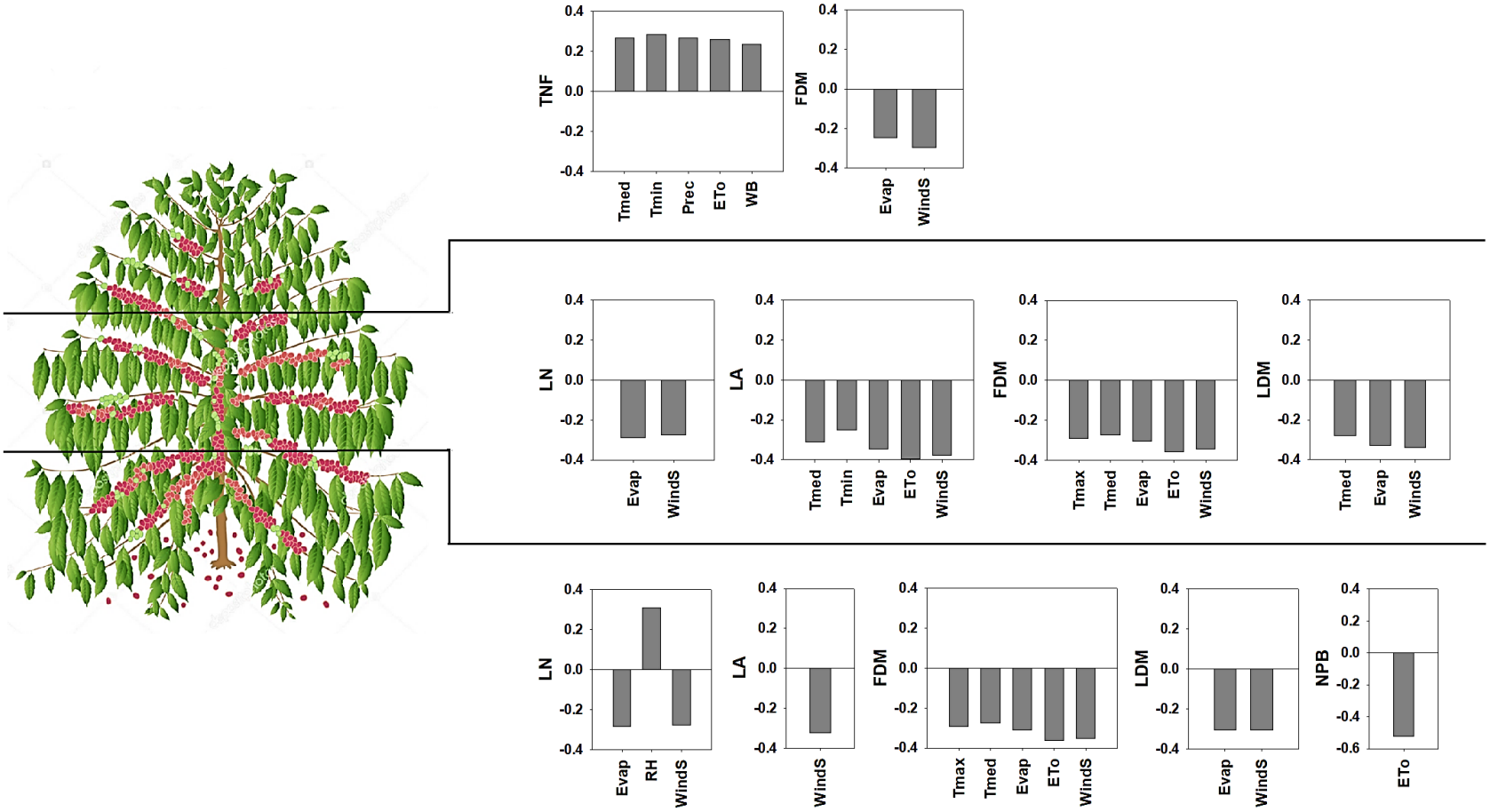

Source: From the author (2022).

Figure 10 - Pearson's correlation analysis between the growth data separated between the sections and the evaluated climate variables. The bars show only the significant correlations obtained ($p<0.05$).

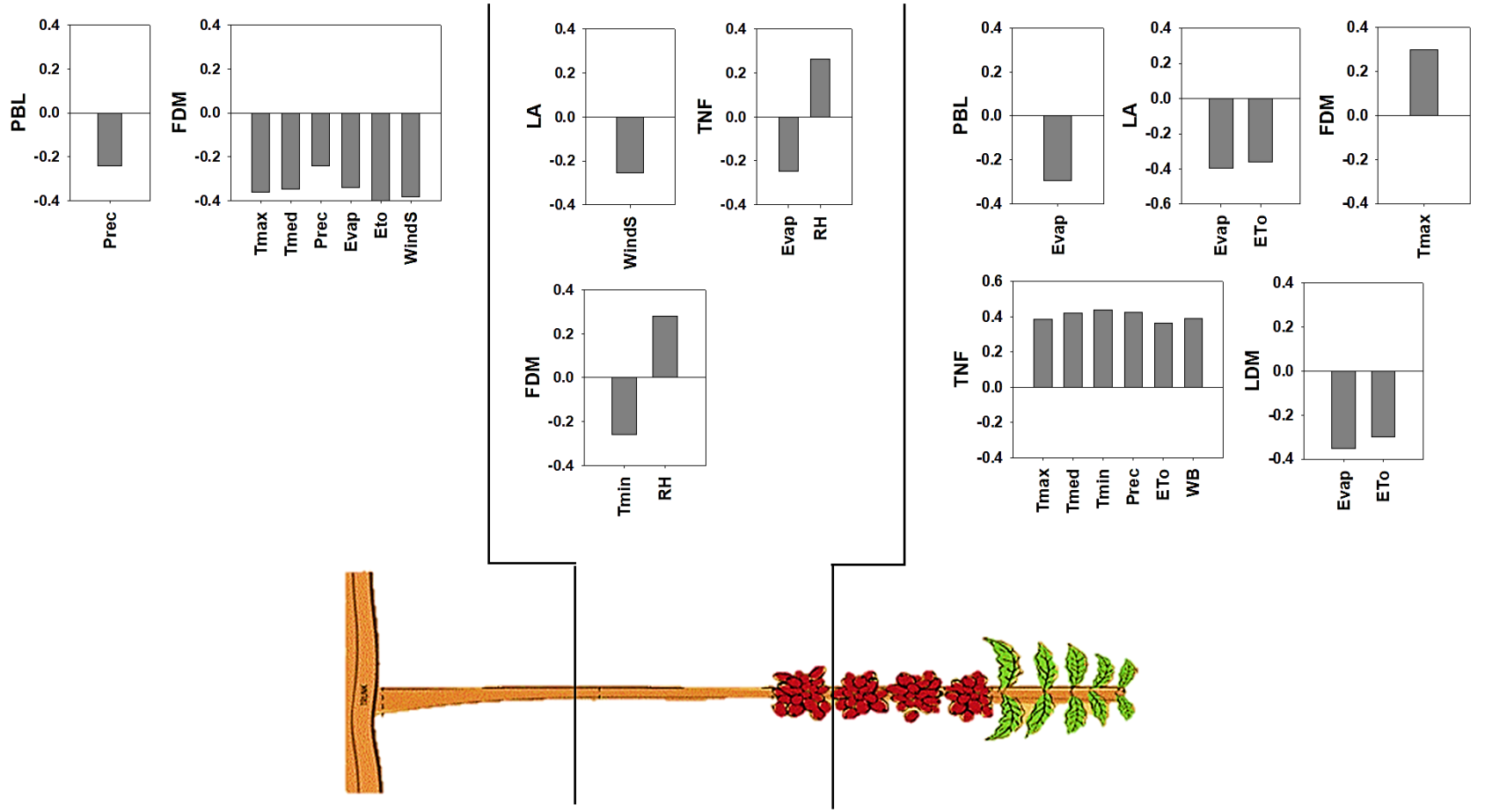

Source: From the author (2022).

3.2 Secondary growth

The results of the influence of climate on the secondary growth of coffee tree can be seen in the published article: “On the use of tree-ring area as a predictor of biomass accumulation and its climatic determinants of coffee tree growth”. **DOI: https://doi.org/10.1111/aab.12680.** Here we show the main results.

The result obtained in the time series normalization process for the growth ring area is shown in Figure 11. When the data is filtered through the first differences, some negative values are obtained. This represent years when the growth of trees was lower than the previous year. However, comparing the growth of a year with reference to the previous year, does not always reflect the relative growth of the plant; nor does it show a clear trend in the growth pattern over time. With that, the normalization of the time series always by the first ring allowed to establish a growth pattern per plant always relative to its initial growth. This showed a tendency for rapid growth in the early years of the tree and later a stabilization in the following years until the date of collection. Considering that we obtained a better result with normalization by the initial ring, all analyzes were performed with this time series of growth ring area.

Figure 11 - Normalization process of time series obtained from the growth ring area. ● - Raw data without normalization, ○ - Data filtered through the first differences, ▼ - Data normalized by the size of the first growth ring.

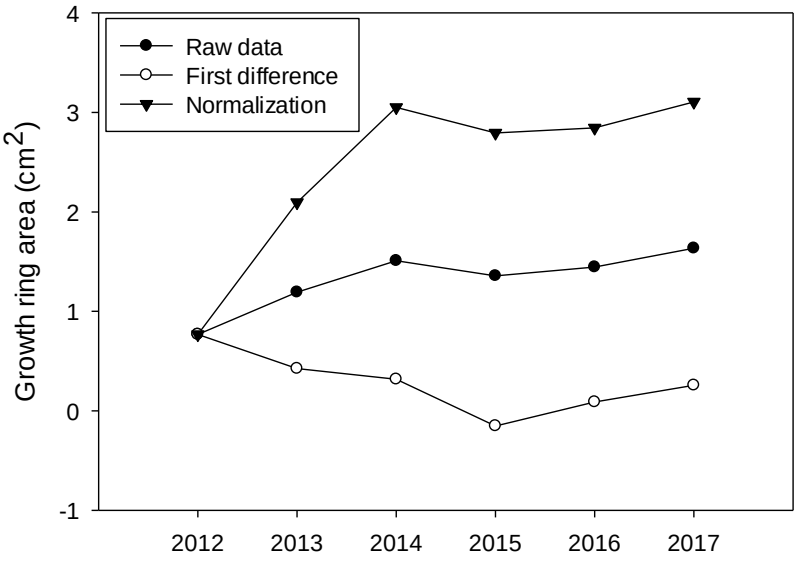

In the coffee growing period between 2012 and 2018, six to seven growth rings were identified, with an average ring width of 0.266 cm and an average ring area of 1.30 cm^2. The trees reached an average accumulated ring area of 7,628 cm^2 and an average increase in the basal area of 1.27 $cm^2\ year^{-1}$. From the identified growth rings, the first one corresponds to the seedling stage and then one ring per year until the complete growth cycle of 2017/2018. In terms of growth rate, the 2012/2013 period had the highest growth rates, and the 2014/2015 period had the lowest rate (Table 4).

Table 4 - Growth ring area values (cm^2) obtained for each year. Each value represents the average of the 17 samples from the base of the orthotropic stem and each year is characterized by its bienniality (CONAB, 2021).

Year	**2012**	**2013**	**2014**	**2015**	**2016**	**2017**	**2018**
Bienniality	**+**	**-**	**+**	**-**	**+**	**-**	**+**
Raw data	0.776	1.188	1.513	1.354	1.453	1.597	1.845
Normalized data	0.776	2.095	3.051	2.794	2.844	3.106	

Note. Year of positive (+) and negative (-) bienniality. Source: From the author (2022).

The results obtained for the linear models between secondary growth, primary growth, and dry matter of the different organs of the plan, show that several significant models ($p<0.05$) were obtained (Figure 12). This may represent a possibility of modeling/monitoring the carbon dynamics in coffee plants using allometric equations that include the parameters of ring area and volume of the orthotropic stem. On the other hand, the results of Pearson's correlation between the data from the normalized growth ring area and the evaluated climatic variables showed several significant correlations that demonstrate thar there is a link between the radial growth of coffee trees and the climate in the southern region of the state of Minas Gerais. For example, on the annual scale (Figure 13), both in the current growing season (T, TD and TW) and in the previous growing season (T-1, T-1D and T-1W), the main determinants responsible for the variation of the area of the tree rings were the water balance (conditioned by its components, Prec and ETo), the relative humidity and the maximum temperature.

Figure 12 – Fit of linear model between allometric variables and dry matter and growth rings accumulated area (GRAA). SV, stem volume (cm^3); PH, plant height (cm); NL, number of leaves; LA, leaf area (cm^2); NP, number of plagiotropic branches; BDM, branch dry matter (g); LDM, leaf dry matter (g); FDM, fruits dry matter (g); TDM, total dry matter (g).

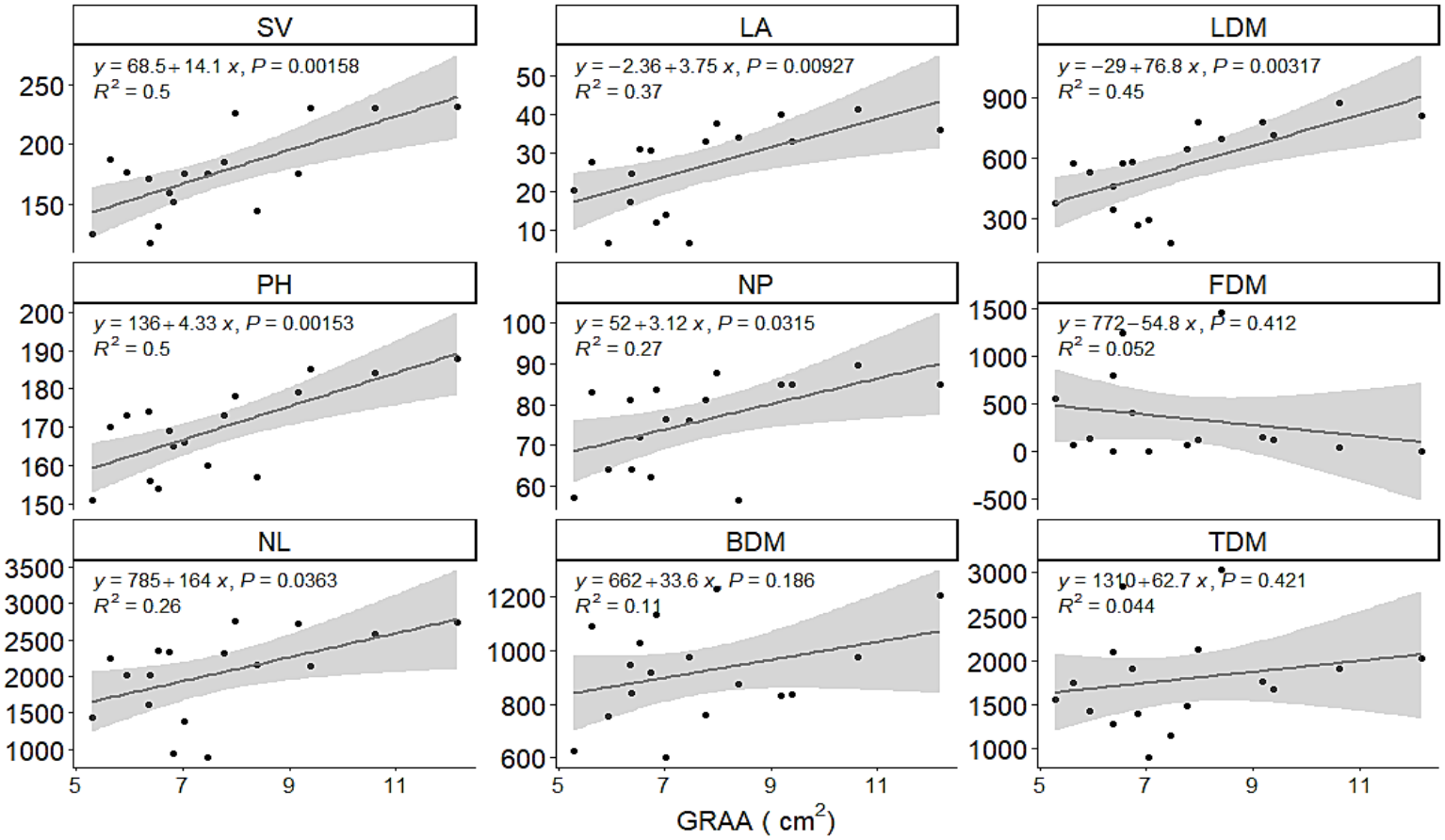

Source: From the author (2022).

Figure 13 – Fit of linear model between the normalized growth rings accumulated area (GRAA) and the climatic variables. Climate: current growth season (T), dry season of the current growth season (TD), climate of the previous year (T-1), dry season of the previous year (T-1D) and wet season of the previous year (T-1W). Climatic variables: Prec, Precipitation (mm); ETo, Evapotranspiration (mm); WBETo, Water Balance (mm); MaxTmaxAv, Average of Maximum Tmax of all months (°C); MinTmaxY, Minimum Tmax in the Year (°C); SLs, Sum of sun hours; RH, Relative humidity (%).

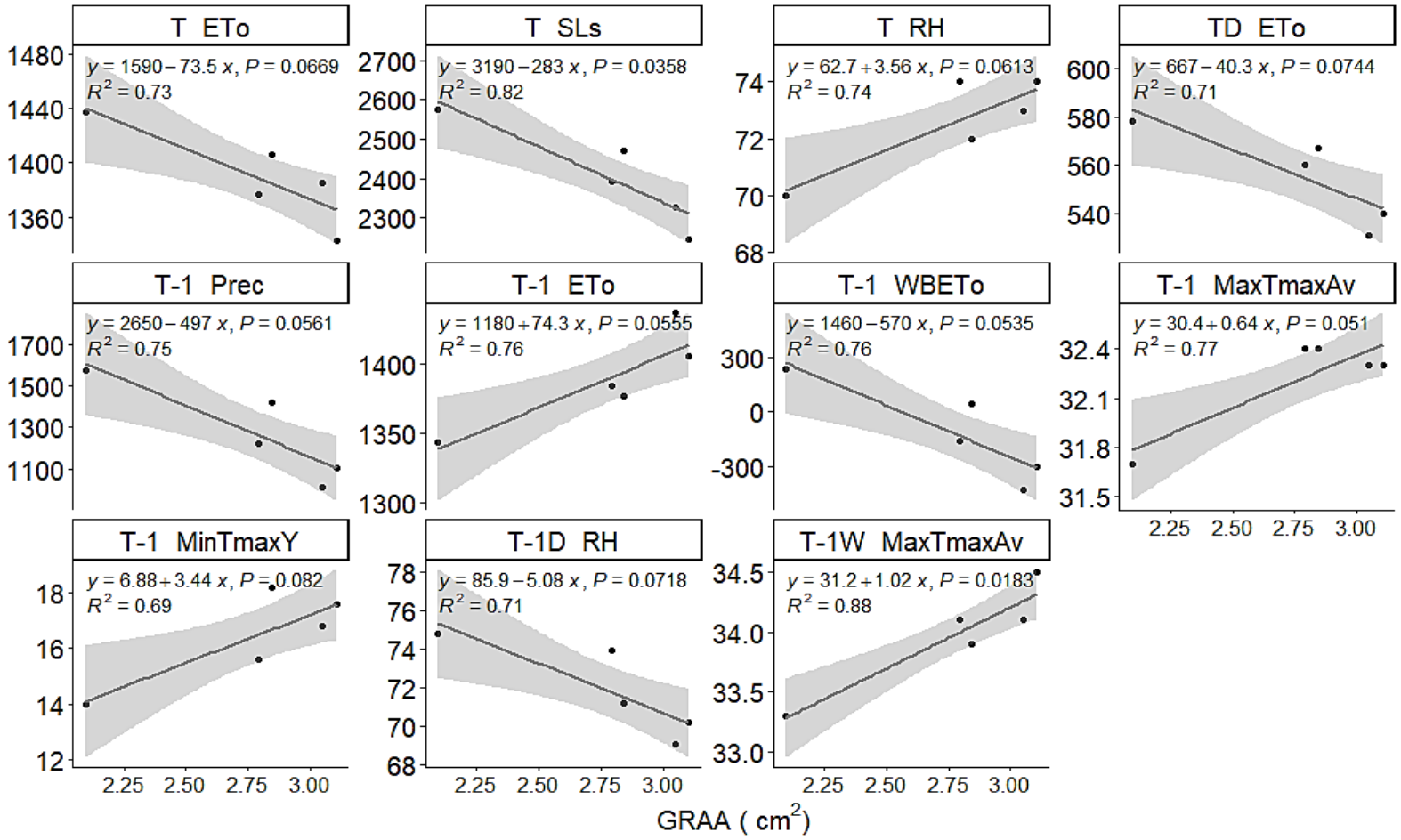

3.3 Gas exchange variables

Five gas exchange variables were analyzed considering all the variation factors (samplings – S, thirds - Th, sections – Se, and the interactions between them) (Table 5). All variables except stomatal conductance were significantly influenced ($p < 0.05$, F-test) by all factors individually and only leaf temperature was influenced by the triple interaction between the factors.

Table 5 - F-values and significance levels in three-way ANOVA of gas exchange variables from coffee plants in production evaluated in 17 samplings over time and sampled in 36 regions distributed in thirds and sections along the tree.

Factor	LeT	BrT	*A*	*gs*	*E*
Sampling (S)	10.2617 ***	100.9995 ***	12.1332 ***	1.6754 ns	17.0063 ***
Third (Th)	108.7551 ***	32.8008 ***	31.4023 ***	1.8954 ns	34.1524 ***
Section (Se)	158.1329 ***	5.8804 **	115.4405 ***	1.4092 ns	76.9790 ***
S x Th	3.5757 ***	4.2636 ***	1.6038 *	1.6294 *	2.5275 ***
S x Se	3.0149 ***	0.8804 ns	8.1574 ***	0.7493 ns	8.2835 ***
Th x Se	65.4840 ***	0.8813 ns	4.1896 **	0.6365 ns	4.6779 **
S x Th X Se	2.0108 ***	0.5973 ns	0.7021 ns	0.6593 ns	0.8267 ns

Note. LeT, leaf temperature (°C); BrT, branch temperature (°C); *A*, net photosynthetic rate (μmol m^{-2} s^{-1}); *gs*, stomatal conductance (mol H_2O $m^{-2}.s^{-1}$); *E*, transpiration rate (mmol H2O $m^{-2}.s^{-1}$). Significance levels are: *** ($p < 0.001$), ** ($p < 0.01$), * ($p < 0.05$), " ($p < 0.1$), ns, not significant. Source: From the author (2022).

Considering the temporal variation, leaf and branch temperature did not show a clear trend between samplings. The photosynthetic rate showed the highest values in the months of January to March in the two years evaluated (S2 to S4 and S11 to S13) and the transpiration rate similarly presented the highest values in the months of December to February for each year evaluated (S2 - S3 and S10 - S11). Throughout the growing season, A reached maximum values of 4.1 and 3.7 μmol m^{-2} s^{-1}, against 1.6 – 1.8 μmol m^{-2} s^{-1} over the reduced growth period. In terms of spatial variation, the LT and MT had the highest values for gas exchange, with the UT, which is the youngest region of the tree on the vertical axis, presenting the lowest values. On the horizontal axis, there was an increasing trend from the proximal to the distal section, with higher values in this younger and constantly growing region (Table 6).

Table 6 - Gas exchange variables from coffee plants in production evaluated in 17 samplings over time and sampled in 36 regions distributed in thirds and sections along the tree.

Factor	LeT	BrT	*A*	*gs*	*E*
Sampling (S)					
S2	16.00±2.180	---	4.05±0.790	0.59±0.431	1.67±0.369
S3	15.25±1.943	---	1.54±0.324	0.04±0.009	1.22±0.237
S4	16.61±1.763	22.19±0.161	3.22±0.492	0.04±0.008	0.69±0.112
S5	13.21±1.685	20.08±0.154	1.84±0.321	0.04±0.008	0.63±0.111
S6	22.76±1.835	25.89±0.468	0.53±0.188	0.03±0.004	0.45±0.063
S7	19.62±2.235	29.43±0.522	1.84±0.264	0.02±0.003	0.90±0.121
S8	22.90±1.820	27.34±0.412	1.89±0.239	0.05±0.006	1.60±0.193
S9	21.58±1.513	26.36±0.464	1.80±0.202	0.03±0.003	0.62±0.075
S10	23.12±1.852	27.97±0.475	1.94±0.293	0.05±0.006	1.51±0.201
S11	21.04±2.054	27.21±0.759	1.70±0.329	0.04±0.005	1.46±0.186
S12	18.38±1.543	22.57±0.153	3.68±0.448	0.08±0.011	1.00±0.132
S13	21.88±2.025	28.89±0.527	2.56±0.371	0.03±0.004	0.70±0.098
S14	19.20±1.843	24.56±0.475	2.10±0.299	0.02±0.003	0.38±0.071
S15	19.82±1.438	23.23±0.518	1.50±0.191	0.01±0.002	0.25±0.046
S16	13.05±0.988	15.52±0.219	1.60±0.261	0.02±0.005	0.36±0.079
SED	7.001	1.533	1.416	0.432	0.628
Third (Th)					
LT	22.60±0.476	23.61±0.352	2.37±0.156	0.15±0.087	1.05±0.081
MT	21.01±0.733	24.74±0.369	2.61±0.181	0.04±0.003	1.10±0.084
UT	13.27±1.028	25.77±0.370	1.38±0.171	0.02±0.003	0.54±0.067
SED	1.350	0.630	0.294	0.087	0.134
Section (Se)					
D	24.98±0.451	25.22±0.395	3.51±0.213	0.14±0.082	1.41±0.095
I	18.96±0.811	24.58±0.353	1.76±0.129	0.06±0.030	0.75±0.059
P	12.95±0.914	24.34±0.359	1.08±0.107	0.02±0.002	0.52±0.065
SED	1.302	0.640	0.272	0.087	0.129

Note. LeT, leaf temperature (°C); BrT, branch temperature (°C); *A*, net photosynthetic rate (μmol m^{-2} s^{-1}); *gs*, stomatal conductance (mol H_2O m^{-2} s^{-1}); *E*, transpiration rate (mmol H2O m^{-2} s^{-1}). Residual degrees of freedom = 351 for BrT and 405 for the rest of variables. SED, standard error of the difference between two treatment means. Values are reported as the means ± standard error (n=156 for BrT and n=180 for the other variables). Source: From the author (2022).

To visualize the distribution and grouping of data more clearly, the PCA performed is shown in Figure 14. Between the first two components the 72% of the data variation is explained.

Figure 14 - Biplot with confidence ellipses (95%) as a result of the Principal Component Analysis – PCA - of gas exchange variables evaluated in a three-way ANOVA from coffee plants in production evaluated in 17 samplings over time and sampled in 36 regions distributed in thirds and sections along the tree. (a) PCA grouped by tree thirds (b) PCA grouped by sections of plagiotropic branches (c) PCA grouped by samplings -S (d) PCA grouped by phenological stages: FFM, Fruit formation and filling; VS/BF, Vegetative stage and bud formation; BM, Bud maturation; QP, Quiescent phase.

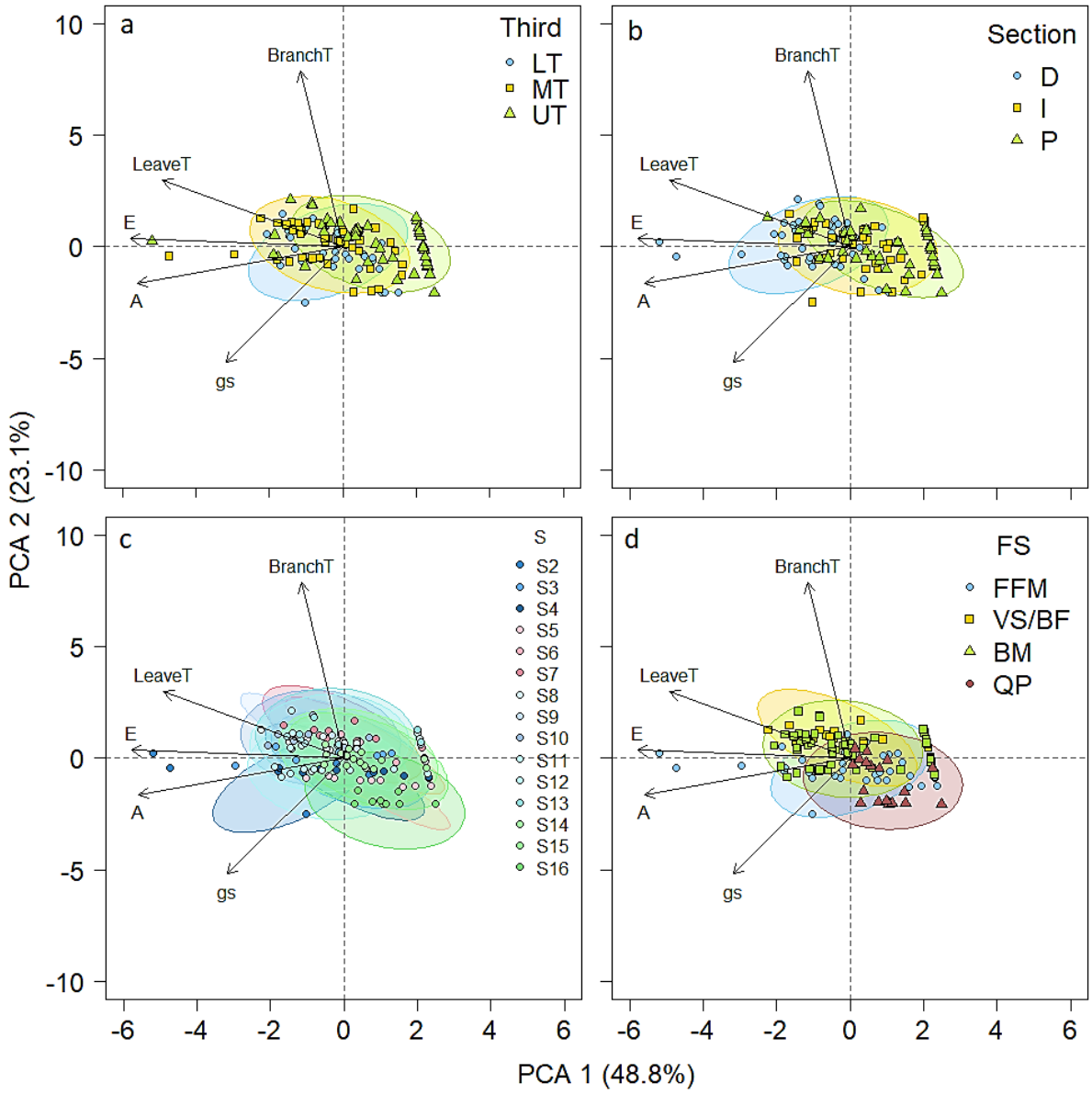

Source: From the author (2022).

While the leaf temperature, *A* and *E* have large negative loadings on component 1, the branch temperature and *gs* have large positive and negative loadings on component 2, respectively. By the proximity of the vectors, it is possible to infer that there is a significant correlation between leaf temperature, E, A and gs. In turn, the temperature of the branch is not correlated with any of the gas exchange variables. Considering the scores in the biplot, it is not easily recognized a grouping in the graph that might indicate two or more separate distributions in the data. In general, both the points and the confidence ellipses are superimposed on each other for all the cases.

Regarding annual climate variability, considering all the temporal variation (S2 to S16), the results of Pearson's correlation between the gas exchange data and the evaluated climatic variables (Figure 15a) showed that leaf temperature did not correlate with any of the climatic variables, gs correlated positively only with precipitation and water balance, A positively correlated with temperature, prec and WB and transpiration together with branch temperature correlated significantly with almost all variables evaluated. SL was the only climate variable that did not correlate with any of the gas exchanges variables.

When data is analyzed in a PCA (Figure 15b), it is possible to observe that the first two components explain just the 56% of the data variation. Temperature, ETo and wind speed have large negative loadings on component 1, Prec, WB and RH have large positive loadings on component 2, and Evap and SL have large negative loadings on component 2. Considering the scores in the biplot, it is easily recognized a grouping of data supported by the confidence ellipse between the phenological stage. The PCA clearly shows the division between the samplings conditioned by climatic conditions. The same trend explained in Figure 8 was maintained, in which the vectors point to the months and phenological stages in which they had the greatest influence. It is also possible to verify that the gas exchange vectors are very small so that it is more difficult to find differences between the groups based on these parameters. Most of the angles between the gas exchange vectors and the climatic variables vectors are small, corroborating the positive correlations obtained in Pearson's correlation analysis. Likewise, the larger angle with RH corroborates the only two negative correlations obtained.

On the other hand, considering the spatial variation, the results of the Pearson correlation show, in general, that almost all gas exchanges were influenced by at least one climatic variable.

In UT, the only variable that correlated significantly was BrT, while in MT and LT, almost all gas exchanges correlated significantly with several of the climate variables analyzed, mainly BrT, *gs* and *E*. Similarly with the results of the growth data, among the climate variables evaluated, sunlight hours, precipitation and relative humidity were the ones that showed the least significant correlations, while medium and minimum temperature, evaporation, water balance and wind speed were the ones that most correlated with gas exchanges in the thirds (Figure 16).

In the case of sections of plagiotropic branches, the results of the Pearson correlation show in general that the influence of climate variables in the study period reached all gas exchanges variables, being all influenced by at least one climatic variable. In sections P and I, there were mainly significant correlations for the variables BrT, *gs* and *E*. On the other hand, section D presented significant correlations with almost all evaluated variables, being the branch section more dynamic in response to the climate, the which also applied to growth variables (Figure 17).

Figure 15 - Analysis between gas exchange data and the evaluated climatic variables (a) Pearson's correlation analysis. Positive significant correlations (blue squares), negative significant correlations (red squares) and no correlation (white squares). Significant correlation: $p<0.05$. (b) Principal component analysis—PCA with confidence ellipses (95%) grouped by phenological stage.

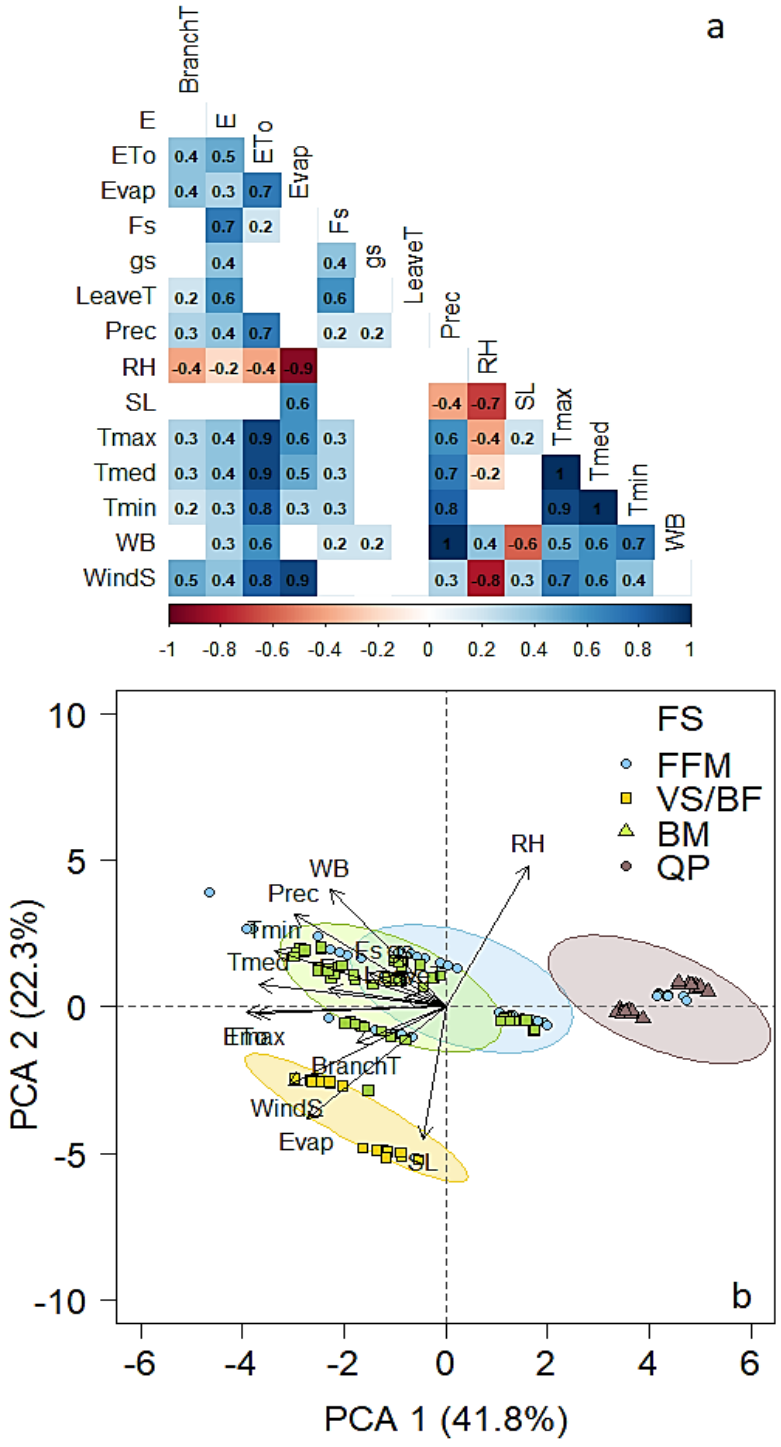

Figure 16 - Pearson's correlation analysis between the gas exchange data separated between the thirds and the evaluated climate variables. The bars only show the significant correlations obtained ($p<0.05$).

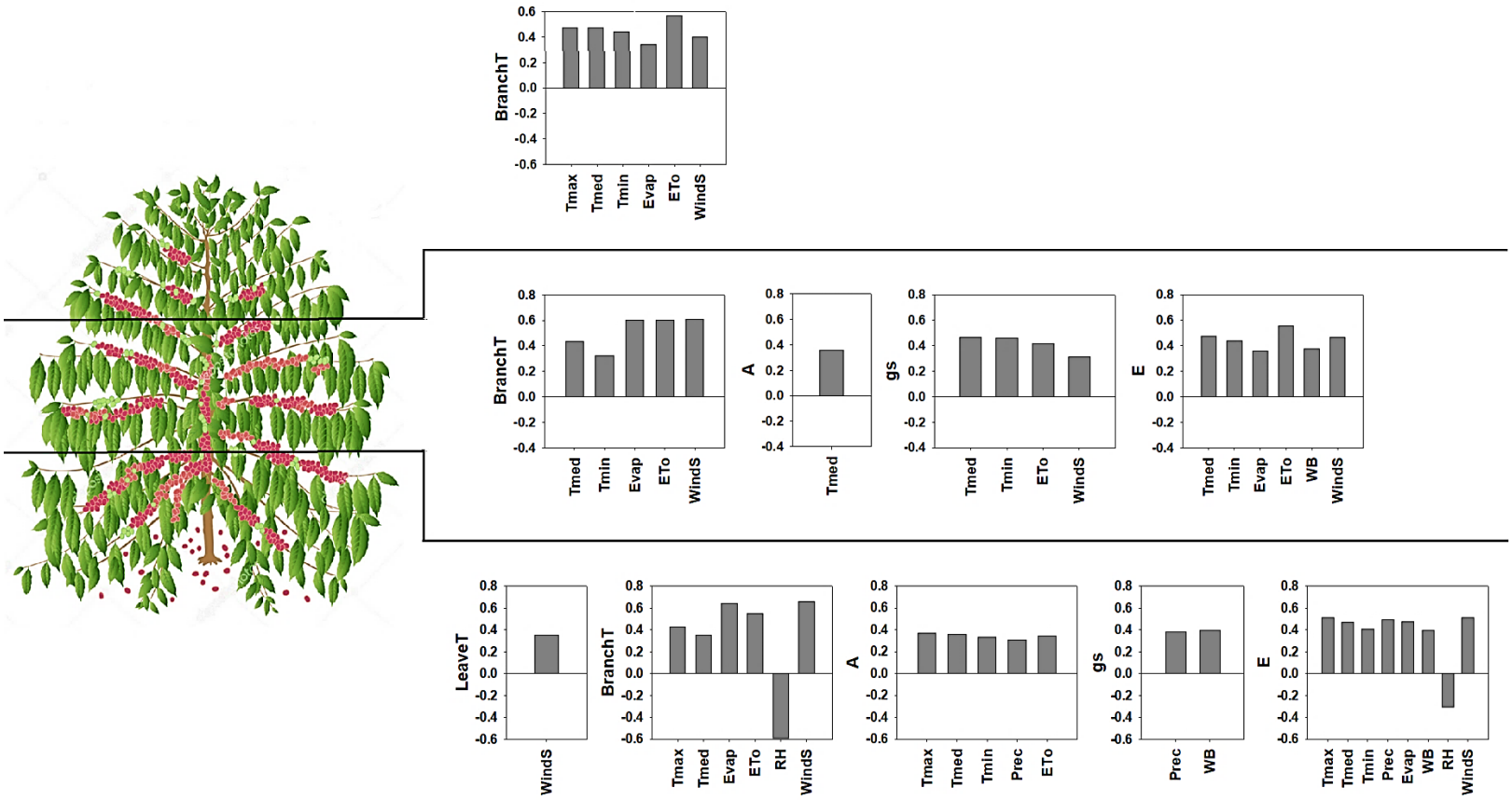

Source: From the author (2022).

Figure 17 - Pearson's correlation analysis between the gas exchange data separated between the sections and the evaluated climate variables. The bars only show the significant correlations obtained ($p<0.05$).

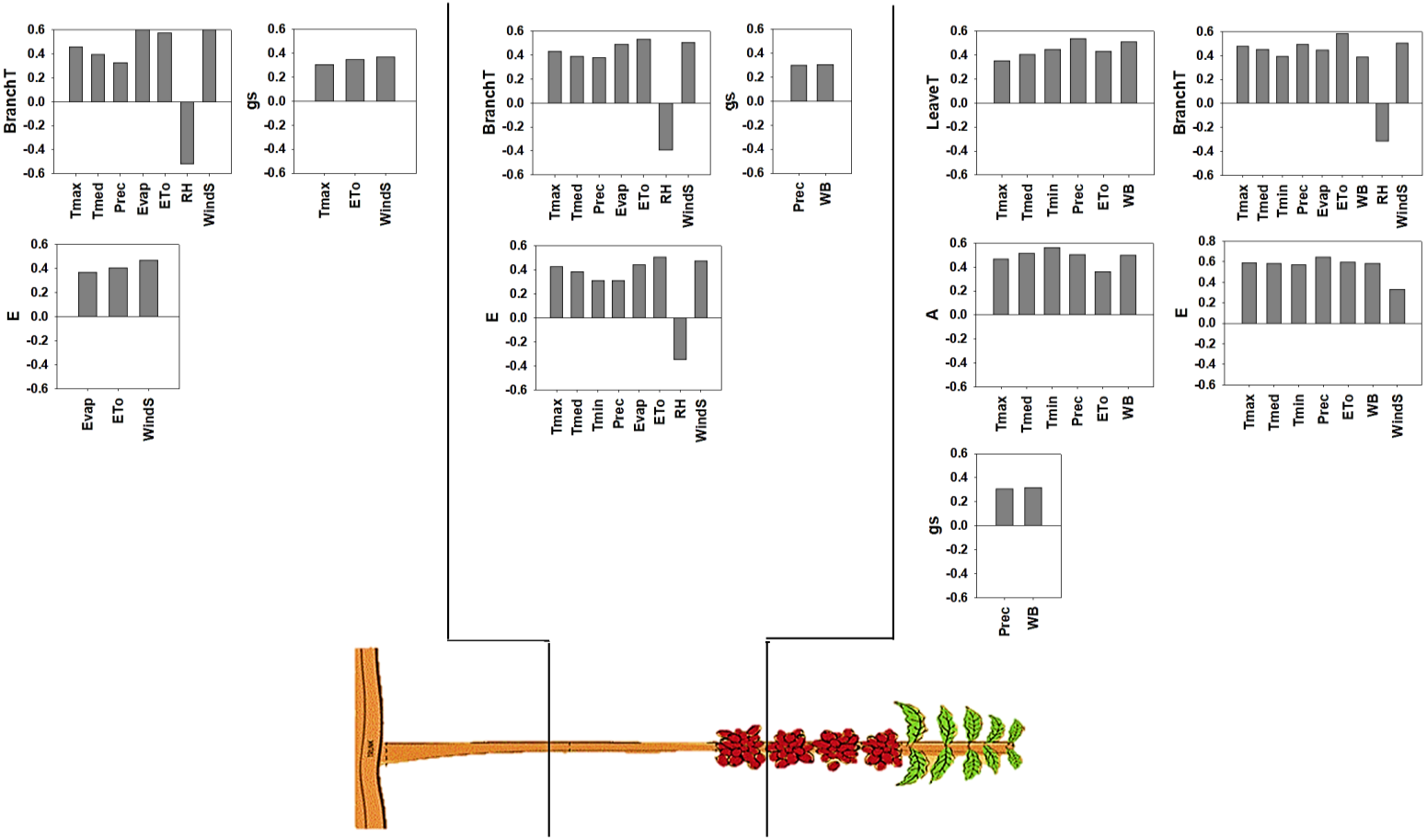

Source: From the author (2022).

3.4 Production of the experimental plot

As mentioned earlier in the general introduction, coffee is a product of great global importance, reaching a production of 176 million bags in the 20220/2021 season and an estimated 167 million bags in the 2021/2022 season (USDA Foreign Agricultural Service, 2021). Brazil is the largest producer and exporter of coffee in the world, with the state of Minas Gerais concentrating the largest coffee production, corresponding to approximately 50% of national production.

The National Supply Company (CONAB by its acronym in Portuguese) carries out the monitoring/surveying of the Brazilian coffee crop, publishing technical bulletins with important information on planted area, productivity, and production at national and state level. In Minas Gerais, production is concentrated in some characteristic mesoregions, such as the South and Midwest of Minas Gerais, the Triângulo area, the Alto Paraíba, the Northwest, the Zona da Mata, the Vale do Rio Doce and the Central Zone. For the current season of 2022, the perspective is to allocate approximately 1.3 million hectares, of which 24% are destined for coffee plantations in formation and the remaining 76% are destined for crops in production (Companhia Nacional de Abastecimento - CONAB, 2022).

When considering the biennial cycle with the alternation of a year with great flowering followed by another with less intense flowering, at the national level and in the state of Minas Gerais, it has been reported that even years normally present positive bienniality in relation to odd years that, from subsequently show negative bienniality (Companhia Nacional de Abastecimento - CONAB, 2022). Thus, in this context, the 2017 season was, both nationally and statewide, a season characteristic for a low flowering with lower production and productivity compared with 2018 characterized by positive bienniality. Thus, considering the dynamics of the experimental plot at the Experimental Farm of Fundação Procafé, it is possible to affirm that the plot presented a situation opposite to the dynamics of bienniality of most of the producing regions of the state and the country. **Thus, whenever we mention positive or negative bienniality in this document, we always refer to the bienniality dynamic of the experimental plot and not the region.**

This situation may be related to the technological level of the experimental plot, which was conducted with high quality standards in terms of management and plant health, so that possibly the first high flowering and productions took place in years of negative bienniality in the state, leading to the dynamics opposite to that of the region. Table 7 shows the main growth and production variables considering the positive and negative bienniality seasons for the experimental crop and the months of the quiescent phase. The positive bienniality phase comprised samplings 1 to 6 from December 2016 to June 2017. The quiescent phase comprised samplings 7 and 8 in the months of September and October 2017 and the negative bienniality phase comprised samplings 9 to 16 in the months of November 2017 to June 2018.

Additionally, from the values of planting density and dry weight of fruits in the cherry development stage that were harvested, the approximate number of bags per hectare for each year evaluated was calculated as follows:

- Planting density:

  The trees were planted with a spacing of 3.5m between rows and 0.5m between plants. Thus, each plant occupies a space of 1.75 m^2, leading to an approximate total of 5700 plants per hectare.
- Dry weight of cherry fruits in the positive bienniality season (2017):

  Between samplings 5 and 6 the fruits harvested in the cherry stage were dried leading to a dry weight of 902g of dry coffee / plant. Considering a value of 0.902Kg per plant multiplied by the total number of plants, this leads to a value of 5141.4 Kg of dry coffee per hectare.
- It is important to consider/fix some factors:

  (a) On average 0.62 kg of coffee cherry weighs 0.23 kg of dry coffee

  (b) On average, 1 L of coffee cherry weighs 0.62 kg

  (c) On average, 1 bag of processed coffee contains 500 L of coffee cherry
- Then in 1 ha:

  If 0.62 kg of coffee cherry weighs 0.23 kg of dry coffee (a), then 5141.4 kg of dry coffee weighs 13859.4 kg of coffee cherry

  If 1L of coffee cherry weighs 0.62 kg (b), then 13859.4 kg of coffee cherry has a volume of 22353.87 L of coffee cherry

If 1 bag of processed coffee has 500 L of coffee cherry, then 22353.87 L is equivalent to 44.7 bags

- Result:

  The experimental plot in the positive bienniality season had a productivity result of **44.7 bags/ha**, which is a higher value in relation to the value found in the region and in the country. In recent years, the national average productivity has been between 27-30 bags/ha. This result is also a reflection of the technological level of the experimental plot.

- Dry weight of cherry fruits in the negative bienniality season (2018):

  Between samplings 15 and 16 the fruits harvested in the cherry stage were dried leading to a dry weight of 46g of dry coffee / plant. Considering a value of 0.046Kg per plant multiplied by the total number of plants, this leads to a value of 262.2 Kg of dry coffee per hectare.

- Then in 1 ha:

  If 0.62 kg of coffee cherry weighs 0.23 kg of dry coffee (a), then 262.2 kg of dry coffee weighs 706.8 kg of coffee cherry

  If 1L of coffee cherry weighs 0.62 kg (b), then 706.8 kg of coffee cherry has a volume of 1140L of coffee cherry

  If 1 bag of processed coffee has 500 L of coffee cherry, then 1140L is equivalent to 2.3 bags

- Result:

  The experimental plot in the negative bienniality season had a productivity result of **2.3 bags/ha**, which is a lower value in relation to the value found in the region and in the country. It also represents a lower value compared to the productivity obtained in the previous season in the same experimental plot.

Table 7 - Primary growth variables from coffee plants evaluated in 17 samplings over time and sampled in 36 regions distributed in thirds and sections along the tree. Values reported considering the positive and negative bienniality seasons as the sum of the plant portions evaluated.

Factor		LN	LA	TNF	BDM	LDM	FDM	NPB	PH	Fruits/Leaves
Considering bienniality and thirds										
Positive bienniality	LT	28561	1.14	9863	8746.80	6463.15	1864.90	717	70.98	0.35
	MT	11546	0.51	12394	3572.94	3516.12	2798.67	473	40.60	1.07
	UT	9167	0.39	3143	1307.90	2898.52	454.65	397	48.54	0.34
Quiescent phase	LT	3075	0.31	4	2680.36	579.38	0.02	206	68.56	0.00
	MT	1459	0.15	0	2112.19	307.55	0.00	204	45.25	0.00
	UT	2819	0.32	0	824.84	869.85	0.00	229	48.56	0.00
Negative bienniality	LT	32880	1.14	478	12162.07	7693.12	90.29	880	71.09	0.01
	MT	22410	0.82	1397	9163.98	6833.27	220.23	891	54.08	0.06
	UT	15715	0.58	2225	3327.78	5481.77	308.03	902	50.92	0.14
Considering bienniality and sections										
Positive bienniality	D	22685	1.04	3490	1604.43	7065.94	456.79	---	---	0.15
	I	16200	0.57	16537	6689.95	3653.67	3371.42	---	---	1.02
	P	10389	0.44	5373	5333.26	2158.18	1290.02	---	---	0.52
Quiescent phase	D	2987	0.31	4	198.61	856.97	0.02	---	---	0.00
	I	2075	0.22	0	2674.06	458.12	0.00	---	---	0.00
	P	2291	0.25	0	2744.72	441.69	0.00	---	---	0.00
Negative bienniality	D	25405	0.99	1274	1725.20	8943.73	86.16	---	---	0.05
	I	21870	0.67	2216	11131.16	4929.99	397.97	---	---	0.10
	P	23730	0.89	609	11797.47	6134.44	134.42	---	---	0.03

Note. LN, leaves number; LA, leaves area (cm^2); TNF, total number of fruits; BDM, branch dry matter (g); LDM, leaves dry matter (g); FDM, fruits dry matter (g); NPB, number of plagiotropic branches; PH, plant height (cm). Positive bienniality: sampling 1 to sampling 6 (dez/16 – jun/17); Quiescent phase: sampling 7 and 8 (Sep and Oct/17); Negative bienniality: sampling 9 to sampling 16 (Nov/17 – Jun/18). **Values are reported as the sum of the plant portions** (n=36 for S, n=204 for Th, n=204 for Se). Source: From the author (2022).

4 DISCUSSION

In this chapter we address source-sink patterns on coffee trees and their relationship to annual climate variability through traditional growth analysis and gas exchange analysis. As in all subsequent chapters, these analyzes were approached from the point of view of temporal variation (over the sampling period) and spatial variation (between different parts of the tree).

Trees or perennial woody plants are long-lived sessile organisms. Because of their multi-year longevity, they have to adapt their growth and development to the sometimes extremely contrasting environmental conditions that occur in different seasons (Ding and Nilsson, 2016; Trumbore, Brando, and Hartmann, 2015). Thus, when thinking about forests and/or productive systems composed mostly of evergreen trees, it is important to know how these plants adjust their metabolic processes to survive in a rapidly changing climate. For this purpose, the development of carbon allocation and growth and productivity models has been seen as an adequate tool to improve the understanding of these processes. Most of these models have a perspective centered on carbon metabolism (Körner, 2015; Sala, Woodruff, and Meinzer, 2012).

At its most basic, the models consider net primary productivity (NPP) as the difference between total carbon assimilation (gross primary productivity, GPP) minus respiration (R, including root export). How these resources are allocated/distributed depends mainly on the balance between how much C is obtained and available through photosynthesis (source activity) and how much C is needed to sustain the various metabolic processes of the plant (sink activity) (Gessler and Grossiord, 2019). Thus, the understanding of carbon allocation and the source-sink relationship is vital to understand how resources are distributed either to compartments or to specific chemical compounds, supporting the three basic processes of the plant: growth, reproduction, and defense (which will not be discussed in this thesis) (Dietze et al., 2014; Gessler and Grossiord, 2019; Huang et al., 2019).

In terms of growth, the coordinated distribution of C is needed, both for structural components and for storage compounds that ensure a stable supply of carbon (Kölling et al., 2015). In our results, almost all growth and gas exchange variables evaluated (except for gs) were influenced by all variation factors, which indicates that there is a constant dynamic of

metabolic processes that influence resource allocation for growth and/ or reproduction of coffee trees, both in time and space.

4.1 Temporal variation

During the study period, there were some trends and dynamics in the data related to the phenology of coffee trees reported by Camargo and Camargo (2001). Recalling, the period spanned 17 months between December 2016 and October 2018 spanning two years of production (Figure 3). It is important to consider that the 2016/2017 season was characterized as a year of positive bienniality, therefore the 2017/2018 season was a year of negative bienniality (CONAB, 2022).

Formation, filling and ripening of fruits (S1 to S6)

Starting with the chronology, the trees started to be sampled in the period of formation and filling of the fruits for the harvest in mid-2017. That year, there was an allocation of biomass to fruits of approximately 40%, compared with only 5% that was allocated in 2018. In this sense, it is possible to see how the values of the leaf variables LN, LA and LDM and the variables of the NPB, PBL and BDM branches were lower in 2017, when there was a high fruit load, compared with 2018 in which it was presented a new growing season. These lower values demonstrate the priority of trees in allocating resources in the formation and filling of fruits, with the highest values for TNF and FDM in samplings 5 and 6 (Table 2). The fruit formation, filling and ripening stage was accompanied by some of the highest photosynthetic rates (Table 6).

It has been reported for both coffee and other woody species and fruit species from the tropics, subtropics and temperate climates that fruits are dominant sinks against vegetative structures (DaMatta et al., 2007; Kozlowski, 1992; Rosati et al., 2018; Samach and Smith, 2013a; Smith and Samach, 2013b). This is demonstrated by preferential movement of stored carbohydrates and current photosynthate to rapidly growing reproductive tissues. In the results of chapter 4, it is possible to see that most of the evaluated NSC are found in greater quantity in the fruits (Table 13) and when the two factors are split together - samplings and plant organs - for all evaluated biochemical properties except for sucrose , the highest values are presented in the fruits in samplings 6 and 15, close to the harvest in the two years evaluated (data not shown).

The ability of reproductive structures to import carbohydrates varies with factors such as age, vigor, species, fruit growth characteristics, etc. (Kozlowski, 1992). Since the sink strength of developing fruits changes seasonally, the import of carbohydrates changes with variations in fruit growth rates, increasing the import with the grain growth and filling process, which can be observed by the gain in dry matter between S2 and S6 and between S11 and S16 (Table 2). The sampled trees were 6-7 years old trees that have already gone through the juvenile stage, being actively productive, showing this alternation between the allocation of C to vegetative and reproductive structures between one year and another. The co-occurrence of the vegetative and reproductive phases leads to a biennial pattern, in which the high fruit load in one year predisposes the trees to low yields in the next harvest, mainly because of a concomitant imbalance in the formation of leaf area, fewer new flowering nodes and presumably because of fewer flowers per node (Alves et al., 2011; Bote and Jan, 2016; DaMatta et al., 2007; Wilkie, Sedgley, and Olesen, 2008).

When correlated with climate (Figure 8), the positive correlation of RH with TNF and the negative correlation of Evap with TNF and FDM suggest that the water factor has great relevance in the process of fruit formation and ripening. It has been reported that rain is a key ecological factor in determining the interval between flowering and seed maturation, and water scarcity affects fruit growth mainly in the rapid expansion phase, so the ovules do not reach their potential full size (Cannell, 1974, 1985; DaMatta et al., 2007). Although we did not have significant correlations directly with Prec, the positive correlation with RH and negative with Evap suggest that an increase in soil evaporation can affect the TNF, as well as their dry matter, and a greater degree of relative humidity in the environment can favor the process of growth and expansion. In addition, at this time of fruit expansion, high transpiration rates were presented (Table 6), possibly due to the high temperatures of these months, with increases in Evap favoring the loss of soil moisture.

Quiescent phase (S7 to S8 and S17)

Continuing the chronology, in the quiescent phase – S7 to S8 – the lowest values were presented for most of the variables: LN, LA, LDM, TNF and DMF. At this time of year, the lowest temperatures are present, as well as the lowest precipitation rates, which triggers

decreasing growth rates, leaf fall and possibly a drop in photosynthetic rates such as those presented in S6, a sampling that precedes the quiescent phase.

This phase is important for some physiological processes of the plant, as the short period and drought stimulates the flowering process and the formation of a new growth ring. The formation of these rings is the result of the exchange activity of the tree between the vegetative period and the quiescent phase. In ecosystems with climatic seasonality, plants produce cyclical growth patterns, due to a period of seasonal stress that induces dormancy of the exchange meristem, interrupting growth in diameter and inducing the formation of growth rings (Alves and Angyalossy-Alfonso, 2000; Nath et al., 2016; dos Santos Silva et al., 2017; Worbes, 2002).

In the published results for secondary growth we find that each new ring started to form at the start of the rainy period after the dry season, which in the region generally lasts more than 3 months (May-August), which is enough to invoke a dormancy which triggers the formation of growth rings (Toro-herrera et al., 2021). This means that the process is directly influenced by the climate just as shown by some of the correlations obtained between the climatic variables and the radial growth rate (Figure 13). So, for this time of year, the correlations show that the increase of sunlight hours may have promoted an increase in ETo that induces a decrease in the growth ring area. Likewise, the increase in HR promotes less ETo, and less negative influence in the ring area.

On the other hand, it is also possible that this is a time when the greatest accumulation of reserves occurs in structures such as branches. Although storage has traditionally been thought of as a passive process/sink and the fraction of C allocated to storage in relation to structural growth and metabolism may be minimal, on an annual basis, over time this fraction typically accumulates as NSC. Thus, storage pools in mature trees become large and can provide a large fraction of C needed for growth in certain situations of starve and/or environmental stresses (Dietze et al., 2014; Kozlowski, 1992; Sala et al., 2012). In recent years, the view has shifted towards considering storage as a strong sink, which can be an active or semi-active process. Active when up-regulation of storage occurs at the expense of growth, even with favorable conditions for it, and semi-active when storage occurs due to down-regulation of growth (Chapin F S, 1990; Dietze et al., 2014). This subject will be discussed further in chapter 4.

New vegetative phase (S9 to S16)

The new season characterized by negative bienniality comprised the new vegetative growth after a high fruit load. The coffee tree has an abundant floral initiation with a low rate of fruit abscission, so that with the force of the sink (the endosperm of the seeds is a primary sink) there is an imbalance in the leaf/fruit ratio and, as a consequence, a competition between reproductive and vegetative growth (Chaves et al., 2012) As a consequence, the following year the production is lower as shown by the lowest values of TNF and FDM in 2018 (Table 2).

The production of nodes in the lateral branches and the formation of leaves are parallel to the oscillations in the growth of the plagiotropic branches (DaMatta et al., 2007). The NPB as well as its length – PBL – increased throughout the experimental period, as well as the growth in height (Table 2). Thus, with the new growth of plagiotropic branches, in 2018 there were higher values for all leaf and branch characteristics: number, area and dry matter; accompanied by higher photosynthetic rates (Table 6). The new vegetative growth coincides with the beginning of the rains in the month of September – October (S9 and S10), being the leaf growth rates and the increase in leaf area characteristic that vary seasonally. Consequently, there is also leaf fall in the dry season, which usually coincides with the harvest and post-harvest periods. When correlated with climate (Figure 8), the negative correlation between wind speed and LN and LA indicate that strong winds may have an influence on this leaf fall process.

Additionally, negative correlations for leaf variables with Tmed, Tmin, Evap, ETo suggest that increases in soil evaporation and plant evapotranspiration depending on the time of year can affect leaf growth and expansion rates, as well as increases in minimum temperature in the months traditionally with higher temperatures they can also interfere negatively.

4.2 Spatial variation

The main objective of the cultivation of perennial fruit trees is to promote the transport of photoassimilates to the fruits, the main product of economic importance. During each new growing season the growth center changes with plant development, promoting a strong ability to transport photoassimilates between different areas of the tree (Sadar et al., 2016). However, the distribution patterns of photoassimilates between sources and sinks are complex and diverse among species. Due to the different ages and characteristics of the branches, the photosynthetic

and nutrient transport capacity of the leaves in each of these types are different, depending on their contribution to fruit growth and development (Fanwoua et al., 2014; Sha et al., 2021; Yang et al., 2019). Thus, knowledge of the spatial variation of growth characteristics and gas exchange can help to understand these patterns between sources and sinks.

In our results, there was an increasing trend for most vegetative growth variables among the thirds (Table 2). The highest values in the lower third may be due to the longevity of this area of the tree, which has older and longer branches with more buds and leaves. However, the fact that this third has, for example, more leaves or leaves with greater area, does not necessarily mean that they are more productive or photosynthetically active. This can be demonstrated by the values of TNF and FDM that are higher in MT, commonly known as the most productive third due to the characteristic of the leaves. These values are supported by higher photosynthetic and transpiration rates in the same third (Table 6).

In other types of fruit trees such as apple, cherry, and melon, it has been shown that different types of leaves have different growth characteristics and contributions to fruit growth and development. Thus, photoassimilates from younger and vegetative branches (like those characteristic of UT) are mainly self-consumed to support growth with poor transferability. Meanwhile, in the middle region of the tree, the synthesis of photoassimilates from the leaves is in good agreement with its photosynthetic intensity, transporting the photoassimilates to the fruits in greater abundance. This also indicates that the distance between leaves and fruits significantly affects the transport of photoassimilates and corroborates that fruits are strong sinks, driving the movement of photoassimilates from sources (Ayala and Lang, 2018; Barzegar et al., 2013; Sha et al., 2021).

These results agree with the correlations with the climate in which the main influenced variables were the leaf variables LN, LA and LDM in the thirds LT and MT, where the highest number of fruits were found to be concentrated. This supports the idea of being the main sources for the growth of these fruits. The main variables that influenced these leaf variables (Figure 9), as well as gas exchange (Figure 16) were associated with the water factor - Evap and ETo - with mean air temperature and wind speed. The importance of these climatic variables in the process of fruit growth and expansion, and in leaf longevity, affecting leaf fall, has already been discussed.

Among the sections, there was no clear trend between the variables, only showing that both TNF and FDM had higher values in section I of the plagiotropic branches (Table 2). However, it was section D - the youngest - that had the highest photosynthetic and transpiration rates (Table 6), as well as the greatest correlation dynamics with the climatic variables (Figure 10, Figure 17). This may be due to the fact that it is the region most exposed to light, with less shading between the leaves, especially in trees with dense crowns where the leaves of the branches located in the interior have lower photosynthetic rates (Fanwoua et al., 2014). The photoassimilates from this region may have been self-consumed to support the growth of new branches and leaves or also allocated to section I with more fruits. This second option is based on the leaf/fruit ratio that has been reported to influence the direction and magnitude of carbon flux (Fanwoua et al., 2014). Since section I has a lower ratio (SI:2.20 < SD: 6.38 < SP: 10.23 - calculated data from Table 2), it would be possible that this promotes the allocation of C in this region of the branch coming from the others. This can also apply to the thirds, with the MT being the one with the lowest ratio.

5 CHAPTER HIGHLIGHTS

1. It is important to know how coffee trees adjust their metabolic processes to survive in a rapidly changing climate. Understanding carbon allocation and the source-sink relationship is vital to understanding how resources are distributed between growth and reproduction.
2. The growth and reproduction data showed the dynamics of bienniality that is present in the region with a high fruit load followed by a lower one. In a specific way, this dynamic represents a negative correlation between growth and reproduction.
3. Reproductive structures have a high capacity to import carbohydrates, constituting strong competing sinks for C that could be allocated to other types of structures and/or metabolic processes.
4. The growth and reproduction variables evaluated have a high influence of seasonality, showing high compatibility with the reported phenology for the coffee tree.
5. The most dynamic regions of the tree were the middle and lower thirds and the intermediate and distal sections.

6. The main climatic variables that influenced vegetative/reproductive growth and gas exchange were evaporation, evapotranspiration, wind speed and, in some cases, minimum temperature.
7. Dendrochronology and the use of growth rings dimensional parameters is a tool that allows indirect, but long-term, assessment of biomass allocation and growth in coffee trees.

REFERENCES

ALVES, E. S.; ANGYALOSSY-ALFONSO, V. Ecological trends in the wood anatomy of some Brazilian Species. 1. Growth rings and vessels. **IAWA Journal**, v. 21, n. 1, p. 3–30, 2000.

ALVES, J. D. et al. Manipulação da relação fonte-dreno em Coffea arabica L. e seu efeito no crescimento da parte aérea e do sistema radicular. **Ciencia e Agrotecnologia**, v. 35, n. 5, p. 956–964, 2011.

AYALA, M.; LANG, G. Current season photoassimilate distribution in sweet cherry. **Journal of the American Society for Horticultural Science**, v. 143, n. 2, p. 110–117, 2018.

BABST, F. et al. Above-ground woody carbon sequestration measured from tree rings is coherent with net ecosystem productivity at five eddy-covariance sites. **New Phytologist**, v. 201, n. 4, p. 1289–1303, 2014.

BARZEGAR, T. et al. 13C-labelling of leaf photoassimilates to study the source-sink relationship in two Iranian melon cultivars. **Scientia Horticulturae**, v. 151, p. 157–164, 2013.

BEADLE, C. L. Chapter 2: Plant Growth Analysis. **Techniques in Bioproductivity and Photosynthesis**, p. 20–25, 1985.

BOTE, A. D.; JAN, V. Branch growth dynamics, photosynthesis, yield and bean size distribution in response to fruit load manipulation in coffee trees. **Trees - Structure and Function**, v. 30, n. 4, p. 1275–1285, 2016.

CAMARGO, A. P.; CAMARGO, B. P. Definição e Esquematização das Fases Fenológicas do Cafeeiro Arábica nas Condições Tropicais do Brasil. **Bragantia**, v. 60, n. 1, p. 65–68, 2001.

CANNELL, M. G. R. Factors affecting Arabica coffee bean size in Kenya. **Journal of Horticultural Science**, v. 49, n. 1, p. 65–76, 1974.

CANNELL, M. G. R. Physiology of the Coffee Crop. **Coffee**, p. 108–134, 1985.

CHAPIN F S. The ecology and economics of storage in plants. **Annual Review of Ecology, Evolution, and Systematics**, v. 21, p. 423–427, 1990.

CHAVES, A. R. M. et al. Varying leaf-to-fruit ratios affect branch growth and dieback, with little to no effect on photosynthesis, carbohydrate or mineral pools, in different canopy positions of field-grown coffee trees. **Environmental and Experimental Botany**, v. 77, p. 207–218, 2012.

COMPANHIA NACIONAL DE ABASTECIMENTO - CONAB. Acompanhamento da Safra Brasileira. Café. 1° Levantamento 2022. v. 9, n. 1, p. 1–61, 2022.

DAMATTA, F. M. et al. Ecophysiology of coffee growth and production. **Brazilian Journal of Plant Physiology**, v. 19, n. 4, p. 485–510, 2007.

DIETZE, M. C. et al. Nonstructural carbon in woody plants. **Annual Review of Plant Biology**, v. 65, n. November, p. 667–687, 2014.

DING, J.; NILSSON, O. Molecular regulation of phenology in trees-because the seasons they are

a-changin'. **Current Opinion in Plant Biology**, v. 29, n. Figure 1, p. 73–79, 2016.

DOS SANTOS SILVA, M. et al. Growth rings in woody species of Ombrophilous Dense Forest: occurrence, anatomical features and ecological considerations. **Revista Brasileira de Botanica**, v. 40, n. 1, p. 281–290, 2017.

FANWOUA, J. et al. The role of branch architecture in assimilate production and partitioning: The example of apple (Malus domestica). **Frontiers in Plant Science**, v. 5, n. JUL, 2014.

GEA-IZQUIERDO, G. et al. Modelling the climatic drivers determining photosynthesis and carbon allocation in evergreen Mediterranean forests using multiproxy long time series. **Biogeosciences**, v. 12, n. 12, p. 3695–3712, 2015.

GESSLER, A.; GROSSIORD, C. Coordinating supply and demand: plant carbon allocation strategy ensuring survival in the long run. **New Phytologist**, v. 222, n. 1, p. 5–7, 2019.

HUANG, J. et al. Eyes on the future – evidence for trade-offs between growth, storage and defense in Norway spruce. **New Phytologist**, v. 222, n. 1, p. 144–158, 2019.

HUNT, R. **Basic Growth Analysis**. London: [s.n.].

HUNT, R. et al. A modern tool for classical plant growth analysis. **Annals of Botany**, v. 90, n. 4, p. 485–488, 2002.

KÖLLING, K. et al. Carbon partitioning in Arabidopsis thaliana is a dynamic process controlled by the plants metabolic status and its circadian clock. **Plant, Cell and Environment**, v. 38, n. 10, p. 1965–1979, 2015.

KÖRNER, C. Paradigm shift in plant growth control. **Current Opinion in Plant Biology**, v. 25, p. 107–114, 2015.

KOZLOWSKI, T. T. Carbohydrate sources and sinks in woody plants. **The Botanical Review**, v. 58, n. 2, p. 107–222, 1992.

MBOW, C. et al. Potential of dendrochronology to assess annual rates of biomass productivity in savanna trees of West Africa. **Dendrochronologia**, v. 31, n. 1, p. 41–51, 2013.

NATH, C. D. et al. Growth rings in tropical trees: role of functional traits, environment, and phylogeny. **Trees - Structure and Function**, v. 30, n. 6, p. 2153–2175, 2016.

PEZZOPANE, J. R. M. et al. Metodologia e técnica experimentais. **Bragantia**, v. 62, n. 3, p. 499–505, 2003.

RIGHI, C. A. Avaliação ecofisiológica do cafeeiro (Coffea arabica L.) em sistema agroforestal e em monocultivo. **Tese de Doutorado**, p. 113, 2005.

ROSATI, A. et al. Resource investments in reproductive growth proportionately limit investments in whole-tree vegetative growth in young olive trees with varying crop loads. **Tree Physiology**, v. 38, n. 9, p. 1–11, 2018.

SADAR, N. et al. Development and distribution of quality related compounds in apples during growth. **Scientia Horticulturae**, v. 213, p. 222–231, 2016.

SALA, A.; WOODRUFF, D. R.; MEINZER, F. C. Carbon dynamics in trees: Feast or famine? **Tree Physiology**, v. 32, n. 6, p. 764–775, 2012.

SAMACH, A.; SMITH, H. M. Constraints to obtaining consistent annual yields in perennials. II: Environment and fruit load affect induction of flowering. **Plant Science**, v. 207, p. 168–176, 2013.

SEVANTO, S.; DICKMAN, L. T. Where does the carbon go?-Plant carbon allocation under climate change. **Tree Physiology**, v. 35, n. 6, p. 581–584, 2015.

SHA, J. et al. Characteristics of Photoassimilates Transportation and Distribution to the Fruits from Leaves at Different Branch Positions in Apple. **Journal of Plant Growth Regulation**, v. 40, n. 3, p. 1222–1232, 2021.

SMITH, H. M.; SAMACH, A. Constraints to obtaining consistent annual yields in perennial tree crops. I: Heavy fruit load dominates over vegetative growth. **Plant Science**, v. 207, p. 158–167, 2013.

STOKES, M. A.; SMILEY, T. L. **An introduction to tree ring dating**. Tucson, AZ: The University of Arizona Press. 1968.

THOMAS, H.; OUGHAM, H. On plant growth and form. **New Phytologist**, v. 216, n. 2, p. 337–338, 2017.

TORO-HERRERA, M. A. et al. On the use of tree-ring area as a predictor of biomass accumulation and its climatic determinants of coffee tree growth. **Annals of Applied Biology**, n. August 2020, p. 1–15, 2021.

TRUMBORE, S.; BRANDO, P.; HARTMANN, H. Forest health and global change. **Science**, v. 349, n. 6250, p. 814–818, 2015.

USDA FOREIGN AGRICULTURAL SERVICE. Coffee: World Markets and Trade. **Coffee: World Markets and Trade**, n. December, p. 1–9, 2021.

WILKIE, J. D.; SEDGLEY, M.; OLESEN, T. Regulation of floral initiation in horticultural trees. **Journal of Experimental Botany**, v. 59, n. 12, p. 3215–3228, 2008.

WORBES, M. One hundred years of tree-ring research in the tropics - A brief history and an outlook to future challenges. **Dendrochronologia**, v. 20, n. 1–2, p. 217–231, 2002.

YANG, S. et al. Branch age and angle as crucial drivers of leaf photosynthetic performance and fruiting in high-density planting: A study case in spur-type apple “Vallee Spur” (Malus domestica). **Scientia Horticulturae**, v. 246, n. November 2018, p. 898–906, 2019.

CHAPTER 3: STABLE ISOTOPIC ANALYSIS – FLUX VIEW

ABSTRACT

Stable isotope signatures of carbon and nitrogen are often used as markers to measure the effect of climate change on various chemical, physical, and biological processes. Thus, the values of the isotopic composition of carbon ($\delta^{13}C$) and nitrogen ($\delta^{15}N$), reflect the interaction between all aspects of the carbon/water and nitrogen relationships, allowing to unravel the mechanisms of their differential investment under different environments. In this context, the aim of this chapter was to evaluate the spatio-temporal variation of source-sink patterns of coffee trees under field conditions in response to climatic conditions through the assessment of the isotopic ratio of carbon and nitrogen. For this purpose, six samplings were selected for which data on C and N percentages, C/N ratio and C and N isotopic composition ($\delta^{13}C$ and $\delta^{15}N$) were collected in the distal section of the three thirds of the tree. Additionally, data on the percentage of C and $\delta^{13}C$ were collected for the growth rings of the basal portion of the orthotropic branch. The analyzes were conducted at the Center for Stable Isotopes, part of the Biosciences Institute at São Paulo State University (UNESP), Botucatu – SP, Brazil. The results obtained were correlated with the climatic variables of the region through a Pearson correlation analysis ($p<0.05$). In temporal terms, there were no significant differences for $\delta^{13}C$ values, with an average of -27.73‰, traditional values of a C3 plant. In turn, the values of $\delta^{15}N$ showed differences between the collections, with a significantly higher value in S2 - 6.36‰ - probably due to the fertilization of the experimental plot. In spatial terms, heterotrophic tissues (stems and fruits) tended to be enriched in $\delta^{13}C$ compared do leaves, showing values of -27.02‰, -27.20‰ and -28.75‰, respectively. Also, there was an enriched values of $\delta^{15}N$ for the leaves and fruits in relation to stems, showing values of 4.23‰, 4.41‰ and 3.40‰, respectively. In addition, there was a vertical pattern with the lower third being depleted in $\delta^{13}C$ and $\delta^{15}N$ in relation to the upper third, with differences of up to 2.30‰ for C and 0.67‰ for N between the LT and UT. These spatial patterns reflect the use of different sources of C and N such as C derived from soil respiration or refixed after plant respiration; as well as the assimilation of N from a reservoir that has already been exposed to assimilation. Isotopic analyzes on the tree growth rings showed that there are no differences for the same ring of individual plants since they are formed in the same season under the same climatic conditions. However, there are intra-ring differences for the same plant due to being formed under different climatic conditions, with precipitation being the main climatic determinant that influences the fixation and discrimination against C. With these results, it is possible to highlight the importance of this method to characterize how the temporal and spatial patterns of $\delta^{13}C$ and $\delta^{15}N$ emerge and signal the influence of climate on the source-sink relationship of coffee trees under field conditions.

Keywords: Stable isotopes. Isotopic discrimination. Climatic signals. Autotrophic vs heterotrophic tissues. Growth rings.

1 INTRODUCTION

The current climate outlook and the widespread recognition of increasing atmospheric CO_2 concentration and associate climate variability (changes in temperature and precipitation patterns), highlighted the need for an understanding of carbon exchange dynamics by natural ecosystems and productive crops (Rascher, Máguas, and Werner, 2010; Scartazza et al., 2015). For this purpose, the analysis of stable isotopes constitutes a useful tool to identify the processes that control the dynamics of the carbon (C) and nitrogen (N) flow, allowing to unveil the mechanisms of their differential investment in plants under different environments (Dawson et al., 2002). The simple and rapid method to determine isotope ratios in various plant materials has promoted the vast utilization of this parameter in a wide range of ecological and physiological studies. For studying C and N balance and allocation (Brüggemann et al., 2011; Dersch et al., 2016; Wegener, Beyschlag, and Werner, 2015), for tracing biogeochemical processes at ecosystem level and over ecological to geological time scales (Dubbert, Rascher, and Werner, 2012; Stein, Sheldon, and Smith, 2021), to assess physiological responses of plants to environmental stresses (Hussain, Al-Dakheel, and Reigosa, 2018), to discriminate and authenticate the origin of products of plant origin (Carter, Yates, and Tinggi, 2015; Liu et al., 2014; Rodrigues et al., 2009), among others.

Chemical, physical, and biological processes generate specific isotopic ratios that can be determined through isotopic discrimination. From the knowledge of fractionation processes, it has been postulated that generally, leaves are isotopically lighter than the other plant organs due to a generic difference between autotrophic (sources - gaining energy from photosynthesis) and heterotrophic (sinks - gaining energy from respiration of organic molecules) organs (Lucas A. Cernusak et al., 2009). And this isotopic pattern has been observed for woody stems (Rascher et al., 2010; Saveyn et al., 2010), roots (Scartazza et al., 2015), seeds (Behboudian et al., 2000; Cernusak et al., 2009) and fruits (Cernusak et al., 2009; Cernusak, Pate, and Farquhar, 2002), incapable of net CO_2 fixation. This difference can be explained by post-photosynthetic fractionation processes such as export / import of photoassimilates and cellular respiration. These processes can alter the isotopic signature of different plant materials, explaining the variation in the abundance of ^{13}C and ^{15}N between the organs of the plant (Badeck et al., 2005; Dubbert et al., 2012; Gessler et al., 2009).

Thus, given the direct relationship between isotopic ratios with climatic conditions and the physiology of the plant during its growth and development, it is proposed to use this technique to characterize the source-sink relationship in different coffee tree organs in field conditions in response to the climate. We hypothesize that the variations in the isotopic composition of carbon ($\delta^{13}C$) and nitrogen ($\delta^{15}N$) in the coffee organs (autotrophic vs. heterotrophic), reflecting the differential use of atmospheric C and N assimilated from the soil, versus C and N relocated from other parts of the plant. To test the hypothesis, specifically, we identify the variation of the isotopic values and the percentages of C and N over time in response to climate for (1) the three organs evaluated; (2) the different portions of the trees; and (3) the growth rings of the basal portion of the orthotropic branch.

2 REVIEW

Each chemical element is defined by the number of protons (Z) present in the nucleus of its atom. In turn, the number of neutrons (N) present within the nucleus can vary, thereby changing the atomic mass (A) of a given element (A = N + Z). Isotopes are defined as atoms of the same chemical element, but with a different number of neutrons, and consequently, with a different number of mass (Caxito and Silva, 2015; Sharp, 2017).

Stable isotopes are those that occur commonly in nature in an almost constant proportion (^{12}C (98,893%), ^{13}C (1,107%), ^{14}N (99,634%) and ^{15}N (0,366%)); in contrast to radioactive isotopes that are unstable and are found in very small amounts, such as ^{14}C (0,01% occurrence). The relative amount of a particular isotope in a sample is represented by the ratio of this isotope and another stable isotope of the same element (δ). δ values are reported in comparison to an internationally recognized standard:

$$\delta = \left[\frac{(R_{sample} - R_{standard}}{R_{standard}}\right] * 1000$$

R_{sample} being the isotopic ratio measured in the sample and $R_{standard}$ the same ratio in the standard. A positive value of δ indicates that the sample has an isotopic ratio greater than the standard and a negative value indicates the opposite (Pereira and Benedito, 2007; Sharp, 2017).

Chemical, physical, and biological processes generate specific isotopic ratios that can be determined by isotopic discrimination, considering changes in the relative abundances of isotopes between reagents and products (isotopic fractionation) (Brüggemann et al., 2011; Farquhar, Ehleringer, and Hubic, 1989). When an element or molecule gets involved in a reaction, the lighter isotope forms weaker atomic bonds than the heavier isotope, being more reactive and concentrating on the products of the reaction; while the heavy isotope, concentrates on the reagents (Caxito and Silva, 2015). In photosynthesis, for example, the degree of fractionation depends on the isotopic composition of the carbon source and its availability in the environment where the plant grows.

In contrast to techniques that provide measurements of gas exchange or photosynthetic rates in a single time, the values of $\delta^{13}C$ and $\delta^{15}N$, reflect the interaction between all aspects of the plant's carbon / water and nitrogen ratios. This highlights the importance of research with stable isotopes to characterize how species adjust their gas exchange metabolism, strategies for the acquisition and use of resources and life history patterns to ensure competitiveness and survival in each habitat (Dawson et al., 2002). The measurement of the isotopic composition is done using isotopic ratio mass spectrometers.

This equipment is based on the principle of deflecting an energetic ion beam and focused on a magnetic / electrostatic field. The degree of deflection is a function of mass and charge, and the relative intensities of ion beams of different masses are used to calculate isotopic ratios. The spectrometer consists of three primary components: a source, where a sample is ionized, accelerated to a certain energy, and collimated into a well-focused beam; the analyzer, which acts to deflect the ion as a function of mass; and the collector set to measure the relative intensities of the different ion beams (Sharp, 2017).

2.1 Carbon isotopic discrimination

Carbon has two stable isotopes: ^{13}C and ^{12}C. Atmospheric CO_2 ($\delta^{13}C$ around 8 ‰) assimilated during photosynthesis by the plant undergoes isotopic fractionation, and the degree of fractionation reflects the specific photosynthetic cycle used for carbon fixation (C3, C4 or CAM) (Brüggemann et al., 2011; Farquhar, Ehleringer, and Hubic, 1989). Thus, the differences in the ratio between ^{13}C and ^{12}C present in these plants reflect the isotopic fractionation processes,

which determine discrimination, against or in favor of ^{13}C. Isotopic compositions are expressed as $\delta^{13}C$ (‰) values (Caxito and Silva, 2015).

Fractionation can vary in response to soil moisture, irradiance, availability of nutrients, CO_2 concentration, among others. Thus, all the factors (ontogenetic or environmental) affecting the diffusion of CO_2 and/or the photosynthetic capacity, can change the photosynthetic discrimination (Badeck et al., 2005). In addition, morphological characteristics impose restrictions on the physiological response to these various environmental conditions through their influence on factors such as resistance of the leaf's border layer, hydraulic conductivity through the xylem and internal resistance of the leaf to CO_2 and H_2O (Dawson et al., 2002; Dawson and Siegwolf, 2007).

In C3 plants, discrimination against ^{13}C occurs in the diffusion of CO_2 through stomata to chloroplasts, due to the carboxylation action of Rubisco and the difference in external and internal CO_2 concentrations (Farquhar, Ehleringer, and Hubic, 1989). The C4 plants, moreover, present the fractionation in the formation of HCO^{-3} and its incorporation by phosphoenolpyruvate carboxylase - PEPCase, in addition to the factor ϕ that represents the rate of CO_2 that escapes from the bundle-sheath cells and may or may not be reincorporated, occurring in these phases, discrimination in favor of ^{13}C. Therefore, plants of the C3 cycle species are poorer at ^{13}C, compared with the plants of the C4 cycle (Dawson et al., 2002; Ducatti et al., 2011).

The discrimination against ^{13}C by Rubisco is linked to photosynthesis through the relationship between the internal and the atmospheric concentration of CO_2 (Ci / Ca). This relationship reflects the relative magnitudes of liquid assimilation (*A*) and stomatal conductance (*gs*) related to CO_2 supply and demand. Therefore, ^{13}C data is a useful index to assess the intrinsic efficiency of water use, defined as the relationship between assimilated carbon and water vapor losses due to stomatal conductance (Dawson et al., 2002; O'Learly, Madhavan, and Paneth, 1992; Rodrigues et al., 2009).

2.2 Nitrogen isotopic discrimination

Nitrogen (N) has two stable isotopes: ^{15}N (0,3663%) and ^{14}N (99,6337%). Fraction occurs through a kinetic process during assimilation in which the heavier isotope (^{15}N) is "broken down", causing a greater fraction of the lighter isotope (^{14}N) to be incorporated in the product.

Nitrate reductase (NR) and glutamine synthetase (GS), the two enzymes necessary for the assimilation of nitrate and ammonium, respectively, are responsible for the discrimination of N isotopes. Isotopic compositions are expressed as $\delta^{15}N$ (‰) values (Hobbie and Högberg, 2012; Kalcsits, Buschhaus, and Guy, 2014).

The N source and the assimilation patterns influence the $\delta^{15}N$ values in the plant. NH_4^+ is assimilated immediately at the root, so the organic N in the aerial part and at the roots is the product of a single assimilation event. In turn, the assimilation of $NO3^-$ can occur both in the roots and in the aerial part, and the fractionation during the assimilation by NR makes the $\delta^{15}N$ of $NO3^-$ enriched in relation to organic nitrogen. The $\delta^{15}N$ of the leaves can be greater than the $\delta^{15}N$ of the roots because the $NO3^-$ available for assimilation is enriched, as it can originate from a pool that has already been exposed to assimilation (Evans, 2001; Kalcsits, Buschhaus, and Guy, 2014).

Also, the reallocation of N during growth causes differences between the organs because most reactions discriminate against ^{15}N. Thus, NO_3^- reduction reactions, GS-GOGAT reactions, transamination and other enzymatic reactions result in products with lower $\delta^{15}N$ values than the original source (Evans, 2001). Thus, the $^{15}N/^{14}N$ isotope ratio has the potential to provide integrated information about the flow process, assimilation, and allocation of N.

3 METHODOLOGY

The isotopic analyzes were conducted at the Center for Stable Isotopes, part of the Biosciences Institute at São Paulo State University (UNESP), Botucatu – SP, Brazil. Initially, the samples were prepared for isotopic determination ($\delta^{13}C$ and $\delta^{15}N$) and elemental contents (C, N and C/N ratio). Leaves, stems, and fruits of the distal region in the upper, middle, and lower thirds (Figure 18a) from samplings 2, 6, 8, 11, 15 e 17 were separated and identified for drying in an oven with forced air circulation at 65º C for 72 hours until constant weight was obtained.

Later they were ground in a hammer mill (MA-090CF, Marconi, Piracicaba- SP, Brazil) with a sieve until reaching a particle size of less than 1mm. The powder obtained from the mill was passed through a sieve of 250 µm (NBR NM 3310-1, SoloTest, São Paulo- SP, Brazil) to further reduce the particle size. Additionally, the basal section of the orthotropic stem with the

growth rings was drilled on one of its three axes with a drill bench (FB13, Schulz, Joinville- SC, Brazil). Consecutive holes were drilled from the medulla to the bark, so that each hole encompassed at least one growth ring. The contents of each hole were deposited in an Eppendorf, with the shank and drill being sanitized between one hole and another (Figure 18b).

Figure 18 - Regions sampled for isotope ratio analysis. (a) Samples of leaves, stems and fruits were selected from the distal region in the three thirds of the tree (b) The content obtained from the growth rings of the most basal portion of the orthotropic stem with a drill

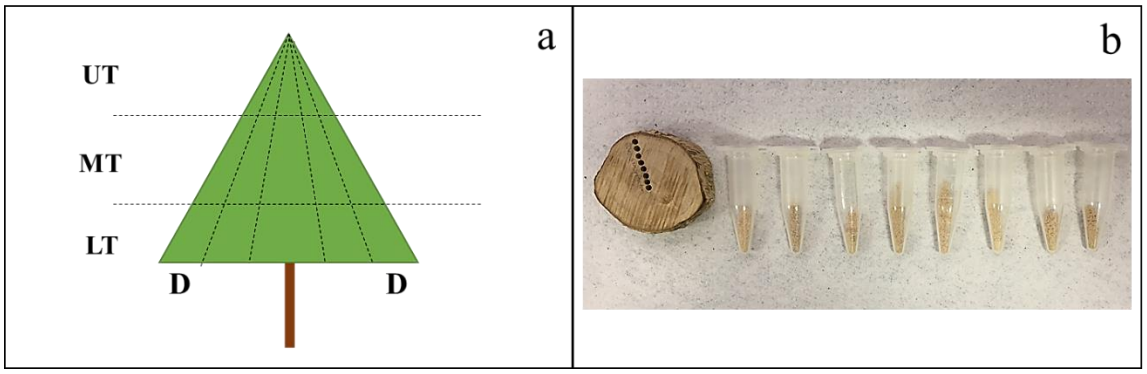

Source: From the author (2022).

There, all the samples were weighed in tin cups (standard weight 5 x 3.5 mm), weight being dependent on the %C and %N of the sample material (50-70 µg for C and 4000-5000 µg for N). The tin capsules were placed and burned in the Flash 2000 Elemental Analyzer (Thermo Fisher Scientific Inc., Bremen, Germany) to obtain CO_2 and N_2. The gases were separated in a gas chromatography column and analyzed in the Delta V Advantage isotope ratio mass spectrometer (Thermo Fisher Scientific Inc., Bremen, Germany) with an interface ConFlo IV Universal (Thermo Fisher Scientific Inc., Bremen, Germany) (Figure 19). In total 48 samples were analyzed (6 samplings x 3 thirds x 3 organs), being that sampling 8 and 17 do not have fruit samples. From the basal section of the orthotropic stem were analyzed 36 samples.

For each sample, the C and N contents (%), the C/N ratio and the isotope ratio (R_{sample} = $^{13}C/^{12}C$ and $^{15}N/^{14}N$) were determined. The ^{13}C and ^{15}N values in isotopic delta ($\delta^{13}C$ - $\delta^{15}N$,

expressed in ‰) were expressed relative to an international standard and were calculated according to the following equations (Coplen, 2011; Craig, 1953):

$$‰\ \delta^{13}C = \left[\frac{(R_{sample} - R_{PDB}}{R_{PDB}}\right] * 1000$$

$$‰\ \delta^{15}N = \left[\frac{(R_{sample} - R_{air}}{R_{air}}\right] * 1000$$

where R_{sample} are the $^{13}C/^{12}C$ and $^{15}N/^{14}N$ ratio in the sample, R_{PDB} is the $^{13}C/^{12}C$ ratio of V-PDB as an international standard for carbon and R_{air} is the $^{15}N/^{14}N$ ratio of atmospheric air as an international standard for nitrogen (Werner and Brand, 2001).

Figure 19 - (a) Analytical balance used for weighing the samples (b) Elemental analyzer coupled to the isotope ratio mass spectrometer with an interface ConFlo IV Universal

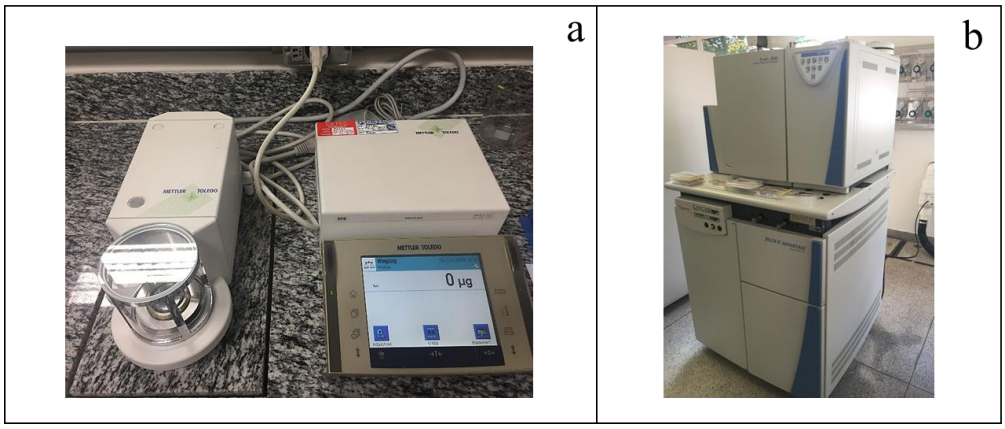

Source: From the author (2022).

4 RESULTS

The five variables were analyzed considering all the variation factors (samplings – S, thirds – Th, organs – O, and the interactions between them). As there is only one repetition for the triple combination of factors (S x Th x O), three two-way ANOVA were made to know the influence of all factors on the response variables (Table 8). The C percentage was significantly influenced ($p < 0.05$, F-test) just by the double interaction between sampling and organs. The N

percentage was significantly influenced ($p < 0.05$, F-test) by the samplings and organs individually. The isotopic ratio of C ($\delta^{13}C$) was significantly influenced ($p < 0.05$, F-test) by the organs and thirds also for each factor in an individual way. The isotopic ratio of N ($\delta^{15}N$) and the C/N ratio were significantly influenced ($p < 0.05$, F-test) by the samplings and organs. In none of the double interactions there was any significant difference except for the C%.

Table 8 - F-values and significance levels in two-way ANOVA of isotopic variables of samples from coffee plants in production evaluated in 6 samplings over time and sampled in 9 regions distributed in thirds and sections along the tree.

Factor	C (%)	N (%)	$\delta^{13}C$ (‰)	$\delta^{15}N$ (‰)	C/N ratio
Sampling (S)	1.970 ns	6.732 ***	0.984 ns	60.514 ***	4.590 **
Organs (O)	0.306 ns	174.221 ***	12.280 ***	17.660 ***	91.098 ***
S x O	2.791 *	1.669 ns	0.326 ns	1.091 ns	1.501 ns
Sampling (S)	1.517 ns	0.531 ns	1.013 ns	34.528 ***	0.653 ns
Third (Th)	0.421 ns	0.104 ns	13.870 ***	3.058 “	0.175 ns
S x Th	1.146 ns	0.085 ns	0.321 ns	0.728 ns	0.186 ns
Organs (O)	0.206 ns	91.219 ***	50.447 ***	2.493 “	58.488 ***
Third (Th)	0.380 ns	0.693 ns	51.912 ***	0.644 ns	0.794 ns
O x Th	1.237 ns	0.554 ns	0.841 ns	0.055 ns	0.762 ns

Note. C (%), carbon percentage; N (%), nitrogen percentage; $\delta^{13}C$, carbon isotope ratio (‰); $\delta^{15}N$, nitrogen isotope ratio (‰); C/N ratio. Significance levels are: *** ($p < 0.001$), ** ($p < 0.01$), * ($p < 0.05$), “ ($p < 0.1$), ns, not significant. Source: From the author (2022).

Considering the temporal variation (as a factor individually), the percentage of C had the highest values in the last samplings - S15 and S17, while the percentage of N had the highest values in the samplings S8 and S11. The C isotope ratio should not vary between samplings because it is an inherent characteristic of the plant's type of photosynthetic metabolism. In this case, in fact, there is no temporal variation. In turn, the N isotope ratio may vary due to several factors, with a higher value in S2 compared with other samples that presented similar values. The

C/N ratio presented the maximum value in the S6 near the harvest period, while reaching the lowest value in the S8 in the quiescent phase after a period of high loading fruits (Table 9).

Table 9 - Isotopic variables of samples from coffee plants in production evaluated in 6 samplings over time and sampled in 9 regions distributed in thirds and sections along the tree

Factor	C %	N %	$\delta^{13}C$ ‰	$\delta^{15}N$ ‰	C/N ratio
Sampling (S)					
S2	50.75±2.321	2.45±0.177	-27.66±0.325	6.37±0.142	21.48±1.473
S6	49.92±0.794	2.15±0.158	-27.19±0.339	3.80±0.292	24.26±1.713
S8	48.77±1.151	2.64±0.316	-28.04±0.566	3.33±0.304	19.97±2.513
S11	48.72±0.366	2.54±0.188	-27.90±0.448	3.04±0.180	20.19±1.666
S15	53.00±1.135	2.38±0.147	-27.61±0.433	3.18±0.177	23.09±1.842
S17	52.81±2.513	2.36±0.247	-28.30±0.684	3.82±0.266	24.16±3.523
Organs (O)					
Leaves	50.14±1.162	2.96±0.062	-28.75±0.228	4.23±0.292	17.10±0.570
Stems	51.08±1.161	1.83±0.039	-27.08±0.252	3.41±0.302	28.06±0.808
Fruits	50.76±0.719	2.45±0.088	-27.20±0.245	4.41±0.406	21.08±0.922
Third (Th)					
LT	49.90±0.934	2.47±0.144	-28.77±0.279	3.66±0.340	21.42±1.420
MT	51.26±1.225	2.37±0.131	-27.63±0.201	4.17±0.321	22.62±1.217
UT	50.77±1.149	2.39±0.143	-26.82±0.243	4.08±0.354	22.58±1.657

Note. C (%), carbon percentage; N (%), nitrogen percentage; $\delta^{13}C$, carbon isotope ratio (‰); $\delta^{15}N$, nitrogen isotope ratio (‰); C/N ratio. UT, upper third; MT, middle third; LT, lower third. Values are reported as the means ± standard error (n=9 for S, n=16 for Th, n=18 for Ti). Source: From the author (2022).

Regarding spatial variation (between thirds and between plant organs), the percentage of C has similar values between organs and thirds, with no apparent differences in terms of spatial variation. In turn, the percentage of N shows similar values in the thirds, however, among the organs, the leaves and fruits have higher values than the branches. The $\delta^{15}N$ also showed higher values for leaves and fruits in relation to the stems, however, there were also differences between the thirds, with the middle and upper thirds having the highest values. The C / N ratio presented the highest value in the stems, followed by the fruits, and leaves without apparent variation

between the thirds. The $\delta^{13}C$ presented the most negative values in the leaves and in the LT (Table 9).

When considering all factors together, it is possible to see that the $\delta^{13}C$ values of the bulk material of leaves, stems and fruits showed notable differences between the thirds of the tree and over time (Figure 20). Throughout the plant profile, leaves were ^{13}C depleted compared with fruits and stems. On average, the difference in $\delta^{13}C$ [‰] of leaf-fruits and leaf-stems were 1.55‰ and 1.68‰, respectively. The three organs showed the same trend of a lower third ^{13}C-depleted compared with the others, being the most pronounced difference in S11 and S17. The difference in $\delta^{13}C$ [‰] of UT – LT for leaves, stems and fruits were 2.54‰, 3.37‰ and 1.96‰, respectively. This may indicate that both the age of the organs in this older region and possibly a little shading may have an influence on the $\delta^{13}C$ values for the LT.

Regarding the $\delta^{15}N$ values, throughout the plant profile, stems were ^{15}N depleted compared with leaves and fruits. On average, the difference in $\delta^{15}N$ [‰] of leaf-fruits, leaf-stems and fruit-stems were -0.18‰, 0.83‰ and 1.00‰, respectively. In this case, the differences between the thirds were smaller, but in some samplings, LT was still ^{13}C-depleted compared with the others. The greatest differences in $\delta^{15}N$ [‰] of UT – LT were found in samplings 8 (1.51‰), 11 (1.20‰), and 17 (0.68‰) for leaves, fruits, and stems, respectively. It is also possible to see that, in general, the values for S2 were higher compared with the other samplings, with a decreasing trend (^{15}N-depletion) between S2 and S6, later a "stabilization" of the data between S6 and S15 and finally a ^{15}N- enrichment in S17 (Figure 20).

Figure 20 - Variation in $\delta^{13}C$ (a–c) $\delta^{15}N$ (d–f) and C/N ratio (g-i) in plant organs from coffee plants in production evaluated in 6 samplings over time. Leaves (a, d, g); fruits (b, e, h); stems (c, f, i).

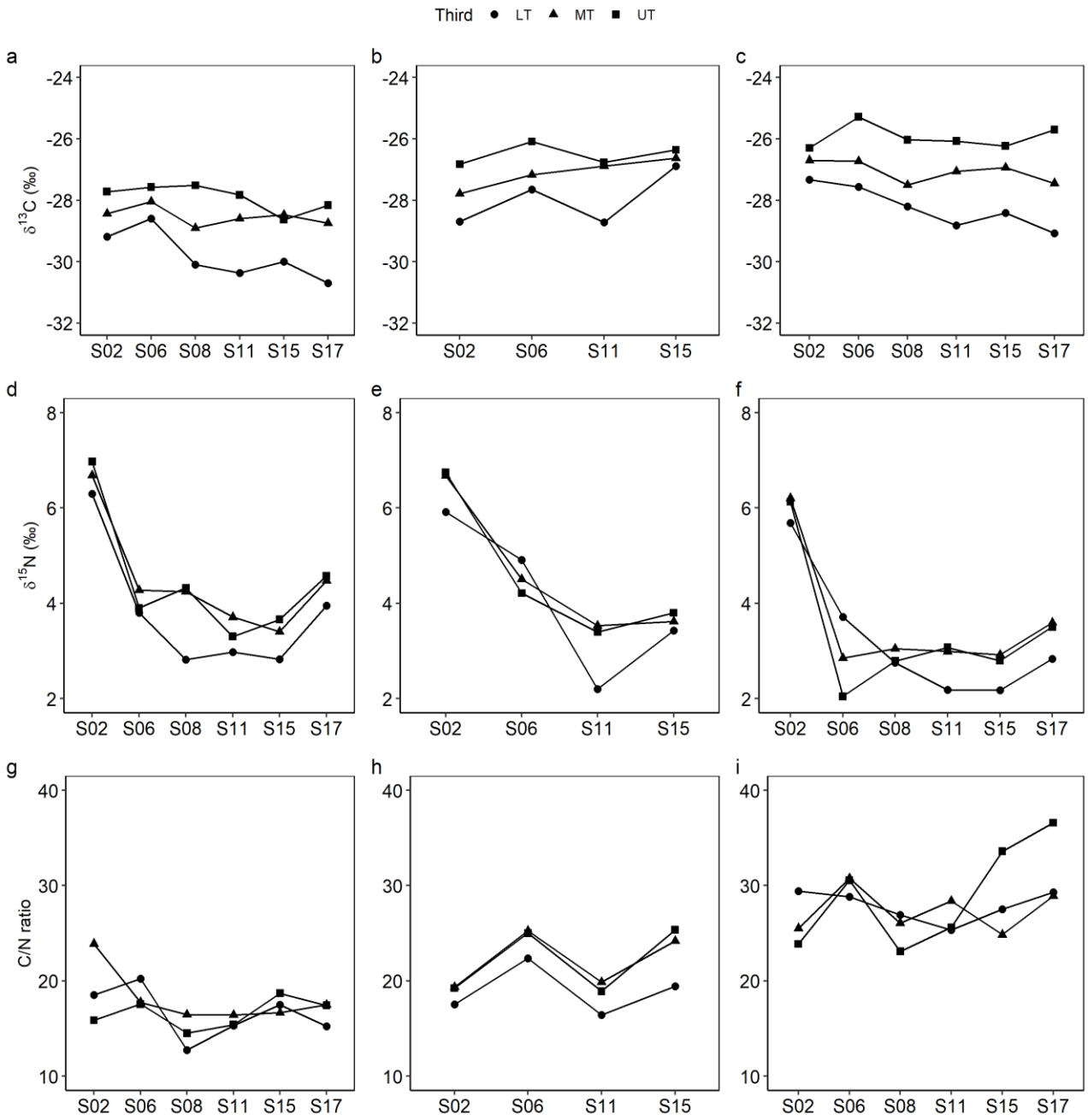

Source: From the author (2022).

For the C/N ratio, there is not a very large difference between the thirds, however, among the organs there are higher values for the stems compared with leaves and fruits, due to their low N content. When analyzed in time, it is possible to see that S6 and S15, which were the harvest time, presented higher values of the C/N ratio in all organs. The decrease in N content that leads to this higher value of the ratio may suggest an intensive use of N to sustain metabolic processes related to fruit growth and expansion.

Growth tree rings

For each of the 6 samplings analyzed samples were obtained from the basal section of the orthotropic stem, being a total of 36 samples corresponding to a determined number of holes between the medulla and the bark for each stem. In turn, each stem had at the time of analysis a determined number of growth rings, and the distribution of holes and growth rings per stem was: S2 with 5 rings and 6 holes, S6 with 5 rings and 5 holes 7, S8, S11 and S15 with 6 rings and 6 holes and S17 with 7 rings and 7 holes. Although the width of the growth rings varies from stem to stem, it is possible to consider that, due to the proximity of the values, each hole has obtained the material of at least one growth ring for the isotopic analysis. For the two variables analyzed (C% and $\delta^{13}C$), the differences between the samplings and between the holes were determined individually (Table 10). Just the carbon isotopic ratio was significantly influenced ($p < 0.05$, F-test) by the holes.

Table 10 - F-values and significance levels in one-way ANOVA of isotopic variables of samples from the basal section of the orthotropic stem with the growth rings.

Factor	C %	$\delta^{13}C$ ‰
Sampling (S)	2.395 "	0.462 ns
Holes (H)	1.205 ns	4.750 **

Note. C (%), carbon percentage; $\delta^{13}C$, carbon isotope ratio (‰); Significance levels are: *** ($p < 0.001$), ** ($p < 0.01$), * ($p < 0.05$), “ ($p < 0.1$), ns, not significant. Source: From the author (2022).

The difference between the samplings indicates the variation of the $\delta^{13}C$ value between hole 1 of the different samples and so on. It was already expected that the difference would not be significant because all the plants grew at the same time, which suggests that each growth ring must have been formed at the same time under the same climatic conditions. In contrast, between holes in the same sample there could be differences due to the different climatic conditions in which each growth ring may have formed. Thus, although all values obtained are characteristic of plants with C3 photosynthetic metabolism such as coffee, the holes closest to the stem pith (H1 and H2) presented fewer negative values (Table 11). Since only one sample had a seventh hole, this value cannot be compared with others.

Table 11 - Isotopic variables of samples from the basal section of the orthotropic stem with the growth rings.

Factor	**C** **%**	**δ13C** **‰**
Sampling (S)		
C2	55.80±0.746	-25.69±0.418
C6	56.52±0.455	-25.69±0.594
C8	56.12±0.331	-25.94±0.349
C11	55.64±0.909	-25.50±0.302
C15	53.03±1.353	-25.44±0.319
C17	54.85±0.516	-25.21±0.309
SED	1.9489	0.9681
Holes (H)		
H1	54.79±1.471	-24.92±0.312
H2	56.00±0.505	-24.84±0.467
H3	55.91±0.838	-26.42±0.205
H4	55.60±0.547	-25.83±0.137
H5	55.99±0.478	-26.20±0.174
H6	53.34±0.984	-25.16±0.298
H7	--	--
SED	2.1490	0.7039

Note. C (%), carbon percentage; $\delta^{13}C$, carbon isotope ratio (‰). Values are reported as the means ± standard error (n=6 for S, n=6 for H). Source: From the author (2022).

Regarding annual climate variability, considering all the temporal variation (S2, S6, S8, S11, S15 and S17), the results of Pearson's correlation between the isotopic data and the evaluated climatic variables showed that the percentage of C and N, the C isotopic ratio and the C/N ratio did not present significant correlations ($p<0.05$) with any of the climatic variables. In turn, the N isotopic ratio was correlated with 6 of them: Tmax, Tmed, Tmin, SL, Prec and WB (Figure 21a).

When data is analyzed in a PCA (Figure 21b), it is possible to observe that the first two components explain the 70% of the data variation. Most climate variables have large loadings both positive and negative on component 1, with the exception of SL, WB and HR which have large loadings on component 2. From the distance and angle between the vectors, it is possible to corroborate some of the correlations determined through Pearson's correlation analysis. For example, the positive correlation between $\delta^{15}N$ and temperature (Tmax, Tmed and Tmin), Prec and WB, and also the negative correlation between $\delta^{15}N$ and SL.

Considering the scores and the confidence ellipses in the biplot, it is easily recognized a grouping of data separating the samplings apparently following a pattern associated with phenology. In the quadrants on the right, S6 and S15 are grouped, samplings at the time of harvest in the two years evaluated. In the quadrants on the left are grouped S8 and S17, samplings in the quiescent phase in the two years evaluated. And S2 and S11, samples at the time of fruit and new vegetative structures growth. This separation evidences the influence of climatic variables on the phenology of the trees, since each phenological phase is conditioned by some climatic characteristics in the region.

On the other hand, when the spatial variation between the thirds is considered, the results of the Pearson correlation show, in general, that only the isotopic ratios were influenced by climatic variables in the study period with no effect for the percentages of C and N. The maximum temperature and sunlight hours showed no significant correlations with any of the isotopic variables. Between the thirds, in the UT and MT there was influence of the climatic variables only for $\delta^{15}N$, while in the LT all the significant correlations were with $\delta^{13}C$. More detailed results can be seen in Figure 22.

Figure 21 - Analysis between the isotopic data and the evaluated climatic variables (a) Pearson's correlation analysis. Positive significant correlations (blue squares), negative significant correlations (red squares) and no correlation (white squares). Significant correlation: $p<0.05$. (b) Principal component analysis—PCA with confidence ellipses (95%) grouped by samplings

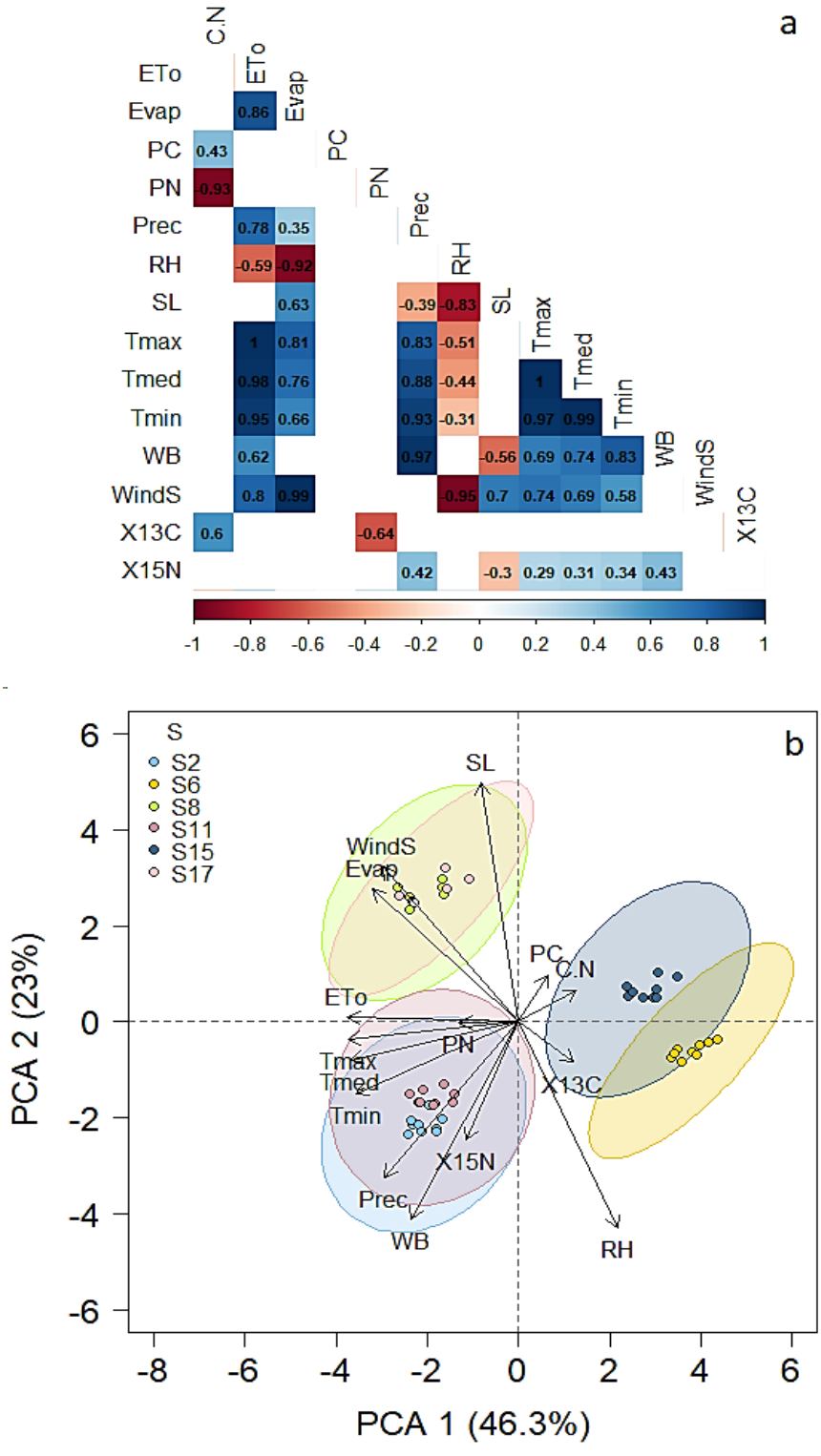

Figure 22 - Pearson's correlation analysis between the isotopic data separated between the thirds and the evaluated climate variables. The bars only show the significant correlations obtained ($p<0.05$).

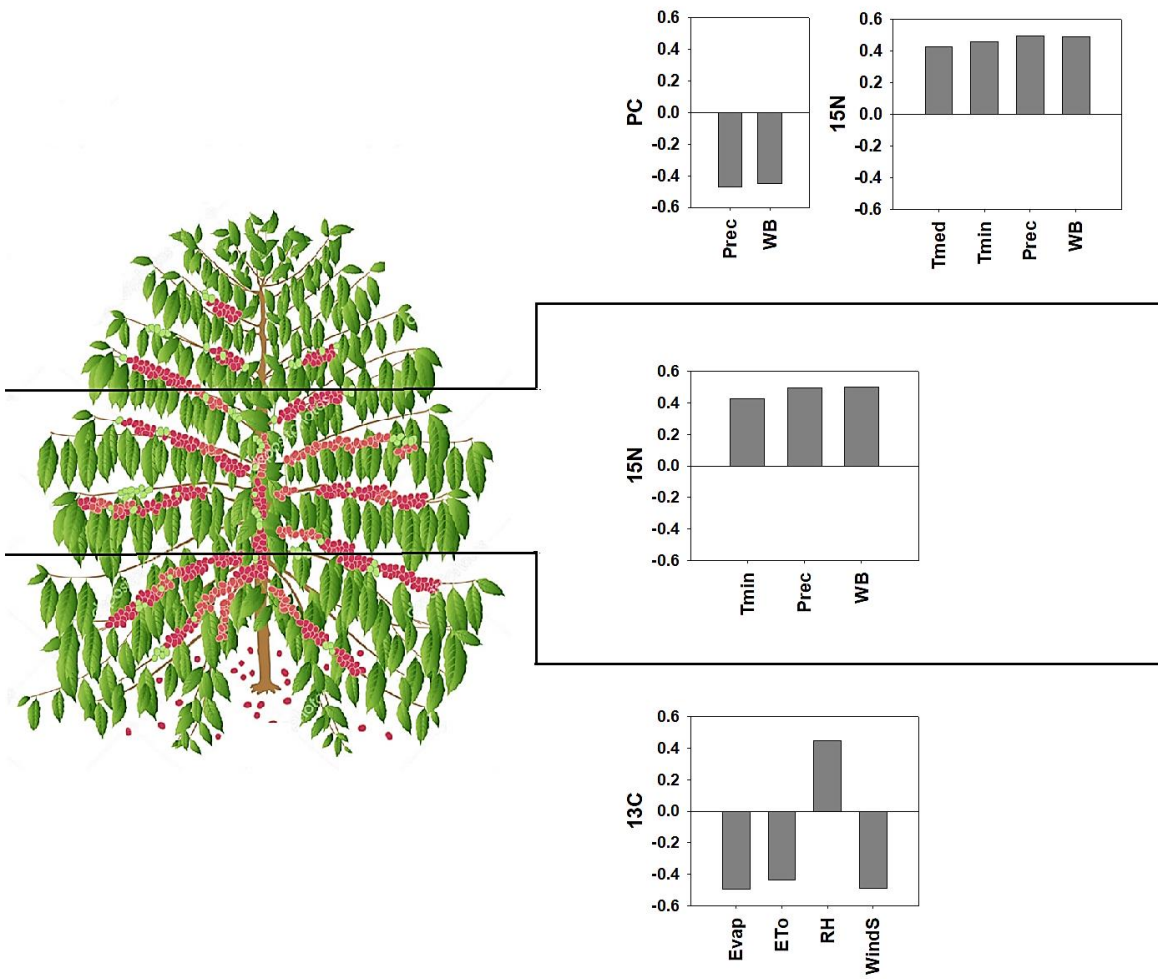

Source: From the author (2022).

5 DISCUSSION

In this chapter we address source-sink patterns on coffee trees and their relationship to annual climate variability through isotopic analysis. The C and N contents of plants are key characteristics with great ecological importance as they are indicators of the distribution and abundance of species, the relationships of plants with other organisms (herbivory, predation, etc.) and adaptation to different environmental conditions (Li et al., 2015). Thus, stable isotope signatures of C and N are often used as markers to measure the effect of environmental changes on various processes such as the photosynthetic and N assimilation process (Dubbert et al., 2012; Sun et al., 2016). A mechanistic explanation of how the temporal and spatial patterns $\delta^{13}C$ and $\delta^{15}N$ emerge is of great relevance, as these values for the dry matter of bulk material from leaves and other plant organs and tissues are commonly used in ecophysiological studies (Badeck et al., 2005; Farquhar and Richards, 1984; Wegener et al., 2015; Werner et al., 2012).

5.1 Temporal variation

Due to changes in plant growth rate between seasons, the allocated proportions of structural, functional, and storage components within organs vary significantly over time to meet plant needs. Previous studies in other species have identified that $\delta^{13}C$ values are affected by temporal variation linked to the change in plant growth stage (Rossatto et al., 2013; Scartazza et al., 2013; Sun et al., 2016). In our results, $\delta^{13}C$ values showed some seasonal signs, reaching a relative maximum in the period of rapid growth of both fruits (S2-S6, -27.43‰) and vegetative structures (S11-S15, -27.75‰) and the lowest values after the quiescent phase in which there is no growth or growth rates are very low (S8-S17, -28.30‰). The mean values of $\delta^{13}C$ in winter (S6 and S15, -27.40‰) were higher than the values in summer (S2 and S11, -27.78‰) and higher than the values at the beginning of the rainy season (S8 and S17, -28.17‰) (Table 9, Figure 20).

It has been reported by some authors (Cao et al., 2011; Sun et al., 2016) that in the early stages of development, there is a “hungry” state of intercellular CO_2 concentrations due to high rates growth and the synthesis of organic matter to meet the demands of development and construction. This process leads to less differentiation and, in turn, to a smaller exclusion of $^{13}CO_2$, resulting in enriched $\delta^{13}C$ values. This information agrees with our results in that the seasonal pattern of $\delta^{13}C$ values implies that the two stages of rapid growth (whether vegetative or reproductive) presented enriched values compared with the time of lower growth rates.

Although no significant correlations were found between $\delta^{13}C$ values and climatic variables (Figure 21), it has been reported for C3 species that there is a negative correlation between leaf $\delta^{13}C$ values and water availability being that low values of $\delta^{13}C$ are often associated with high rainfall, or at least greater availability of water (Codron et al., 2005; Ma et al., 2012; Stewart et al., 1995; Vitória et al., 2018). In our results, on the other hand, the lowest values of foliar $\delta^{13}C$ were found in the samplings S8 and S17 when the rainy season begins, but the previous months are characterized by low rainfall and low water availability. This suggests that there may be another factor besides precipitation that influences the more negative values of $\delta^{13}C$. Considering that the lowest growth rates (Table 2) were presented at this time of year, together with low photosynthetic rates (Table 6) and increased accumulation of reserves (Figure 29), it is possible to suggest that there is a decrease in $^{13}CO_2$ fixation, using other types of C sources in the plant that may have also gone through other fractionation processes against ^{13}C, leaving the values even more negative in relation to the other sampling months. For example, a higher proportion of CO_2 refixation due to low assimilation rates, and growth and maintenance respiration, can lead to ^{13}C-depleted tissues (Lucas A. Cernusak et al., 2009; Sun et al., 2016).

In the case of $\delta^{15}N$ values, a seasonal pattern was not easily observed. The maximum value was reached in S2 (6.37‰), when the growth and expansion of the fruits took place for the 2016-2017 harvest. In the subsequent samplings, relatively close values were found, ranging between 3.04‰ and 3.82‰ with no apparent pattern. The mean values of $\delta^{15}N$ in summer (S2 and S11, 4.71‰) were higher than the values at the beginning of the rainy season (S8 and S17, 3.57‰) and higher than in winter (S6 and S15, 3.49‰) (Figure 20). $\delta^{15}N$ values provide time- and space-integrated information on nitrogen use throughout the plant and at the organ level, being affected by factors such as abiotic stresses, availability of N in the soil, the acquisition of N from alternative sources, the source of CO_2 and environmental effects (Evans, 2001; Kalcsits and Guy, 2013; Vitória et al., 2018).

In general, a decrease in $\delta^{15}N$ values in soil and plants has been observed with increasing precipitation and decreasing dry season (Nardoto et al., 2008; Vitória et al., 2018). This decrease has been associated with processes such as denitrification, which is favored in humid conditions, preventing an increase in $\delta^{15}N$ values (Nardoto et al., 2008). In our results, on average, the lowest values of $\delta^{15}N$ found in the three organs were in S11, the season of January (2018), a month in

which there are high rates of precipitation. These values are maintained until S15, in which, although there is a decrease in rainfall, with a decrease in temperatures, moisture levels in the soil are probably still maintained. Although low values of $\delta^{15}N$ would be expected in S2 also because it was the same time of high rainfall in the previous year (2017), possibly the highest values for this sampling and the subsequent one - S6- are due to factors associated with fertilization with nitrogen sources. These sources were perhaps applied to sustain the high production expected for the 2016/2017 season of positive bienniality, in addition to the beginning of the new vegetative growth. Furthermore, in Pearson's correlation analysis, a positive correlation was found between the values of $\delta^{15}N$ and Prec. This is possibly due to this high value in S2 where, as mentioned, there were high precipitations (Figure 21, Figure 22).

On the other hand, considering the values of N, especially leaf N, it has been reported that a higher concentration of leaf N would be associated with higher values of photosynthesis, maximizing the opportunities for carbon gain, which would lead to lower values of $\delta^{13}C$ (Santiago et al., 2017; Vitória et al., 2018). In our results, although the samplings with higher values of leaf N and lower values of $\delta^{13}C$ coincide (S8 and S11), the two seasons are contrasting in terms of photosynthetic rates. S11 is a time of active growth and higher rates of photosynthesis, in contrast to S8 when growth slows, and photosynthetic rates are also lower.

When considering the C/N ratio, it is important to emphasize that this ratio represents the ability of plants to assimilate C while absorbing N (Rong et al., 2014; Sun et al., 2016). Thus, higher growth rates would be associated with lower proportions of C:N in the plant. In our results, considering the two periods with the highest growth rates (S2 and S11), lower proportions of C:N were always presented in the three organs relating, for example, S2 against S6 and S11 against S15. This difference comprises the months of January with high rates of reproductive and vegetative growth compared to the months of May and June when harvests begin and growth rates cease. It is also possible to see that S8 has even lower values than the other samplings, possibly because it is the quiescent period in which neither of the two processes takes place actively.

5.2 Spatial variation

In C3 plants, it has been reported that heterotrophic tissues/organs tend to be enriched with ^{13}C compared with leaves (Badeck et al., 2005; Bowling, Pataki, and Randerson, 2008; Cao et al., 2011; Codron et al., 2005; Rascher et al., 2010). Given that C4 plants do not show this tendency towards enrichment or even depletion in heterotrophic tissues, it is assumed that the isotopic fractionation processes that lead to the spatial variation of $\delta^{13}C$ are probably located in the leaves, where the difference between C3 and C4 metabolism originates (Hobbie and Werner, 2004; Wegener et al., 2015). However, isotopic fractionation processes associated with metabolic branch points, transport and respiration occur downstream of leaf primary C assimilation, also altering the $\delta^{13}C$ of the different C pools (Badeck et al., 2005).

Among these processes, those that have mainly been associated with isotopic differences between plant organs are phloem transport and loading and respiratory processes. In the case of phloem loading, the isotopic effect may occur depending on the phloem loading strategy used (active or passive) and the sap composition for each species. The sap components, mainly sugars and alcohols, may differ in their isotopic composition, affecting the $\delta^{13}C$ values found (Dubbert et al., 2012; Rascher et al., 2010). In the case of respiration, the CO_2 released during autotrophic respiration is enriched with ^{13}C, leaving behind ^{13}C-depleted C to be incorporated into leaf biomass. Conversely, respiration in heterotrophic tissues releases ^{13}C-depleted CO_2, leaving behind ^{13}C-enriched carbon to be incorporated into their biomass. Thus, fractionation processes during respiration strongly influence the isotopic composition of the remaining C, leading to depleted or enriched C reservoirs being loaded into the phloem (Bathellier et al., 2008; Cernusak et al., 2009; Ghashghaie and Badeck, 2014; Wegener et al., 2015). Thus, an understanding of how the initial signatures of $\delta^{13}C$ are later altered is important for studies that use these signatures from different organs and/or plant tissues as indicators of altered photosynthetic discrimination.

In our results, stems and fruits were less ^{13}C-depleted than the leaves, with average values of -27.02‰ for stems and -27.20‰ for fruits in relation to -28.75‰ for leaves. Also, considering the thirds, it is possible to see that for the three organs, there is a decreasing trend or a vertical pattern in which the UT is enriched in relation with the LT, which presents more negative values of $\delta^{13}C$. Considering the average values, the difference between UT and LT is 1.92‰, 1.48‰ and 2.30‰ for leaves, fruits and stems respectively. This vertical distribution of $\delta^{13}C$ is due, as

discussed earlier, to fractionation processes within the plant as carbon moves between organs, but it may also have a C component derived from soil respiration. This respiration typically has relatively depleted $\delta^{13}C$ values (about -27‰), compared to ambient air which is relatively enriched (−8‰). This favors that leaf material closer to the soil surface tends to show more negative $\delta^{13}C$ values than leaves higher in the canopy (Buchmann et al., 1997; Domingues et al., 2005; Vitoria et al., 2016). C fixation by these lower canopy leaves, which are also more shaded, progressively introduces more depleted C into the trunk phloem. It is then recognized that leaves growing under shady conditions can also be more ^{13}C-depleted (Vitória et al., 2018; Xiao et al., 2013).

This spatial pattern can also be generated by a developmental change in photosynthetic discrimination against ^{13}C. For example, during expansion of young leaves after a heterotrophic stage, ci:ca values are higher than values for mature leaves, producing ^{13}C-depleted photosynthates, resulting in an accumulation of depleted organic material (Sun et al., 2016). Furthermore, since these expanding leaves have higher growth respiration rates and low assimilation rates, there may be CO_2 refixation processes producing depleted tissues (Cernusak et al., 2006; Cernusak et al., 2009). Since leaf samples only from the distal section were evaluated, which are mostly young in the three thirds, this trend of new expanding leaves ^{13}C-depleted and mature leaves ^{13}C-enriched was not so clear. Possibly it would have been clearer when having samples from the intermediate and proximal sections that are more mature than the leaves in the distal section.

Regarding the values of $\delta^{15}N$, values of 4.41‰, 4.23‰ and 3.40‰ were presented on average for fruits, leaves, and stems, respectively. Considering the thirds, there was also a decreasing trend or a vertical pattern in which the UT is enriched in relation to the LT. Thus, seeing the mean values, the difference between UT and LT was 0.42‰, 0.67‰ and 0.17‰ for fruits, leaves and stems, respectively. The discrimination of N isotopes of the whole plant is a function of 4 fluxes. A gross influx from the root medium, partial assimilation by NR from the root, efflux of unassimilated nitrate back into the medium, and nitrate exported to leaves (Evans, 2001). Thus, the main determinants of $\delta^{15}N$ differences between the root and the shoot of the plant are the export of unassimilated nitrate to the leaves together with the export of assimilated N through the xylem (Evans, 2001). Fractionation against ^{15}N during nitrate reduction in the root

leaves behind ^{15}N-enriched nitrate molecules that will be translocated to the shoot (Peuke, Gessler, and Tcherkez, 2013). Although we do not have $\delta^{15}N$ values for the coffee roots, the values obtained would probably be depleted in relation to the values of the shoot.

For this reason, the leaves are normally enriched relative to the roots as demonstrated in our results, since the nitrate enriched from partial assimilation in the roots is transported to the leaves. Thus, foliar nitrogen available for assimilation comes from a pool that has already been exposed to assimilation (Evans, 2001; Kalcsits and Guy, 2013). In the case of stems, although small amounts of activity of enzymes involved in the assimilation of inorganic nitrogen such as NR have been found (Black, Fuchigami, and Coleman, 2002; Hunter, 1985), the assimilatory volume is small compared to roots and leaves. Thus, normally the $\delta^{15}N$ of organic nitrogen assimilated in the stem would be equal to the $\delta^{15}N$ of the source of inorganic nitrogen discharged from the xylem, which may originate from the roots or leaves or both (Kalcsits et al., 2014). In the case of fruits, the values of ^{15}N enriched in relation to the leaves may be due to fractionation processes in the transport and loading of the phloem.

From another point of view, $\delta^{15}N$ values are also considered as a reflection of the distribution of nitrogen fertilizer in the trees and the regularity of migration in the organs (Ding et al., 2017). Thus, our results show that in the positive bienniality season $\delta^{15}N$ was distributed mainly in the fruit in S2 and S6 followed by leaves and stems. With the reduction of the fruit load, the distribution rate of $\delta^{15}N$ in the fruits gradually decreased but remained in the other organs in S8. Subsequently, in the negative bienniality season, $\delta^{15}N$ was distributed mainly in the leaf at S11, in the fruit at S15 and after the harvest it increased again in the leaves and stems, even more than in the previous year. Thus, in agreement with the results reported by Ding et al., (2017), the distribution content of N that was absorbed by the plant to the reproductive organs decreased with the decrease in fruit load, but its distribution to other organs increased. The greater distribution of $\delta^{15}N$ to fruits in S15 may indicate that even in a year of negative bienniality in which vegetative growth with low fruit production predominates, the ability of reproductive organs to compete for $\delta^{13}C$ and $\delta^{15}N$ is stronger than the ability of vegetative and storage structures. However, the content of $\delta^{13}C$ and $\delta^{15}N$ allocated to reproductive organs gradually decreased with the decline in crop load, which can be evidenced by the difference in $\delta^{15}N$ values between S6 and S15 (4.54‰ and 3.29‰ respectively).

The results also show the relationship between the values of $\delta^{15}N$ and the values of the percentage of N, since they followed the same trend with higher values in leaves and fruits in relation to stems. The bulk N pool of plant organs contains various species such as inorganic N, amino acids, proteins, and chlorophylls. Variations in $\delta^{15}N$ can be attributed to different mixing ratios of different N species, each of which could have a distinct $\delta^{15}N$ (Gauthier et al., 2012; Peuke et al., 2013). In our results, the leaves showed higher N values, especially in the months of strong vegetative growth, indicating the high amount of nitrogen compounds in relation to other organs. On the other hand, as mentioned earlier, the C/N ratio represents the ability of plants to assimilate C while absorbing N, and higher growth rates would be associated with lower proportions of C:N in the plant. This agrees with our data in the sense that relatively higher C/N ratios in stems, followed by fruits and leaves, would denote lower growth rates for stems and fruits than leaves.

5.3 Growth tree rings

Tree rings can provide an excellent record of the growth dynamics in trees, especially in conjunction with local climate data. Its formation is the result of the exchange activity of the tree between the vegetative period and the quiescent phase. In ecosystems with climatic seasonality, plants produce cyclical growth patterns, due to a period of seasonal stress that induces dormancy of the exchange meristem, interrupting growth in diameter and inducing the formation of growth rings (Alves and Angyalossy-Alfonso, 2000; Nath et al., 2016; dos Santos Silva et al., 2017; Worbes, 2002). Thus, the width/area of a tree ring indicates how much growth occurred in the vascular cambium of a tree within one year, so climate conditions such as water availability are represented in tree rings because they affect growth rate.

Although the dimensional parameters of the rings provide information about environmental signals, they are associated with several challenges that can make it difficult to understand these signals, such as segments in which the rings become incoherent or indistinguishable, lack of uniformity in the growth of the rings and difficulty in identifying the boundaries between a ring and the other (especially in tropical species) (Tarhule and Leavitt, 2004). However, given the influence of climate on the composition of stable isotopes from cellulose of growth rings, this tool constitutes an analysis that can complement the standard analysis of width and/or area of rings, improving the understanding of growth dynamics and

biomass allocation. in response to climate. Cellulose is the main component of wood tissue and can record the response of trees to climatic conditions throughout the life of the tree. Each late wood ring is constructed with carbon fixed that year just as early wood contains fixed and stored carbon from the previous season. In this way, the C fixed in cellulose is stable and its isotopic proportions do not change, having the potential to act as a proxy for environmental factors such as precipitation and temperature (McCarroll and Loader, 2004).

In our results, the inter-tree variability was minimal, with a value of 0.74 between the maximum and minimum value (and not significant $p<0.05$), while the intra-tree variability varied between -24.84‰ and -26.42‰ showing a greater variation of up to 1.58‰. As mentioned before, no differences were expected between the samplings given that the trees grew under the same climatic and management conditions, so it is expected that the formation of each ring in individual plants took place in the same season. However, the intra-ring variation of $\delta^{13}C$ values shows that the first two years of growth have enriched values in relation to the others, which have more negative values (especially H5 and H6).

From the process of normalization of time series obtained from the area of the growth ring (Figure 11), it was seen that there was a trend of rapid growth in the first years of the tree and later a stabilization in the following years until the date of collection. Thus, the 2012/2013 period had the highest growth rate, while the 2014/2015 period had the lowest rate (Table 4). As discussed earlier, early developmental stages characteristic of high growth rates are associated with lower discrimination against ^{13}C, resulting in enriched values (Cao et al., 2011; Sun et al., 2016). Possibly, these first years with less negative values of $\delta^{13}C$ represent this period of accelerated growth (H1 and H2). Subsequently, growth stabilizes with the lowest growth rate (H3 - period 2014/2015), possibly showing greater discrimination.

On the other hand, considering the negative correlation between $\delta^{13}C$ values and water availability (Codron et al., 2005; Ma et al., 2012; Stewart et al., 1995; Vitória et al., 2018), $\delta^{13}C$ values follow the region's precipitation dynamics (data not shown in this document, but reported in Toro-herrera et al., 2021). The periods of 2012/2013 and 2013/2014 (H1 and H2) presented average annual rainfall of up to 400mm below the period 2014/2015. Thus, as precipitation increases, the values become more negative. This because when water availability is low, stomatal conductance decreases, reducing both leaf CO_2 concentrations and ^{13}C discrimination

during carbon fixation. Thus, in times of limited water availability, the carbon fixed by the tree in sugars and eventually cellulose should have higher $\delta^{13}C$ values than in times of abundant water where the opposite happens (McCarroll and Loader, 2004).

6 CHAPTER HIGHLIGHTS

1. Stable signatures of C and N isotopes are highly relevant markers to measure the effect of environmental changes on various physiological processes in the plant.
2. Values of $\delta^{13}C$ and $\delta^{15}N$ are affected by temporal/seasonal variation linked to changes in the plant growth stage. $\delta^{13}C$ values showed more seasonal signals than $\delta^{15}N$ values, mainly influenced by plant organ growth rates and precipitation.
3. As reported for many other species, in this study heterotrophic tissues (stems and fruits) tended to be enriched in $\delta^{13}C$ compared to leaves. This is due to post-photosynthetic isotopic fractionation processes such as transport and loading in the phloem or respiratory and CO_2 refixation processes.
4. There was a vertical pattern in the values of $\delta^{13}C$ and $\delta^{15}N$, with the lower third being depleted in relation to the upper third enriched. This pattern is mainly due to the fixation of other non-atmospheric sources of C such as C derived from soil respiration and the assimilation of N originating from a pool that has already been exposed to assimilation.
5. The $\delta^{15}N$ values reflect the distribution of nitrogen fertilizer in the trees and the regularity of migration in the organs. Reproductive structures continued to demonstrate a strong ability to compete for resources, constituting strong sinks in relation to vegetative and storage structures.
6. The standard analyzes of the width and/or area of the growth rings present challenges related to the instability of the measurements due to several factors. Given that the C fixed in cellulose - the main component of wood - is stable and its isotopic proportions do not change, the isotopic analysis of growth rings allows to improve the understanding of growth dynamics and biomass allocation in response to climate.

REFERENCES

ALVES, E. S.; ANGYALOSSY-ALFONSO, V. Ecological trends in the wood anatomy of some Brazilian Species. 1. Growth rings and vessels. **IAWA Journal**, v. 21, n. 1, p. 3–30, 2000.

BADECK, F. W. et al. Post-photosynthetic fractionation of stable carbon isotopes between plant organs - A widespread phenomenon. **Rapid Communications in Mass Spectrometry**, v. 19, n. 11, p. 1381–1391, 2005.

BATHELLIER, C. et al. Divergence in δ13C of dark respired CO2 and bulk organic matter occurs during the transition between heterotrophy and autotrophy in Phaseolus vulgaris plants. **New Phytologist**, v. 177, n. 2, p. 406–418, 2008.

BEHBOUDIAN, M. H. et al. Discrimination against 13CO2 in leaves, pod walls, and seeds of water stressed chickpea. **Photosynthetica**, v. 38, n. 1, p. 155–157, 2000.

BLACK, B. L.; FUCHIGAMI, L. H.; COLEMAN, G. D. Partitioning of nitrate assimilation among leaves , stems and roots of poplar. **Tree Physiology**, v. 22, p. 717–724, 2002.

BOWLING, D. R.; PATAKI, D. E.; RANDERSON, J. T. Carbon isotopes in terrestrial ecosystem pools and CO2 fluxes. **New Phytologist**, v. 178, n. 1, p. 24–40, 2008.

BRÜGGEMANN, N. et al. Carbon allocation and carbon isotope fluxes in the plant-soil-atmosphere continuum: A review. **Biogeosciences**, v. 8, n. 11, p. 3457–3489, 2011.

BUCHMANN, N. et al. Interseasonal comparison of CO2 concentrations , isotopic composition , and carbon dynamics in an Amazonian rainforest (French Guiana). **Oecologia**, v. 110, p. 120–131, 1997.

CAO, S. K. et al. Research on the water use efficiency and foliar nutrient status of Populus euphratica and Tamarix ramosissima in the extreme arid region of China. **Environmental Earth Sciences**, v. 62, n. 8, p. 1597–1607, 2011.

CARTER, J. F.; YATES, H. S. A.; TINGGI, U. Isotopic and Elemental Composition of Roasted Coffee as a Guide to Authenticity and Origin. **Journal of Agricultural and Food Chemistry**, v. 63, n. 24, p. 5771–5779, 2015.

CAXITO, F. A.; SILVA, A. V. Isótopos Estáveis: Fundamentos e técnicas aplicadas à caracterização e proveniência geográfica de productos alimentícios. **Geonomos**, v. 23, n. 1, p. 10–17, 2015.

CERNUSAK, L. A. et al. Large variation in whole-plant water-use efficiency among tropical tree species. **New Phytologist**, v. 173, p. 294–305, 2006.

CERNUSAK, L. A. et al. Why are non-photosynthetic tissues generally 13C enriched compared with leaves in C3 plants? Review and synthesis of current hypotheses. **Functional Plant Biology**, v. 36, n. 3, p. 199–213, 2009a.

CERNUSAK, L. A. et al. Why are non-photosynthetic tissues generally 13C enriched compared with leaves in C3 plants? Review and synthesis of current hypotheses. **Functional Plant Biology**, v. 36, p. 199–213, 2009b.

CERNUSAK, L. A.; PATE, J. S.; FARQUHAR, G. D. Diurnal variation in the stable isotope composition of water and dry matter in fruiting Lupinus angustifolius under field. **Plant Cell and Environment**, v. 25, p. 893–907, 2002.

CODRON, J. et al. Taxonomic, anatomical, and spatio-temporal variations in the stable carbon and nitrogen isotopic compositions of plants from an African savanna. **Journal of Archaeological Science**, v. 32, n. 12, p. 1757–1772, 2005.

COPLEN, T. B. Guidelines and recommended terms for expression of stable-isotope-ratio and gas-ratio measurement results. **Rapid Communications in Mass Spectrometry**, v. 25, n. 17, p. 2538–2560, 2011.

CRAIG, H. The geochemistry of the stable carbon isotopes. **Geochimica et Cosmochimica Acta**, v. 3, n. 2–3, p. 53–92, 1953.

DAWSON, T. E. et al. Stable isotopes in plant ecology. **Annual Review of Ecology and Systematics**, v. 33, p. 507–559, 2002.

DAWSON, T.; SIEGWOLF, R. **Stable isotopes as indicators of Ecological Change**. 1st Edition. Elsevier Academic Press. 417p. 2007.

DERSCH, L. M. et al. Novel approach for high-through out metabolic screening of whole plants by stable isotopes. **Plant Physiology**, v. 171, n. 1, p. 25–41, 2016.

DING, N. et al. Effects of crop load on distribution and utilization of 13 C and 15 N and fruit quality for dwarf apple trees. **Scientific Reports**, v. 7:14172, n. November 2016, p. 1–9, 2017.

DOMINGUES, T. F. et al. Parameterization of Canopy Structure and Leaf-Level Gas Exchange for an Eastern Amazonian Tropical Rain Forest (Tapajós National Forest , Pará , Brazil). **Earth Interactions**, v. 9, n. 17, p. 1–23, 2005.

DOS SANTOS SILVA, M. et al. Growth rings in woody species of Ombrophilous Dense Forest: occurrence, anatomical features and ecological considerations. **Revista Brasileira de Botanica**, v. 40, n. 1, p. 281–290, 2017.

DUBBERT, M.; RASCHER, K. G.; WERNER, C. Species-specific differences in temporal and spatial variation in δ13C of plant carbon pools and dark-respired CO2 under changing environmental conditions. **Photosynthesis Research**, v. 113, n. 1–3, p. 297–309, 2012.

DUCATTI, C. et al. Revista Brasileira de Zootecnia Utilização de isótopos estáveis em ruminantes. **Revista Brasileira de Zootecnia**, v. 40, p. 68–75, 2011.

EVANS, R. D. Physiological mechanisms influencing plant nitrogen isotope composition. **Trends in Plant Science**, v. 6, n. 3, p. 121–126, 2001.

FARQUHAR, G. D.; EHLERINGER, J. R.; HUBIC, K. T. Discrimination and Photosynthesis. **Annu. Rev. Plant Physiol. Plant Mol. Bioi**, v. 40, p. 503–537, 1989.

FARQUHAR, G. D.; RICHARDS, R. A. Isotopic composition of plant carbon correlates with water-use efficiency of wheat genotypes. **Australian Journal of Plant Physiology**, v. 11, n. 6, p. 539–552, 1984.

GAUTHIER, P. P. G. et al. Metabolic origin of d15N values in nitrogenous compounds from

Brassica napus L . leaves. **Plant, Cell & Environment**, p. 1–10, 2012.

GESSLER, A. et al. Tracing carbon and oxygen isotope signals from newly assimilated sugars in the leaves to the tree-ring archive. **Plant, Cell and Environment**, v. 32, n. 7, p. 780–795, 2009.

GHASHGHAIE, J.; BADECK, F. W. Opposite carbon isotope discrimination during dark respiration in leaves versus roots - a review. **New Phytologist**, v. 201, n. 3, p. 751–769, 2014.

HOBBIE, E. A.; HÖGBERG, P. Nitrogen isotopes link mycorrhizal fungi and plants to nitrogen dynamics. **New Phytologist**, v. 196, n. 2, p. 367–382, 2012.

HOBBIE, E. A.; WERNER, R. A. Bulk carbon isotope patterns in C 3 and C 4 plants : a review and synthesis. **New Phytologist**, v. 161, n. 2, p. 371–385, 2004.

HUNTER, W. J. Soyabean stem in vivo Nitrate Reductase activity. **Annals of Botany**, v. 55, n. 5, p. 759–761, 1985.

HUSSAIN, M. I.; AL-DAKHEEL, A. J.; REIGOSA, M. J. Genotypic differences in agro-physiological, biochemical and isotopic responses to salinity stress in quinoa (Chenopodium quinoa Willd.) plants: Prospects for salinity tolerance and yield stability. **Plant Physiology and Biochemistry**, v. 129, n. February, p. 411–420, 2018.

KALCSITS, L. A.; BUSCHHAUS, H. A.; GUY, R. D. Nitrogen isotope discrimination as an integrated measure of nitrogen fluxes, assimilation and allocation in plants. **Physiologia Plantarum**, v. 151, n. 3, p. 293–304, 2014.

KALCSITS, L. A.; GUY, R. D. Whole-plant and organ-level nitrogen isotope discrimination indicates modification of partitioning of assimilation, fluxes and allocation of nitrogen in knockout lines of Arabidopsis thaliana. **Physiologia Plantarum**, v. 149, n. 2, p. 249–259, 2013.

LI, Z. et al. Spatial patterns of leaf carbon, nitrogen stoichiometry and stable carbon isotope composition of Ranunculus natans C.A. Mey. (Ranunculaceae) in the arid zone of northwest China. **Ecological Engineering**, v. 77, p. 9–17, 2015.

LIU, H. C. et al. Geographic determination of coffee beans using multi-element analysis and isotope ratios of boron and strontium. **Food Chemistry**, v. 142, p. 439–445, 2014.

MA, J. Y. et al. Variation in the Stable Carbon and Nitrogen Isotope Composition of Plants and Soil along a Precipitation Gradient in Northern China. **PLoS ONE**, v. 7, n. 12, p. 1–7, 2012.

MCCARROLL, D.; LOADER, N. J. Stable isotopes in tree rings. **Quaternary Science Reviews**, v. 23, n. 7–8, p. 771–801, 2004.

NARDOTO, G. B. et al. Understanding the influences of spatial patterns on N availability within the Brazilian Amazon Forest. **Ecosystems**, v. 11, p. 1234–1246, 2008.

NATH, C. D. et al. Growth rings in tropical trees: role of functional traits, environment, and phylogeny. **Trees - Structure and Function**, v. 30, n. 6, p. 2153–2175, 2016.

O'LEARLY, M. H.; MADHAVAN, S.; PANETH, P. Physical and chemical basis of carbon isotope fractionation in plants. **Plant, Cell & Environment**, v. 15, n. 9, p. 1099–1104, 1992.

PEREIRA, A. L.; BENEDITO, E. Isótopos estáveis em estudos ecológicos : métodos , aplicações

e perspectivas. **Revista Biociência**, v. 13, n. 1–2, p. 16–27, 2007.

PEUKE, A. D.; GESSLER, A.; TCHERKEZ, G. Experimental evidence for diel d15 N-patterns in different tissues , xylem and phloem saps of castor bean (Ricinus communis L .). **Plant, Cell & Environment**, v. 36, p. 2219–2228, 2013.

RASCHER, K. G.; MÁGUAS, C.; WERNER, C. On the use of phloem sap δ13C as an indicator of canopy carbon discrimination. **Tree Physiology**, v. 30, n. 12, p. 1499–1514, 2010.

RODRIGUES, C. I. et al. Stable isotope analysis for green coffee bean: A possible method for geographic origin discrimination. **Journal of Food Composition and Analysis**, v. 22, n. 5, p. 463–471, 2009.

RONG, Q. et al. Leaf carbon, nitrogen and phosphorus stoichiometry of Tamarix chinesis Lour. in the Laizhou Bay coastal wetland, China. **Ecological Engineering**, p. 1–9, 2014.

ROSSATTO, D. R. et al. Seasonal variation in leaf traits between congeneric savanna and forest trees in Central Brazil: Implications for forest expansion into savanna. **Trees - Structure and Function**, v. 27, n. 4, p. 1139–1150, 2013.

SANTIAGO, L. S. et al. Functional strategies of tropical dry forest plants in relation to growth form and isotopic composition. **Environmental Research Letters**, v. 12, n. 115006, p. 1–9, 2017.

SAVEYN, A. et al. Woody tissue photosynthesis and its contribution to trunk growth and bud development in young plants. **Plant, Cell and Environment**, v. 33, n. 11, p. 1949–1958, 2010.

SCARTAZZA, A. et al. Seasonal and inter-annual dynamics of growth, non-structural carbohydrates and C stable isotopes in a Mediterranean beech forest. **Tree Physiology**, v. 33, n. 7, p. 730–742, 2013.

SCARTAZZA, A. et al. Combining stable isotope and carbohydrate analyses in phloem sap and fine roots to study seasonal changes of source-sink relationships in a Mediterranean beech forest. **Tree Physiology**, v. 35, n. 8, p. 829–839, 2015.

SHARP, Z. Principles of Stable Isotope Geochemistry. v. Second Edi, p. 416, 2017.

STEIN, R. A.; SHELDON, N. D.; SMITH, S. Y. C3 plant carbon isotope discrimination does not respond to CO2 concentration on decadal to centennial timescales. **New Phytologist**, v. 229, n. 5, p. 2576–2585, 2021.

STEWART, G. R. et al. 13C natural abundance in plant communities along a rainfall gradient: A biological integrator of water availability. **Australian Journal of Plant Physiology**, v. 22, n. 1, p. 51–55, 1995.

SUN, L. et al. Temporal and spatial variations in the stable carbon isotope composition and carbon and nitrogen contents in current-season twigs of Tamarix chinensis Lour. and their relationships to environmental factors in the Laizhou Bay wetland in China. **Ecological Engineering**, v. 90, p. 417–426, 2016.

TARHULE, A.; LEAVITT, S. W. Comparison of stable-carbon isotope composition in the growth rings of Isorberlinia doka, Daniella oliveri, and Tamarindus indica and West African

climate. **Dendrochronologia**, v. 22, n. 1, p. 61–70, 2004.

TORO-HERRERA, M. A. et al. On the use of tree-ring area as a predictor of biomass accumulation and its climatic determinants of coffee tree growth. **Annals of Applied Biology**, n. August 2020, p. 1–15, 2021.

VITORIA, A. P. et al. Using leaf d13C and photosynthetic parameters to understand acclimation to irradiance and leaf age effects during tropical forest regeneration. **Forest Ecology and Management**, v. 379, p. 50–60, 2016.

VITÓRIA, A. P. et al. Isotopic composition of leaf carbon (δ13C) and nitrogen (δ15N) of deciduous and evergreen understorey trees in two tropical Brazilian Atlantic forests. **Journal of Tropical Ecology**, v. 34, p. 145–156, 2018.

WEGENER, F.; BEYSCHLAG, W.; WERNER, C. Dynamic carbon allocation into source and sink tissues determine within-plant differences in carbon isotope ratios. **Functional Plant Biology**, v. 42, n. 7, p. 620–629, 2015.

WERNER, C. et al. Progress and challenges in using stable isotopes to trace plant carbon and water relations across scales. **Biogeosciences**, v. 9, n. 8, p. 3083–3111, 2012.

WERNER, R. A.; BRAND, W. A. Referencing strategies and techniques in stable isotope ratio analysis. **Rapid Communications in Mass Spectrometry**, v. 15, n. 7, p. 501–519, 2001.

WORBES, M. One hundred years of tree-ring research in the tropics - A brief history and an outlook to future challenges. **Dendrochronologia**, v. 20, n. 1–2, p. 217–231, 2002.

XIAO, L. et al. Stable isotope compositions of recent and fossil sun/shade leaves and implications for palaeoenvironmental reconstruction. **Review of Palaeobotany and Palynology**, v. 190, p. 75–84, 2013.

CHAPTER 4: BIOCHEMICAL ANALYSIS – METABOLIC VIEW

ABSTRACT

Carbohydrates are one of the main constituents of plants as they are building blocks of various structures and provide the energy needed for metabolic processes and the synthesis of other organic compounds. Among them, non-structural carbohydrates (NSC) play a central role, as they are the main substrates for the primary and secondary metabolism of plants. Its dynamics in the plant reflects the relationship between sources and sinks, mediating the carbon allocation process. Thus, understanding how environmental changes affect patterns and stocks of these compounds is of vital importance. In this context, the aim of this chapter was to evaluate the spatio-temporal variation of source-sink patterns of coffee trees under field conditions in response to climatic conditions through the evaluation of the NSC profile. For this purpose, in each of the samplings and portions established in the trees, data from the near infrared spectrum of leaves, stems and fruits were collected. The raw spectral data obtained were scaled into measures of NSC contents using three predictive models: Partial Least Squares Regression -PLS, Principal Components Regression -PCR and Random Forest regression - RFR. The models were calibrated with values of the six biochemical properties that make up the NSC profile, determined in the laboratory using wet chemistry methods. Thus, for each organ of the plant, a profile of NSC was obtained containing values for protein, amino acids, reducing sugars, total soluble sugars, sucrose, and starch. The complete NSC time series was correlated with the gas exchange data and the climatic characteristics of the region, using Pearson's statistical correlation analysis. The best performance in NSC prediction was with the PCR model in the spectral range of 9000-4000 cm^{-1} for leaves and stems, with no clear trend for fruits. Based on the R^2 of the models, in general, the PCR model efficiently predicted ($R^2 > 0.5$) the NSC values, showing a good agreement between the predicted and observed values. The variation of the NSC was influenced by the growth rates and by the strength of the drains, presenting higher values for leaves and fruits in relation to the stems, especially in the months of active growth. In spatial terms, the most dynamic section in NSC concentrations was the distal section in the three thirds, which may be due to being the youngest section of the tree, in addition to the most exposed to light. The main climatic determinants of these variations were temperature and precipitation, which are closely linked to the phenology of the tree. With these results, it is possible to highlight the importance of this method to characterize how the temporal and spatial patterns of the NSC signal the influence of climate on the source-sink relationship of coffee trees under field conditions.

Keywords: Carbohydrates. NSC profile. Biochemical analysis. Spectral analysis. Climatic signals.

1 INTRODUCTION

Carbohydrates are a large family of macromolecules and one of the main constituents of plants, with a central role in its functioning. They are building blocks for the construction of various plant structures, and energy carriers for plant metabolic processes. So, they are partitioned among different sinks and metabolic uses, like growth, life-maintaining functions (respiration, tissue repair/replacement, osmoregulation, etc.), reproduction or storage (Chapin F S, 1990; Tharanathan et al., 1987). Among them, non-structural carbohydrates (NSC) play a central role, as they are the main substrates for primary and secondary plant metabolism (transport, energy metabolism and osmoregulation) and are considered an indicator of the plant's carbon status, as they reflect any shortage (depletion) or surplus (accumulation), that is, the balance of the source-sink activity; mediating the carbon allocation process (Hartmann et al., 2018; Hartmann and Trumbore, 2016; Körner, 2003). These compounds are simple soluble sugars (glucose, fructose, and sucrose), starch, lipids, amino acids, fatty acids, and alcohols, being the first two the most significant portion of the energy reserves stored in plants (Hoch, Richter, and Körner, 2003).

The ongoing climate change, characterized by rising temperatures and an increase in the frequency and intensity of drought events, has repercussions on several physiological processes of plants, affecting the phenology and the process of accumulation and/or remobilization of NSC (Hoch and Körner, 2012; Tixier et al., 2020). Given the importance of NSC reserves especially in periods of carbon deficit, variations in patterns and stocks of these compounds due to climate change can lead to an overall reduction in NSC reserves, leaving plants highly vulnerable (Huang et al., 2016). Therefore, it is essential to understand how plants regulate NSC metabolism and differential carbon allocation in response to different environmental signals at different time scales. A quick and straightforward approach to assessing a plant's carbon status is to measure the size of its overall non-structural carbon stock in periods of variable demand (Körner, 2003).

This stock can be quantified using wet chemistry methods. In this type of approach, the total concentration of NSC is determined through several protocols already established in the laboratory, being time-consuming and expensive methods, especially when studying the dynamics of carbohydrates over time, which implies in very large groups of samples. In contrast, near infrared (NIR) spectroscopy is a fast and easy technique that has shown favorable for the

analysis of the chemical composition of several compounds, being used to evaluate the composition of NSC in various tissues and plant organs. After the raw spectral information is obtained, several predictive models can be used to scale the data into measures of NSC content, starting from measured values as a reference.

The development of these models from reflectance spectroscopy of different plant organs helps not only in the prediction of biochemical characteristics at different spatial and temporal scales, but also in a later step, in improving the knowledge about the relationship of these characteristics with the environment in which the plant develops. In this study, we examine beyond the ability to make generalized estimates of a set of biochemical properties in stems, fruits and leaves of coffee trees in production (*Coffea arabica* L. cv. Arara), the relationship of these properties with biomass allocation patterns and plant growth patterns in response to climate over time. Specifically, we (1) evaluated the ability to accurately estimate six biochemical properties in coffee organs from NIRS; (2) we identified the main regions of the spectrum important for the correct prediction of these properties, as well as the main models for each organ-property combination; (3) we establish the changes in the profiles of these metabolites over time in response to variation in climate.

2 REVIEW

2.1 NSC profile

Carbon can bond with many other elements, such as hydrogen and oxygen, to form large macromolecules composed of many repeated subunits. Carbohydrates are a large family of these macromolecules and one of the main constituents of plants. They are formed through photosynthesis and provide the building blocks for the construction of various plant structures, as well as the energy needed for metabolic processes and the synthesis of other organic compounds (Bernadier, 1976; Tharanathan et al., 1987).

Plant carbohydrates are generally divided in groups: monosaccharides (glucose and fructose), disaccharides (sucrose), polysaccharides (starch and fructans), oligosaccharides (raffinose) and sugar alcohols (inositol, sorbitol, and mannitol) (Magel, Einig, and Hampp, 2000; Stick and Williams, 2010; Tharanathan et al., 1987). Among these groups, there is the formation

of structural carbohydrates, which are long chain molecules used to build and solidify biomass components and structures (hemicellulose and cellulose as the main constituents of cell walls); and non-structural carbohydrates (NSC), which are the main substrates for primary and secondary plant metabolism (transport, energy metabolism and osmoregulation) (Hartmann and Trumbore, 2016).

Figure 23 - Scheme of macromolecules in plants. The colored boxes represent the molecules that were quantified in leaves, stems, and fruits of coffee plants in response to the climate.

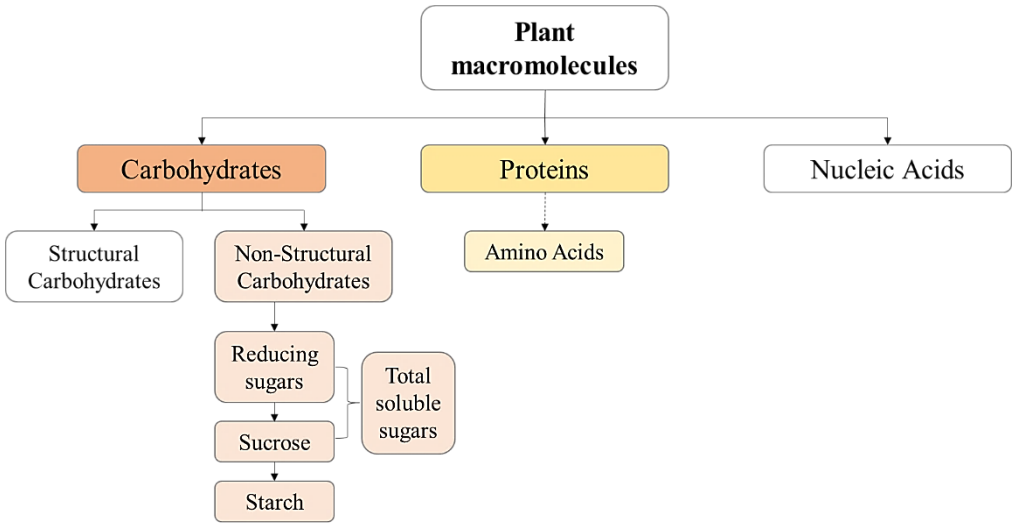

Source: From the author (2022).

For the profile constructed in this research, non-structural carbohydrates were determined, divided into total soluble sugars (TSS), reducing sugars (RS), sucrose and starch (Figure 23):

- Total soluble sugars (TSS): Nonstructural carbohydrates can be soluble like sucrose, glucose, and fructose; or insoluble like amylose and amylopectin (starch). Thus, we consider the fraction of TSS as the sum of the fraction of reducing sugars and sucrose. TSS = RS + Sucrose.
- Reducing sugars (RS): Sugars containing functional groups capable of being oxidized and, in tum, bringing about reduction of other components. The main RS known are glucose and

fructose that may be differentiated based on the location of their respective functional carbonyl group (Zoecklein et al., 1989).

- Sucrose: Most of the organic carbon produced during photosynthesis is channeled to the synthesis of this metabolite. It is the main form of carbohydrate transport in the plant, being distributed from the source to the sink tissues/organs, for the construction of permanent structural elements and as a metabolic fuel to produce energy. In addition, it is usually the major carbon source for starch synthesis in reserve tissues, acting as a temporary reserve, providing most of the carbohydrate needed for use in future growth periods (Avigad, 1982; Peat, 1946; Preiss, 1982). As a disaccharide, it does not contain free acetal hydroxyl groups, so it has no reducing action.
- Starch: It is a common constituent of higher plants present in almost all organs of the plant. Represents a more permanent form of storage, being that the starch found in chloroplasts has a more transitory nature than the starch found in reserve organs. The regulation of its biosynthesis and catabolism is a fundamental process for the control of carbon reserves in the plant (Preiss, 1982).

On the other hand, amino acids are the building blocks for proteins (another type of macromolecules in plants). Besides being traditionally regarded as precursors and constituents of proteins and other nitrogenous compounds such as nucleic acids (Kumar et al., 2017; Rai, 2002); amino acids are also involved in various functions and processes such as plant growth and development, intracellular pH control, generation of metabolic energy or redox power, signaling, and resistance to both abiotic and biotic stress (Häusler, Ludewig, and Krueger, 2014; Hildebrandt et al., 2015).

In turn, proteins are high-molecular-weight polymers of amino acids. Each protein has a specific amino acid sequence, the order of which is determined by the genetic code. Each protein can consist of a single polypeptide chain considered to be the primary structure. An aggregate of several chains linked through a peptide bond can generate a coiled structure in the form of an a-helix (secondary structure), which can fold on itself and adopt a particular three-dimensional shape (tertiary structure). Each arrangement is associated with a particular function. Proteins can

be classified based on solubility properties, according to molecular weight and based on function. They occur throughout the plant in all types of tissues and organs (Harbone, 1984).

2.2 NIRS technique

The near infrared (NIR) spectroscopy is a fast and easy technique that has lately gained wide acceptance for the analysis of the chemical composition of various plant-derived products such as grains (Batten et al., 1993; Decruyenaere et al., 2012), wine (Cayuela, Puertas, and Cantos-Villar, 2017; Ríos-Reina et al., 2018), and vegetable oils (Farres et al., 2019; Kaur, Sangha, and Kaur, 2017). Also, it has been used to evaluate the composition of NSC in various tissues and organs of plants such as stem (De Bei et al., 2017; Ramirez et al., 2015), leaves (Lohr et al., 2017; Quentin et al., 2017), wood (Tsuchikawa and Kobori, 2015). The technique is mainly used as a secondary method of measurement, validated by comparison with a primary reference method (Marrubini et al., 2017). It has the advantage of providing results with high repeatability, requiring minimal sample preparation when compared to traditional analytical methods, and allowing the evaluation of large samples. Usually, the measurement step is fast (taking less than 2 min per sample), the analyses can be carried out by non-trained personnel, and several constituents can be assayed simultaneously in the same sample (Marrubini et al., 2017).

The measurement technique is based on the absorption of electromagnetic radiation at wavelengths in the 750–2500 nm range (near infrared region) and it is used to gather information on the relative proportions of C-H, N-H and O-H (S-H) bonds, which are the primary constituents of organic compounds of plant tissue (De Bei et al., 2017; Ramirez et al., 2015). When infrared light interacts with a molecule, the analysis can be based on the absorption, emission, and reflection of that light (Pasquini, 2018). Thus, for example, the images derived from some equipment record the sample's absorbance at each wavelength, resulting in a large set of raw spectral information (Türker-Kaya and Huck, 2017).

The analysis of this information is usually done through the development of multivariate data methods and techniques, using predictive methods (calibration vs. validation), such as principal component analysis (PCA) and partial least squares regression (PLS) (Cozzolino, 2015). Initially, the raw spectral data can go through a series of spectral pretreatments (first and second derivatives) in combination with various standardization techniques to improve the quality of the information. Depending on the number of samples, it is possible to perform the analysis through

cross-validation or external validation approaches, leading to the selection of the best predictive model. Each model allows to measure the precision of the relationship between the NIR spectral values and the laboratory reference values using regression equations. Thus, it can be expected that each model has associated some statistical parameters that provide a measure of the uncertainty that can be expected for the predicted values (Lohr et al., 2017; Quentin et al., 2017).

3 METHODOLOGY

3.1 Biochemical analyzes

The biochemical analyzes were conducted at the Laboratory of Biochemistry and Molecular Physiology of Plants form the Plant Physiology Sector, Department of Biology, Federal University of Lavras, Lavras - MG, Brazil. The levels of proteins, amino acids, reducing sugars (RS), total soluble sugars (TSS), starch and sucrose were quantified in samples of leaves, stems, and fruits following the methodologies indicated in Figure 24.

For the extraction of carbohydrates, the methodology adapted from Zanandrea et al., (2009) was used. For each sample, 200 mg of dry and ground mass were homogenized in 10 mL of 0.1 M potassium phosphate buffer, ph = 7, and then subjected to a water bath at 40 ° C for 30 minutes. Subsequently, the samples were centrifuged at 5,000 g for 10 minutes and the supernatant was collected and stored to determine the levels of proteins, amino acids, RS, and TSS. In turn, the pellet was stored, in a -20 ° C freezer, for further determination of starch.

Figure 24 - Methodologies used to quantify the profile of carbohydrates, amino acids, and proteins.

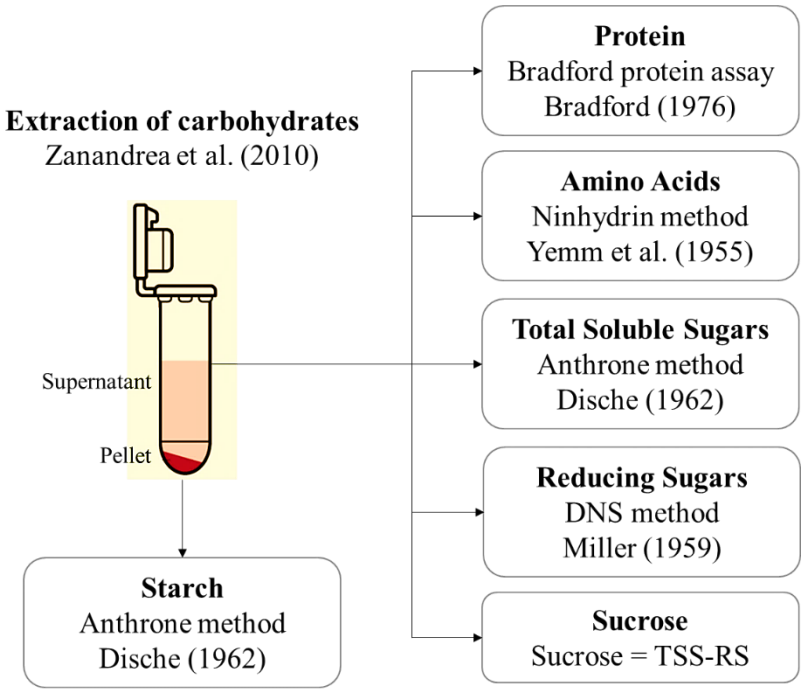

Source: From the author (2022).

3.1.1 Protein

The total protein content was quantified from the crude carbohydrate extract by the Bradford protein assay (Bradford, 1976). This method is based on a standard curve, whose standard used is Bovine Albumin Serum (BSA - 2.5mg / mL) in increasing concentrations. 294 µl of the Comassie Blue reagent is added to both, the curve and the aliquots of the samples and the volume is made up to 6 µl with water. To prepare the Comassie Blue, a day before analysis 100 mg of Comassie blue was dissolved in 50 ml of 95% ethanol and then 100 ml of 85% H_3PO_4 was added, making up to 1 L with water. After overnight in constant agitation, the reagent was filtered and stored in glass protected from degradation by light. The mixture was directly pipetted onto the plate for reading on the spectrophotometer at 595 nm.

3.1.2 Amino Acids

The total amino acids content was quantified from the crude carbohydrate extract by the ninhydrin method (Yemm, Cocking, and Ricketts, 1955). For each amino acid quantification

session, the following reagents were prepared: (A) 0.2M sodium citrate buffer, pH = 5.0, (B) 5% ninhydrin in methyl celosolve (Ethylene glycol monomethyl ether), (C) 2% KCN in methyl celosolve (2 ml of 0.01M KCN in 100 ml of methylcelosolve), 60% (v / v) ethanol and glycine or any other amino acid in 0.1µmol / ml concentration, which will be the standard used on the standard curve in increasing concentrations. Initially, 1.7 ml of the mixture of reagents A, B and C (0.5 ml, 0.2 ml, and 1 ml, respectively) was added to both, the curve, and the aliquots of the samples and then the glass tubes were shaken and taken to a water bath at 100ºC for 20 minutes to develop the color. Then, the volume to 4 ml was made up with 60% ethanol and shaken again. After cooling, a reading was made on the spectrophotometer at 570 nm.

3.1.3 Total soluble sugars

The total soluble sugars were quantified from the crude carbohydrate extract by the anthrone method (Yemm and Willis, 1954) (Dische, 1962). This method is based on a standard curve, whose standard used is glucose 60µg / mL in increasing concentrations. Both the curve and the aliquots of the samples was added 2 ml of anthrone reagent, and the volume was made up to 3 ml with water. The anthrone was prepared from 40 g of anthrone, 1 ml of water and 20 ml of sulfuric acid PA. After cooling to room temperature or on ice, the reading was made at 620 nm in a spectrophotometer.

3.1.4 Reducing sugars (RS)

The reducing sugars were quantified from the crude carbohydrate extract by the dinitro salicylic acid (DNS) method (Miller, 1959). The quantification of reducing sugars is based on a standard curve, whose standard used is 10 mM glucose in increasing concentrations. 0.5 ml of the Dinitrosalicylic Acid reagent (DNS) is added both the curve and the aliquots of the samples, and the volume is made up to 1.25 ml with water. To prepare the DNS, 50 ml of 2N sodium hydroxide (NaOH) was added to 2.5 g of DNS and approximately 125 ml of distilled water, stirring until dissolved. Subsequently, 75g of Rochelle salt was added and the volume of the solution was made up to 250 ml. Since the reagent is unstable in the presence of light and CO_2, whenever it was prepared it was stored in a dark glass in the refrigerator. After adding the DNS in each glass tube, they were shaken and taken to the water bath at 100 ºC for 5 minutes. After cooling to room temperature, the volume to 5 ml was made up with distilled water. Plates were filled with the contents of each tube and a reading was made on the spectrophotometer at 540 nm.

3.1.5 Sucrose

Sucrose was determined by subtracting the TSS value minus the RS value, as described in the following equations:

$$TSS = RS + Sucrose \quad (1)$$

$$Sucrose = TSS - RS \quad (2)$$

3.1.6 Starch

After obtaining the crude carbohydrate extracts, the resulting pellet was resuspended with 4 mL of the 200 mM potassium acetate buffer, pH 4.8 and 1 mL of the 1 mg / mL amyloglucosidase enzyme solution (1 mg of the enzyme in 1 mL of buffer). Subsequently, the samples were incubated in a water bath at 40 ° C for 2 hours and then centrifuged at 5,000 g for 10 minutes. The supernatant was collected, and the starch was quantified by the Antrona method described previously (Dische, 1962; Yemm and Willis, 1954).

3.2 Spectral analysis

The spectral analyzes were conducted at the Department of Forestry, Federal University of Lavras, Lavras - MG, Brazil. The near-infrared spectra were acquired using the Bruker spectrometer (model MPA, Bruker Optik GmbH, Ettlingen, Germany) based on a Fourrier transform and equipped with an integrating sphere. Spectral acquisition was performed within a spectral range between 12,500 and 3600 cm^{-1} with a spectral resolution of 8 cm^{-1} in the diffuse reflectance mode with an integrating sphere. Each dried and ground sample of leaf, stem or fruit was placed into a 7 ml vial for NIRS analysis (Figure 25). Each spectrum represented the average of 16 scans and for each sample or background, two readings were taken; the background readings being represented by a standard Bruker gold reference that was used every 30 samples. The resulting data was stored on the computer with the extension "Sample_name.0" and " Sample_name.1" for the two readings per sample, respectively. These files were converted to a ".txt" format, using the Spectragrypgh software (https://www.effemm2.de/spectragryph/).

Figure 25 - Equipment and tools used to acquire the spectra of samples (a) Bruker spectrometer (model MPA, Bruker Optik GmbH, Ettlingen, Germany) (b) Vials with coffee leaf samples

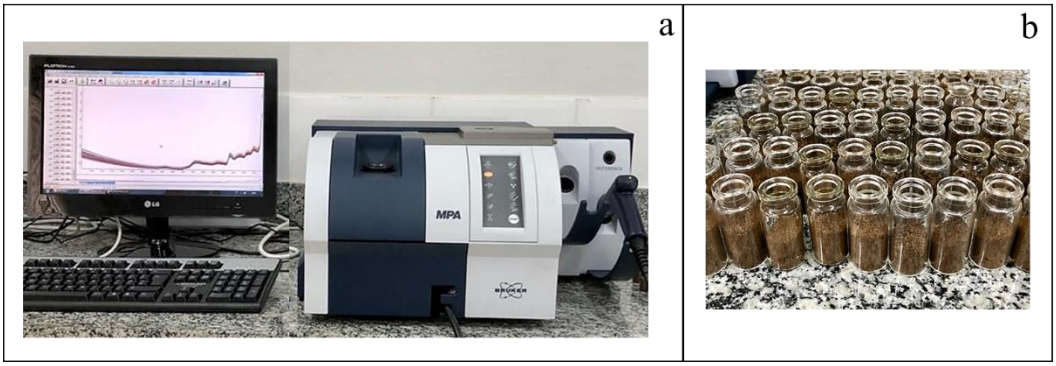

Source: From the author (2022).

Spectral information was determined for all samples from the 17 samplings, totaling more than 3200 samples that passed through the spectrometer. With the samples from the six samplings that were also analyzed by biochemical methods in the laboratory, three different regression models were calibrated and validated in order to predict the values of the 11 remaining samplings. In a general way, these regressions models were applied to associate the variations in the spectra (Matrix X) with the variations in the NSC (Matrix Y). For each combination of biochemical property and organ type, the three models were calibrated in the three spectral ranges for a total of 162 models tested (6 biochemical traits x 3 models x 3 ranges x 3 organs). For example, the three regression models (PLSR, PCR and RFR) were calibrated in the three spectral ranges mentioned above for the leaf-protein, stem-protein, and fruit-protein combination, and so on for the other biochemical properties evaluated in the laboratory. In all cases, 75% of the matrix was used for the "training" process and the remaining 25% for the "testing" process. The selection of the best regression models for each combination was based on the coefficient of determination (R^2) and the root mean square error (RMSE), resulting from the testing step. More specific details of the model calibration and validation process can be found in the Supplementary Material – Annex A.

4 RESULTS

4.1 Biochemical analyzes

Six biochemical properties were analyzed considering four variation factors (samplings – S, Organs – O, thirds – Th and sections – Se, and the interactions between them) (Table 12). Considering the factors individually, all properties evaluated were significantly influenced ($p < 0.05$, F-test) by the samplings and organs, all properties except AA were significantly influenced ($p < 0.05$, F-test) by the thirds and only RS and TSS were significantly influenced ($p < 0.05$, F-test) by the sections. Likewise, there were several properties that were significantly influenced by the double, triple, and quadruple interactions of the factors (Table 12).

Table 12 - F-values and significance levels in four-way ANOVA of biochemical properties of samples from coffee plants in production evaluated in 6 samplings over time and sampled in 9 regions distributed in thirds and sections along the tree.

Factor	PTNA	RS	AA	TSS	Starch	Sucrose
Sampling (S)	30.6451 ***	42.8736 ***	58.8432 ***	81.7898 ***	205.9341 ***	79.4379 ***
Organs (O)	221.1410 ***	867.0445 ***	34.5137 ***	259.8641 ***	363.0889 ***	7.1063 ***
Third (Th)	11.6993 ***	36.1621 ***	1.0900 ns	25.7886 ***	50.2994 ***	3.6331 *
Section (Se)	0.0452 ns	37.6566 ***	1.3158 ns	20.7607 ***	1.5781 ns	1.8950 ns
S x O	56.2035 ***	39.0623 ***	79.7355 ***	28.4172 ***	45.6828 ***	13.0753 ***
S x Th	2.2976 *	3.3537 ***	3.6226 ***	3.7014 ***	1.4366 ns	1.6689 ns
O X Th	1.8092 ns	19.6410 ***	3.3536 ***	13.9042 ***	28.5130 ***	3.2530 *
S x Se	2.7965 **	3.8088 ***	3.0424 ***	1.4659 ns	1.9112 *	0.4284 ns
O x Se	3.2588 *	5.3425 ***	1.0382 ns	4.6000 **	9.9334 ***	4.1121 **
Th x Se	1.4593 ns	1.3198 ns	2.5806 *	1.6367 ns	3.6311 **	1.3213 ns
S x O x Th	3.2224 ***	3.6818 ***	2.8790 ***	1.8816 *	8.1712 ***	2.0808 **
S x O x Se	1.7924 *	2.7496 ***	1.1073 ns	2.6650 ***	2.4345 **	2.1280 **
S x Th x Se	1.0660 ns	0.6647 ns	1.5856 *	1.6141 *	2.0623 **	1.7899 *
O x Th x Se	4.1155 ***	1.1834 ns	0.8961 ns	1.4009 ns	1.1372 ns	2.2747 *
S x O x Th x Se	1.9141 **	1.3077 ns	1.2088 ns	1.7777 *	2.1285 ***	1.7789 *

Note. Protein (µg protein g^{-1} DM); RS, Reducing Sugars (µmol glucose g^{-1} DM); AA, Amino Acids (µmol aa g^{-1} DM); TSS, Total Soluble Sugars (µmol glucose g^{-1} DM); Starch (µmol glucose g^{-1} DM); Sucrose (µmol glucose g^{-1} DM). Significance levels are: *** ($p < 0.001$), ** ($p < 0.01$), * ($p < 0.05$), “ ($p < 0.1$), ns, not significant. Source: from the author (2022).

Considering the temporal variation (between the samplings), in general, there was no clear trend, and for each biochemical parameter evaluated, there was a different trend over time. However, it is possible to identify that TSS presented higher concentrations in relation to starch both in the growing season and in the reduced growth period. Thus, there was no clear increase in starch concentration in the quiescent phase. Regarding spatial variation (between thirds and between plant organs), in general terms, the fruits had the highest content of protein, RS, TSS and starch, followed by leaves and stems. On the other hand, the content of AA and sucrose was higher in stems than in other organs. In relation to the thirds, there was a decreasing gradient for AA, TSS, starch and sucrose with higher contents in the UT (the youngest region of the tree) and smaller ones in the LT (the oldest region of the tree). In turn, the protein and RS contents were higher in the MT of the tree, where the most productive region is found. Between the sections on the horizontal axis there was no clear trend, as there was a short gap between the three sections (close values). The NSC content quantified in each of the sampled divisions of the coffee trees (as an individual factors) is shown in Table 13.

Table 13 - Protein, reducing sugars (RS), amino acids (AA), total soluble sugars (TSS), starch and sucrose contents obtained in the six samplings evaluated in coffee trees.

FACTOR	PROTEIN	RS	AA	TSS	STARCH	SUCROSE
Sampling (S)						
S2	11779.01±692.869	150.89±5.202	97.02±5.525	195.34±5.869	64.52±1.522	44.45±1.877
S6	9705.71±540.674	206.64±10.553	39.21±14.815	318.46±11.439	157.29±5.384	111.82±5.482
S8	11787.68±315.938	151.51±5.634	74.00±4.446	219.14±6.565	114.90±2.467	67.63±4.808
S11	8206.21±291.149	158.44±4.861	139.76±7.620	263.08±6.788	156.22±5.444	104.64±5.226
S15	12021.55±741.944	177.34±6.853	46.32±2.221	324.79±9.251	164.44±6.032	147.45±5.925
S17	14179.07±253.833	142.17±6.349	154.86±10.032	265.29±9.839	134.91±4.615	123.12±5.278
SED	1253.75	16.77	20.82	20.90	11.17	12.12
Organs (O)						
Leaves	11217.40±351.324	203.14±3.223	69.68±1.946	299.21±5.825	135.07±3.008	96.08±4.183
Stems	8892.41±201.934	93.45±1.817	113.55±8.093	201.88±3.519	105.10±1.749	108.44±2.702
Fruits	16144.39±725.912	241.72±7.160	91.66±5.985	324.78±10.383	176.55±7.800	83.06±5.690
SED	831.36	8.06	10.25	12.41	8.54	7.56
Third (Th)						
LT	9961.47±317.633	147.47±4.305	89.66±5.234	238.72±5.556	112.68±3.066	91.25±3.596
MT	11871.22±430.580	175.67±5.090	88.15±4.747	275.83±6.716	134.40±3.799	100.16±4.048

UT	11818.77±429.735	171.41±5.310	100.24±9.239	277.06±7.159	146.51±4.426	105.65±4.186
SED	686.27	8.52	11.63	11.28	6.59	6.84
Section (Se)						
D	10847.28±297.385	177.00±4.285	99.81±8.564	276.40±6.005	127.97±2.926	99.39±4.077
I	11338.38±399.331	166.87±4.865	86.46±4.558	267.81±6.580	131.53±3.771	100.94±3.724
P	11411.48±490.734	147.67±5.589	91.31±5.689	242.80±6.861	132.19±4.786	95.13±4.078
SED	699.09	8.56	11.25	11.24	6.76	6.86

Note. UT, Upper third; MT, Middle third; LT, Lower third; D, Distal; I, Intermediate; P, Proximal. Protein (µg protein g^{-1} DM); RS, Reducing Sugars (µmol glucose g^{-1} DM); AA, Amino Acids (µmol aa g^{-1} DM); TSS, Total Soluble Sugars (µmol glucose g^{-1} DM); Starch (µmol glucose g^{-1} DM); Sucrose (µmol glucose g^{-1} DM). SED, standard error of the difference between two treatment means. Values are reported as means ± standard error (n= for S, n=8 for Ti, n= for Th, n= for Se). Source: from the author (2022).

To visualize the distribution and grouping of data more clearly, the PCA performed is shown in Figure 26. Between the first two components the 63.2% of the data variation is explained. Depending on the way the data was organized, protein and AA have positive loadings on component 2 when grouped by sections and plant organs, and negative loadings on the same component when grouped by thirds and samples. The same trend happened for RS, TSS and sucrose, with positive and negative loadings on component 1, depending on the way the data were grouped. From the proximity and angle between the vectors, it can be inferred that there is a positive correlation between RS, TSS and sucrose. Also, considering the scores in the biplot, the separation of groups between the data is not clearly displayed.

Without further visualization of separate groups through PCA, the data were plotted in the form of a boxplot that allows a good visualization of the data distribution (Figure 27). Starting from a basic visual analysis, in general it is possible to observe that for most properties it is possible to visualize a "cyclicality" in which the trend presented in 2017 (S2 to S8) is the same presented in 2018 (S11 to S17), with some changes in the data amplitude. The widest differences between minimum and maximum values were presented for the fruits, being that the Y-axis scales for these graphs have a greater amplitude. For example, while protein reached values below 20,000 µg protein g^{-1} DM for leaves and stems, fruits reached values close to 50,000 µg protein g^{-1} DM. Likewise, while starch reached values below 250 µmol glucose g^{-1} DM for leaves and stems, fruits reached values close to 400 µmol glucose g^{-1} DM. Furthermore, both sucrose and starch have an increasing trend over the time of the study period for the three organs.

Figure 26 - Biplot with confidence ellipses (95%) as a result of the Principal Component Analysis – PCA - of biochemical properties from samples from coffee plants in production evaluated in 17 samplings over time and sampled in 36 regions distributed in thirds and sections along the tree. (a) PCA grouped by tree thirds (b) PCA grouped by sections (c) PCA grouped by plant organs and (d) PCA grouped by samplings.

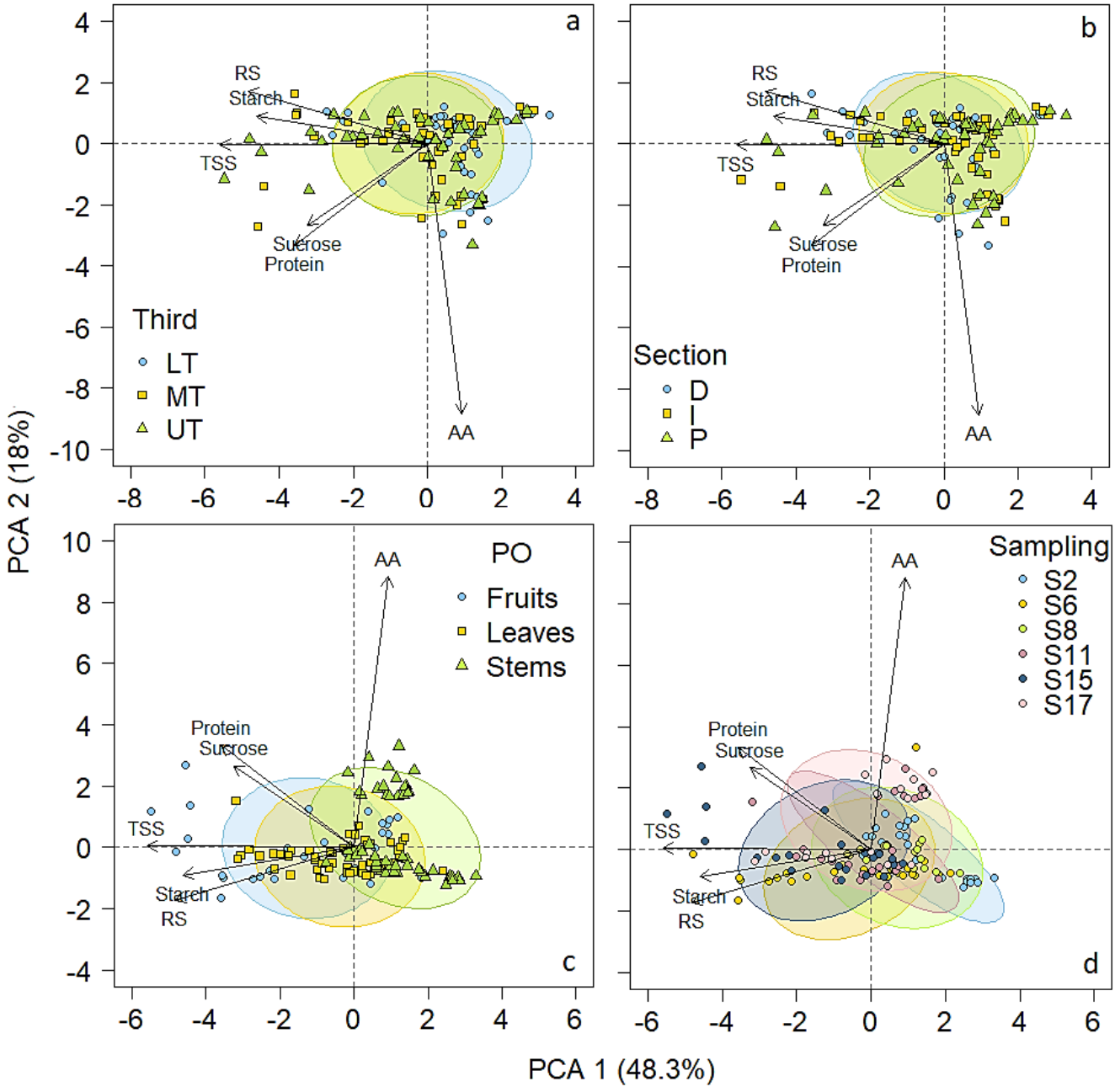

Source: From the author (2022).

Figure 27 - Data distribution of biochemical properties evaluated in laboratory in the three organs (a) leaves (b) stems (c) fruits. Each box represents a different sampling for a total of 6 samplings for leaves and stems and 4 samplings for fruits. Protein (µg protein g^{-1} DM); RS, Reducing Sugars (µmol glucose g^{-1} DM); AA, Amino Acids (µmol aa g^{-1} DM); TSS, Total Soluble Sugars (µmol glucose g^{-1} DM); Starch (µmol glucose g^{-1} DM); Sucrose (µmol glucose g^{-1} DM).

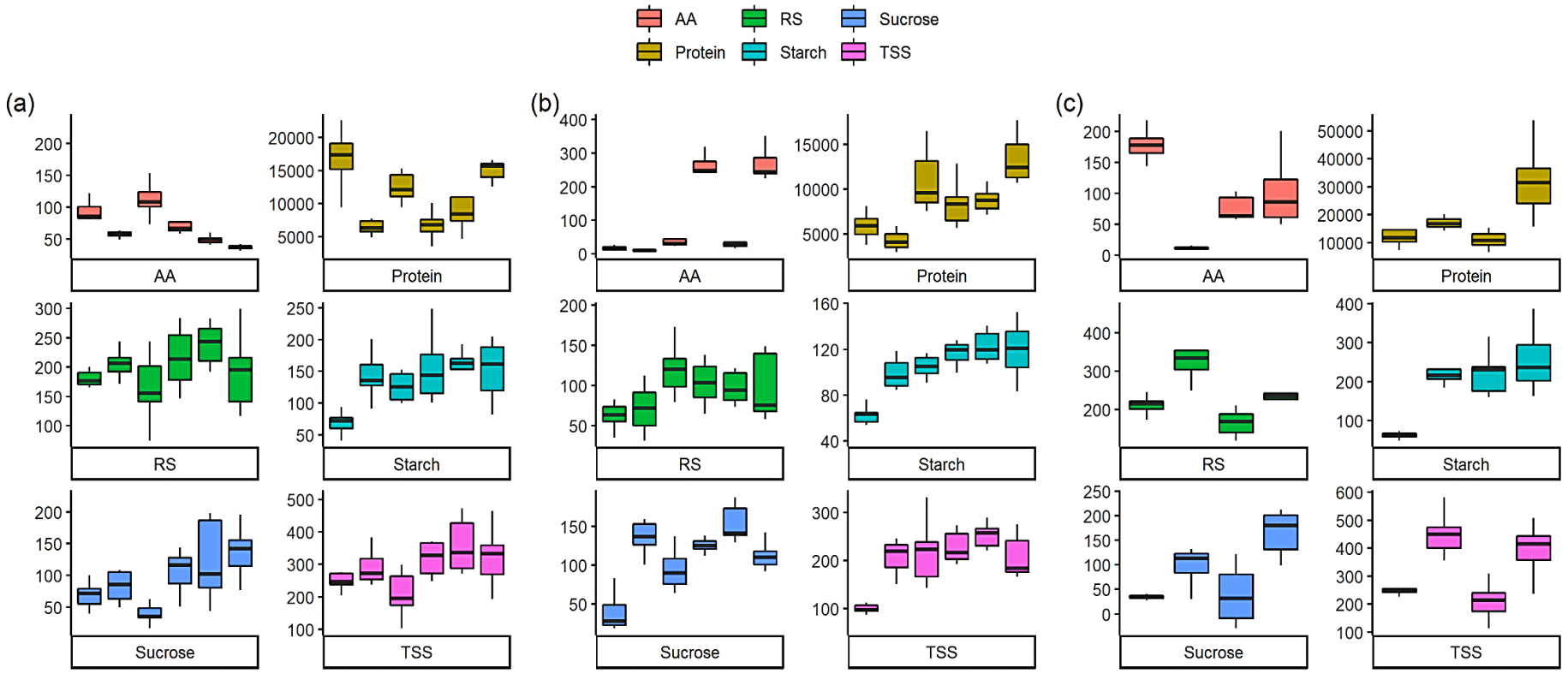

Source: From the author (2022).

4.2 Spectral analyzes

NIR spectral signatures recorded from leaves, stems and fruits from coffee plants are shown in Figure 28. Each line represents the average of NIR spectra taken from the different plant organs. The arrows at the bottom of the graph show the three spectral ranges tested to select the best model-range combination for each organ and NSC. In general, in the region between 12,500 and 9,000 cm^{-1} the spectrum of leaves and fruits are very close, having a different behavior from the spectrum of stems. In the region between 9,000 and 5,500 cm^{-1} the spectrum of leaves and stems are close, being overlapped in some ranges, while the spectrum of fruits presents higher absorbance values. Although the values are different, the trend of the lines follows the same pattern. In the region between 5,500 and 4,000 cm^{-1} the spectrum of leaves and stems remains close and overlapping at some points, and the spectrum of fruits reaches some peaks above 1, which could be associated with noise.

Figure 28 - Original NIR spectra recorded from samples of coffee plants in production. Arrows indicate the three spectral ranges tested to choose the best prediction model. SR1, 12500-4000 cm^{-1}; SR2, 9000-4000 cm^{-1}; SR3, 12500-5500 cm^{-1}.

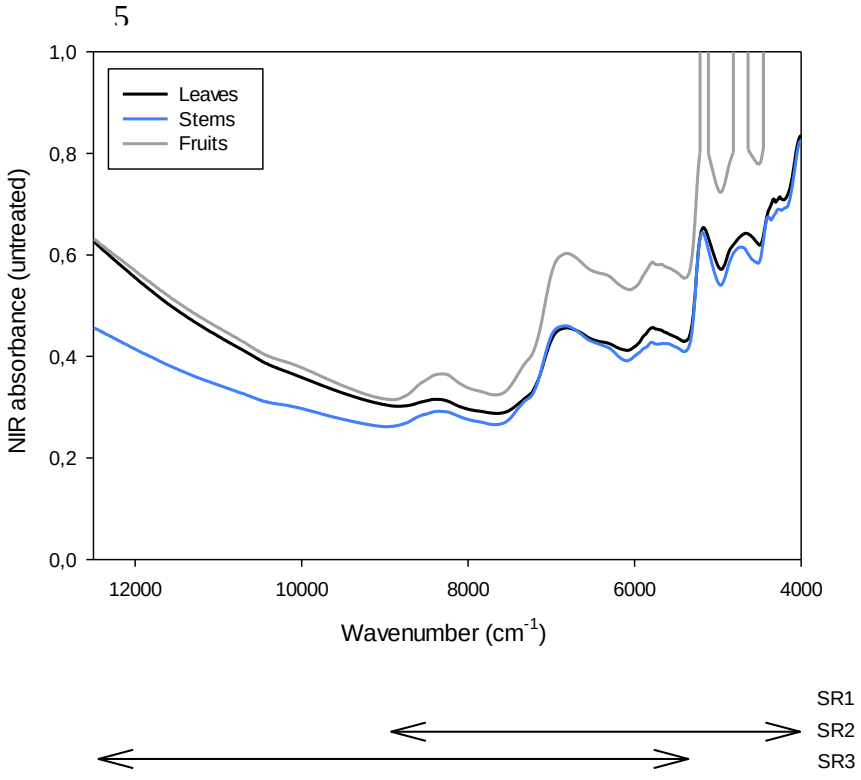

After the calibration and validation process of the prediction models described in Annex A, the complete time series was obtained for the values of biochemical properties. In Figure 29 it is possible to visualize the distribution of the data. Starting from a basic visual analysis, in general it is possible to observe that the predicted values present a smaller dispersion in relation to the measured values, given that the boxes of samplings 2, 6, 8, 11, 15 and 17 are usually larger, representing a greater amplitude/dispersion in the data. Specifically for leaf (Figure 29a), it can be observed that the median of data from measured samplings vs. observed samplings are "relatively similar" for RS, starch, TSS and AA; while, for protein and sucrose, the median of samplings with measured values is lower, in a low proportion, in relation to the median of the samplings with predicted values. This pattern is repeated for the stem for some biochemical properties such as AA, protein, and sucrose (Figure 29b), this time being a much larger and substantial difference, approximately up to 150-200 µmol g^{-1} DM for amino acids, 5000 µg g^{-1} DM for proteins and 100 µmol glucose g^{-1} DM for sucrose.

In the case of fruits, there are data for only 12 samplings, the remaining 5 corresponding to the period from June 2017 to January 2018 (S7 to S11), period in which the quiescent phase and the new vegetative period occur. AA, proteins, and sucrose showed the opposite trend towards leaves and stems, with the medians of the samplings measured greater than the medians of the predicted samplings (Figure 29c), with approximate differences of up to 150 µmol g^{-1} DM for amino acids, 2000 µg g^{-1} DM for proteins and 150 µmol glucose g^{-1} DM for sucrose. Starch had lower medians at samplings 2 and 8 up to 150 µmol glucose g^{-1} DM, and RS and TSS had similar medians for all samplings.

Figure 29 - Complete time series with data distribution of biochemical properties in the three organs evaluated (a) leaves (b) stems (c) fruits. Each box represents a different sampling for a total of 17 samplings for leaves and stems and 12 samplings for fruits. Protein (µg protein g^{-1} DM); RS, Reducing Sugars (µmol glucose g^{-1} DM); AA, Amino Acids (µmol aa g^{-1} DM); TSS, Total Soluble Sugars (µmol glucose g^{-1} DM); Starch (µmol glucose g^{-1} DM); Sucrose (µmol glucose g^{-1} DM).

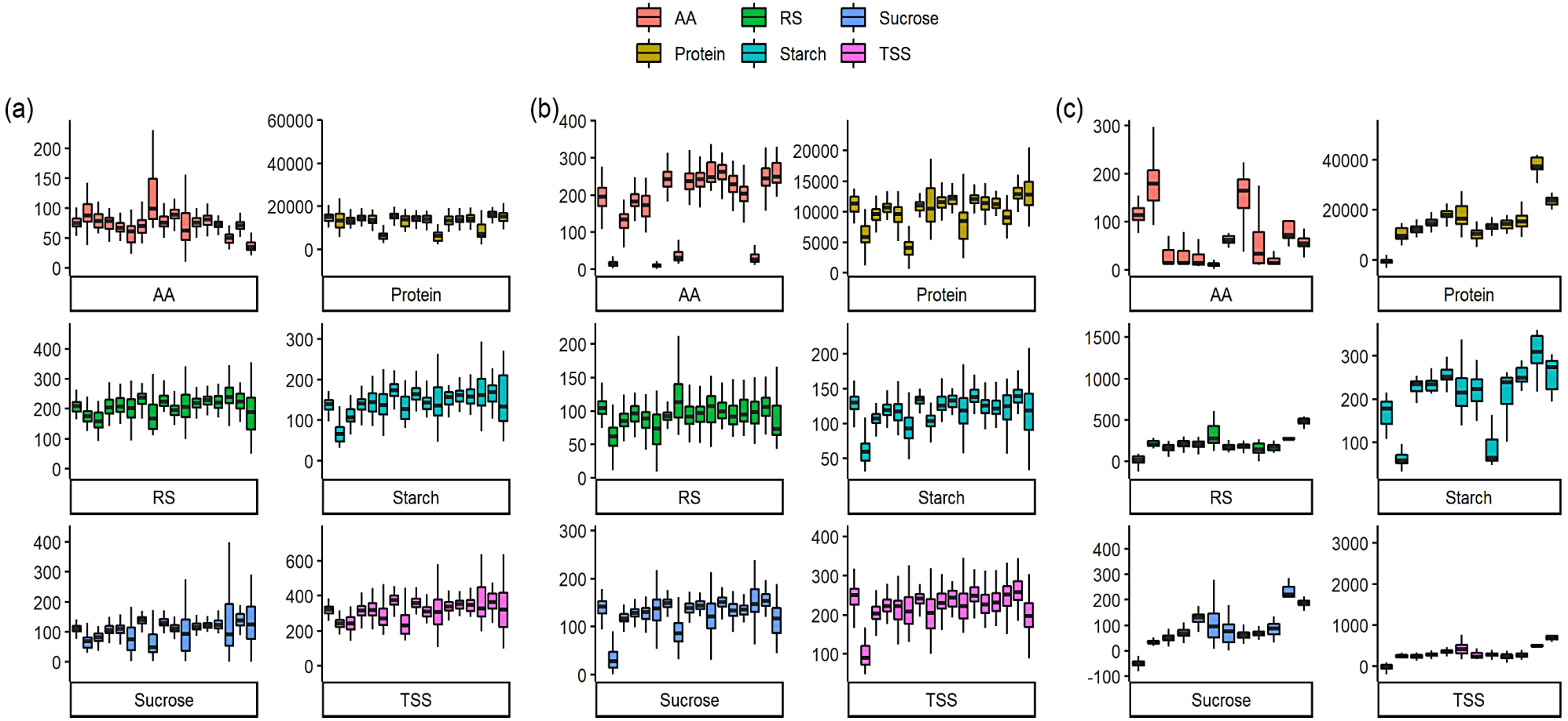

The complete time series was correlated with the gas exchange data, and the results are presented in Table 14. Among the organs, the one that presented more significant correlations ($p<0.05$) with the gas exchange was the fruits, followed by the stems and leaves. In turn, among the measured gas exchanges, transpiration showed more significant correlations ($p<0.05$) with biochemical properties for all plant organs. Leaf temperature was the least correlated variable.

Table 14 - Pearson's correlation analysis between the gas exchange and the biochemical variables. Correlation made by organs.

Fruits			Leaves			Stems		
Variable	**r**	***p***	**Variable**	**r**	***p***	**Variable**	**r**	***p***
LeT (°C)								
			Protein	-0.2080	0.0185	RS	0.3468	0.0001
						TSS	0.2026	0.0252
BrT (°C)								
Protein	-0.2664	0.0149	AA	0.3056	0.0005			
RS	-0.3029	0.0054						
TSS	-0.2830	0.0095						
Sucrose	-0.3069	0.0048						
***A* (µmol m^{-2} s^{-1})**								
AA	0.2571	0.0190	Protein	0.1877	0.0339	Protein	0.1862	0.0400
Starch	-0.2826	0.0096	Starch	-0.1774	0.0451	RS	0.2093	0.0207
Sucrose	-0.2458	0.0251				Sucrose	-0.2123	0.0189
gs (mol H_2O m^{-2} s^{-1})								
AA	0.2648	0.0156	Starch	-0.2839	0.0012	Protein	-0.2106	0.0199
Starch	-0.2817	0.0099				TSS	-0.2736	0.0023
						Starch	-0.2980	0.0009
						Sucrose	-0.2767	0.0020
***E* (mmol H_2O m^{-2} s^{-1})**								
Protein	-0.2679	0.0143	RS	-0.2697	0.0021	RS	0.2427	0.0071
AA	0.2181	0.0477	AA	0.2260	0.0103	Sucrose	-0.3273	0.0002
Starch	-0.2337	0.0335	TSS	-0.2855	0.0011			
Sucrose	-0.3644	0.0007	Starch	-0.3334	0.0001			
			Sucrose	-0.2471	0.0049			

Note. LeT, leaves temperature (°C); BrT, branch temperature (°C); *A*, net photosynthetic rate (µmol m^{-2} s^{-1}); *E*, transpiration rate (mmol H_2O m^{-2} s^{-1}). AA, Amino Acids (µmol aa g^{-1} DM); TSS, Total Soluble Sugars (µmol glucose g^{-1} DM); Starch (µmol glucose g^{-1} DM); Sucrose (µmol glucose g^{-1} DM). Colors are indicators of significant correlations: $p < 0.05$ (red) and $p < 0.1$ (yellow). Source: from the author (2022).

Regarding annual climate variability, considering all the temporal variation (S1 to S17), the results of Pearson's correlation between the NSC data and the evaluated climatic variables showed that minimum, mean and maximum temperature, as well as ETo, correlated significantly ($p < 0.05$) with all NSC, while SL did not correlate with any of them. Precipitation and water balance correlated with only 4 NSC, which were protein, AA, starch, and sucrose. Wind speed correlated with RS, AA, starch and sucrose, and evaporation in turn correlated with the last three. Thus, amino acids, starch and sucrose were the NSCs that showed the most correlations, suggesting that their metabolism is directly associated with climatic influence (Figure 30).

On the other hand, when the spatial variation between the thirds is considered, the results of the Pearson correlation show, in general, that contrary to the growth and gas exchange data presented in chapter 2, this time the most dynamic third in relation to presenting more significant correlations with the climatic variables was the UT, followed by MT and UT. The main NSC that were most influenced by climate were TSS, starch and sucrose. The main climatic variables that most correlated with NSC were temperature (minimum, medium and maximum) and ETo. SL and RH did not show significant correlations with any of the NSCs. More detailed results can be seen in Figure 31.

In the case of the sections, the NSC presented significant correlations with the climatic variables in a similar way in all sections, being representative the section I and P, contrary to the growth and gas exchange data in which the most dynamic section was the D. As in the thirds, the main NSC influenced by climate were TSS, starch and sucrose, and the main climatic variables that had more influence on the NSC were temperature (minimum, medium and maximum), Prec and ETo. More detailed results can be seen in Figure 32.

Figure 30 - Pearson's correlation analysis between the NSC data and the evaluated climatic variables. Positive significant correlations (blue squares), negative significant correlations (red squares) and no correlation (white squares). Significant correlation: $p<0.05$. (b) Principal component analysis—PCA with confidence ellipses (95%)

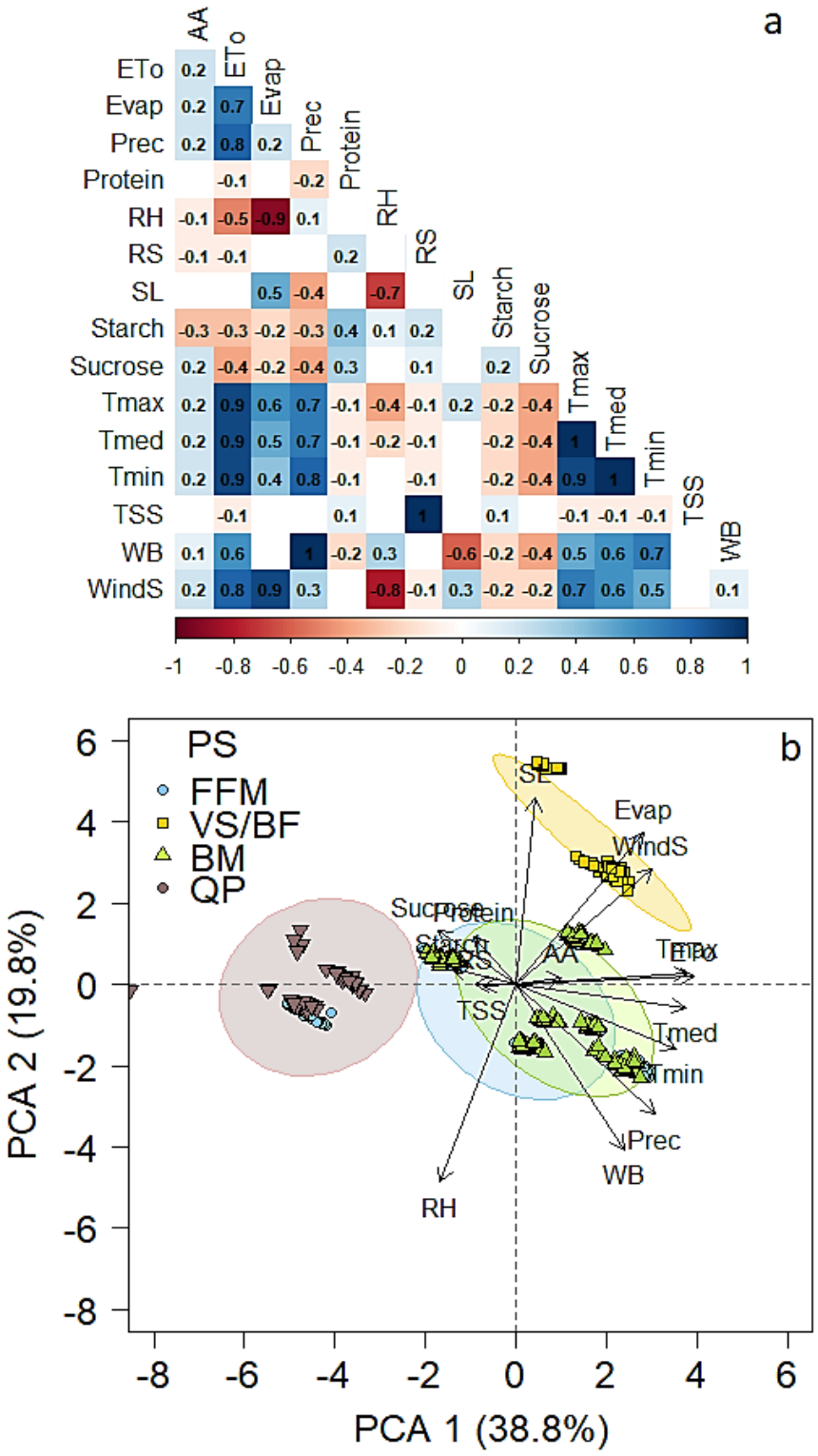

Figure 31 - Pearson's correlation analysis between the isotopic data separated between the thirds and the evaluated climate variables. The bars only show the significant correlations obtained ($p<0.05$).

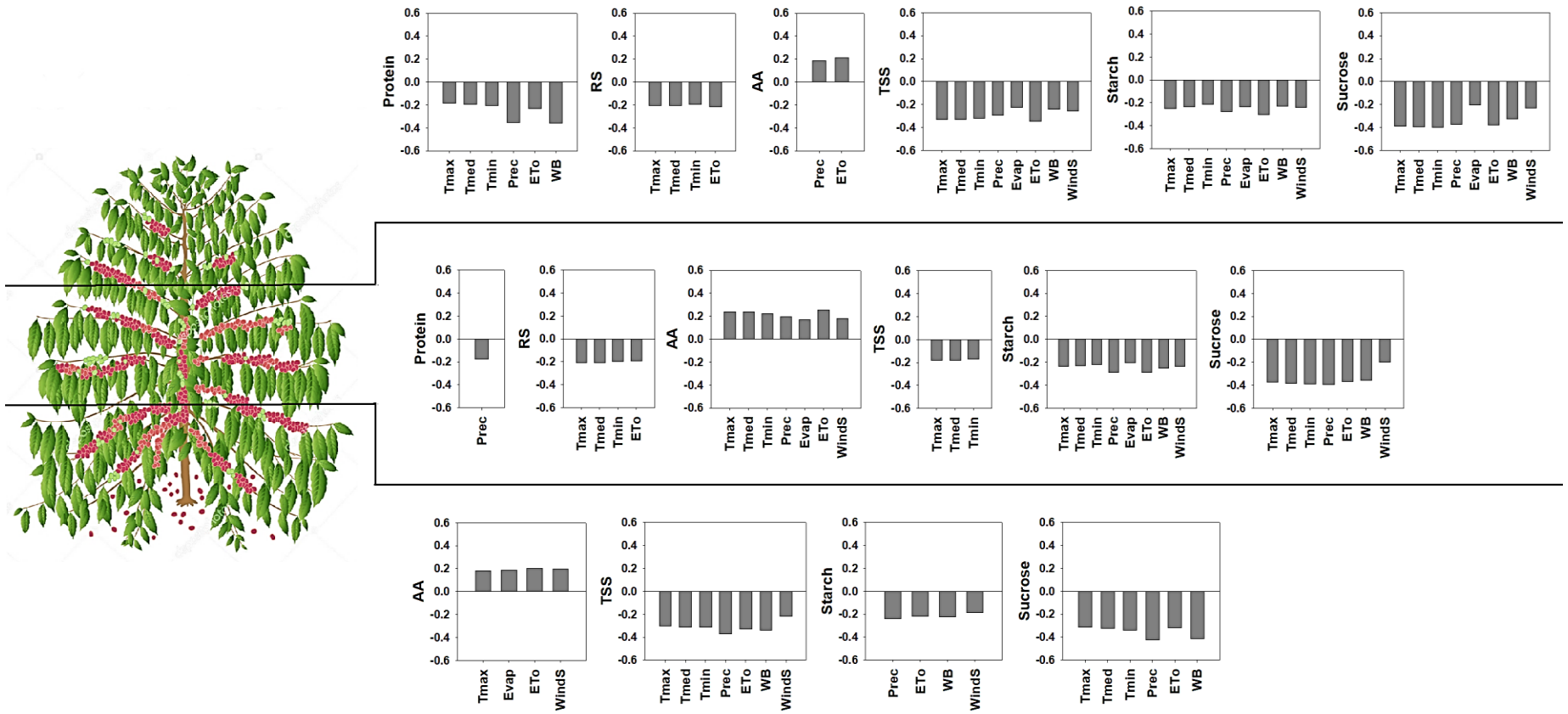

Source: From the author (2022).

Figure 32 - Pearson's correlation analysis between the growth data separated between the sections and the evaluated climate variables. The bars show only the significant correlations obtained ($p<0.05$).

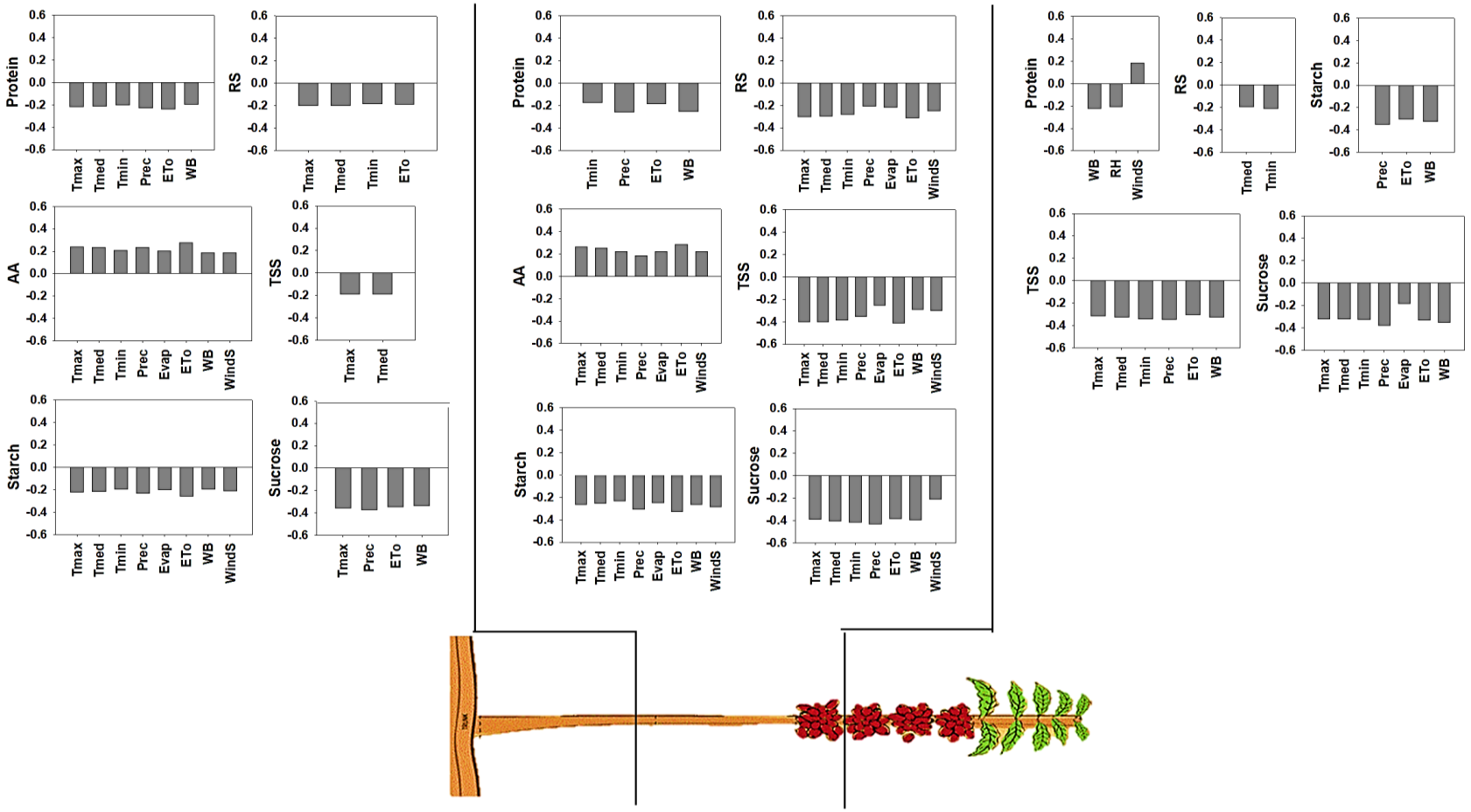

Source: From the author (2022).

5 DISCUSSION

In this chapter we address source-sink patterns on coffee trees and their relationship to annual climate variability through of the dynamics of carbohydrates, proteins, and AA for the complete data series. As mentioned before, the series comprises the data of NSC, proteins and AA for the 17 samplings, six of them of measured data and the remaining 11 of predicted data. The data include the variation between plant organs (Leaves, stems, and fruits), between tree thirds (LT, MT and UT) and between plagiotropic branch sections (P, I and D). Thus, covering the temporal and spatial variation of the dynamics of C compounds for coffee under field conditions.

Carbohydrate metabolism is critical for plant life, which need to assimilate C for the accumulation of structural biomass and for sustaining the metabolism associated with the construction and maintenance of such biomass, including reproductive structures (Sala et al., 2012). Furthermore, due to being sessile, a pool of non-structural stored C is needed in order to buffer periods of stress, especially in long-lived perennial species (Kozlowski and Pallardy, 2002; Sala et al., 2012). NSC storage dampens the asynchrony of C supply and demand at various time scales (daily, seasonal, or decadal) and between plant organs. Although there is a basic understanding of their different functional roles in the plant - transport, energy metabolism and osmoregulation - the understanding of storage dynamics at those different scales is still limited, being essential to improve the understanding of NSC in the face of environmental changes (Hartmann and Trumbore, 2016).

In our results, almost all biochemical variables evaluated were influenced by at least three of the four variation factors, which indicates that there is an influence of both the temporal and spatial scales for the storage of NSC, always varying according to the phenological stage and climate of the region.

5.1 Temporal variation

As trees depend on NSCs and replenish stored ones throughout the year, seasonal variation in storage is driven by the balance between sources and sinks (Furze et al., 2019). The most commonly used measure to determine the dynamics of NSC over time has been tracking/quantifying the concentration of NSC in plant tissues/organs. Depending on tissue type,

these concentrations indicate a range of temporal dynamics, providing insights into how trees manage NSC resources such as 'cash flow' (sugars) and NSC storage (starch) during the growing season (Hartmann et al., 2020; Hartmann and Trumbore, 2016).

Seasonal variations of NSC can be induced by seasonal regimes of temperature or water or by the phenological patterns that these regimes induce (Würth et al., 2005). For example, in temperate regions, NSCs are expected to increase throughout the growing season when photosynthesis is high, accumulate as growth slows, and decrease during the dormant season when photosynthesis is low and reserves are used for respiration (Furze et al., 2019). In the humid tropics, the rainy season represents a period of rapid growth with high consumption of C and lower levels of reserves, with the dry period being characteristic of NSC accumulation and little or no growth (Körner, 2015). This dynamic reflects the trend that when growth is slow or zero, the concentration of NSC is commonly high and vice versa.

Formation, filling and ripening of fruits (S1 to S6)

In the region, the active growth phase of the coffee tree occurs between September and March, a period in which temperatures are high and rainfall is abundant. As seen in chapter 2, the 2016/2017 season of positive bienniality, had between S1 and S6 the growth and expansion of the fruits for the half-year harvest. In this period, without clear increasing or decreasing trends, considering both the measured values (Table 13, Figure 27) and the predicted values (Figure 29, SM Table 5), proteins, TSS and starch were the dominant NSC in the fruits, followed by the leaves and stems. The AA showed the same trend in the measured data, with a contrary trend for the predicted data due to differences in the medians.

The highest photosynthetic rates in these months and the high demand for carbohydrates by the fruits for their growth and expansion (strong sink) support the highest values of NSC in the fruits and leaves. Silva et al., (2004), found similar concentrations between TSS and starch during the coffee growing season, with a small tendency to higher values for TSS, which in our case was not a subtle difference with values up to double. This is related to the information reported by Körner (2015) who argues that in the period of rapid and active growth there are reduced levels of reserves, supporting higher TSS values. On the other hand, stems and thick roots usually have low NSC concentrations (as shown in our results), when compared to other

plant organs; although they comprise a fundamental part of the stock of NSC in trees (Hartmann and Trumbore, 2016).

Quiescent phase (S7 to S8 and S17)

Subsequently, continuing with the chronology, growth rates gradually decrease from April, reaching low values between June and September, periods when temperatures are lower, rainfall is scarce, and photoperiods are shorter. The cessation of growth is associated with internal and external factors such as phenology, low temperatures, and low availability of soil water. Thus, the accumulation of NSC occurs because the potential for absorption exceeds the potential for structural investment (Körner, 2015). This same trend has been reported in other woody species from both the tropics and temperate regions (Furze et al., 2019; Richardson et al., 2013, 2015; Würth et al., 2005).

At this time, TSS and starch peaks are normally reached (Furze et al., 2019; Silva et al., 2004). This agrees with our results that both leaves and stems peaked for protein, TSS, and starch in samplings S7, S16, and S17 in the lowest growth months (Figure 29, SM Table 5). At this point, the reserves can be kept stored to face periods of stress or can be used to support the growth of new branches and new foliage for the renewal of the canopy for the following season.

New vegetative phase (S9 to S16)

The new crop characterized by negative bienniality comprised the new vegetative growth after a high fruit load. After the quiescent phase, the distinction between immediate and future needs is important for forecasting the seasonal dynamics of NSC. While the accumulated starch may be a purely storage compound for future use, TSS play immediate roles in supporting the new demands for growth and respiration (Martínez-Vilalta et al., 2016). Therefore, this may indicate that strong activity from sinks such as new roots, branches and leaves could in principle be built up using the reserves as the demand for C exceeds what is being produced by photosynthesis; or from new C sources (Richardson et al., 2013).

There are studies supporting both types of sources. For example, sprouting and new shoot growth may be independent of storage compounds due to the high concentrations of NSC while these processes take place (Hoch et al., 2003). They can be supplied by the C coming from reserves that were fixed years ago (Herrera-Ramírez et al., 2020). Or they may be supplied by a

mixed pool derived from newer C sources and older C sources (Carbone et al., 2013; Hartmann and Trumbore, 2016). In our results, after the quiescent phase there was no downward trend in the concentrations of NSC, proteins and AA. This may indicate that the supply of C by photosynthesis may be sufficient and is providing all the metabolic and growth needs of the sinks. This without affecting the reserves, keeping the levels in the evaluated organs relatively stable.

However, it is important to note that the concentration values for each organ alone do not provide a detailed or specific source and age of C used by the plant, nor a whole-tree view. For this purpose, other types of tools are necessary, such as those reported by Herrera-Ramírez et al., (2020) and Hartmann et al., (2020).

5.2 Spatial variation

As mentioned before, the distribution patterns of photoassimilates between sources and sinks are complex, due in part to the different ages and characteristics of branches with different photosynthetic and nutrient transport capacity. Although the characteristics of leaves, branches, dry matter, and gas exchange showed a decreasing trend from LT to UT; in terms of NSC, protein and AA concentrations, the trend was opposite in both measured and predicted data (Table 13, SM Table 6). This suggests strong source-sink activity between plant organs and parts of the tree.

In all thirds, the most dynamic section in terms of NSC exchanges and concentrations is the D section, which may be due to its being the most exposed to light. According to Ngao et al., (2020), under high fruit load, maximum investment in C assimilation along with rapid export of photoassimilates from all leaves are necessary to sustain fruit growth. This requires optimizing light capture, which can be achieved by modifying the allocation of C. Thus, the optimal allocation of N within trees to maximize light harvest and photosynthesis occurs as a function of fruit load (Ding et al., 2017). This can be evidenced in our results in the highest values of foliar protein and protein in the fruits in the months in which the highest values of A (SM Table 5, SM Table 6) were presented, with less investment in protein in the branches. Also, the negative correlation between A and the concentrations of TSS, starch and sucrose (Table 14) may support the idea of rapid export of these NSC to the fruits, especially in years of high fruit load.

6 CHAPTER HIGHLIGHTS

1. The concentration of NSC in plant organs can be used as an indication of the temporal and seasonal dynamics of C metabolism in plants.
2. Seasonal temperature and/or water regimes influence the variation in NSC. For many woody species from temperate and tropic regions, it has been reported that when growth is slow or zero, the concentration of NSC is commonly high and vice versa; the growth rates being influenced by the water factor and the temperature.
3. Distinguishing between immediate and future needs is important for understanding the seasonal dynamics of NSC. Source-sink patterns influence how trees manage NSC resources such as 'cash flow' (sugars) and NSC storage (starch) during the growing season.
4. The growth and reproduction processes can be supplied with new sources of C (newly assimilated), sources of C fixed with antiquity or from a mixed pool of the two sources. Our results cannot demonstrate the age or which type of source was used to supply the metabolic and growth processes of the coffee plants.
5. The regions with the highest concentrations of NSC were the distal section of all thirds, especially the upper and middle thirds.

REFERENCES

AVIGAD, C. **Sucrose and other dissaccharides.** In: Storage Carbohydrates in Vascular Plants, ed. Lewis D.H., 53-73, Cambridge University Press, Cambridge. 1982.

BATTEN, G. D. et al. Non-structural carbohydrate: Analysis by near infrared reflectance spectroscopy and its importance as an indicator of plant growth. **Plant and Soil**, v. 155–156, n. 1, p. 243–246, 1993.

BERNADIER, C. D. **Carbohydrate Metabolism: Regulation and Physiological Role.** Hemisphere Pub. Corp. 318p. 1976.

BRADFORD, M. A Rapid and Sensitive Method for the Quantitation of Microgram Quantities of Protein Utilizing the Principle of Protein-Dye Binding. **Analytical Biochemistry**, v. 72, n. 1–2, p. 248–254, 1976.

CARBONE, M. S. et al. Age, allocation and availability of nonstructural carbon in mature red maple trees. **New Phytologist**, v. 200, n. 4, p. 1145–1155, 2013.

CAYUELA, J. A.; PUERTAS, B.; CANTOS-VILLAR, E. Assessing wine sensory attributes using Vis/NIR. **European Food Research and Technology**, v. 243, n. 6, p. 941–953, 2017.

CHAPIN F S. The ecology and economics of storage in plants. **Annual Review of Ecology, Evolution, and Systematics**, v. 21, p. 423–427, 1990.

COZZOLINO, D. Infrared spectroscopy as a versatile analytical tool for the quantitative determination of antioxidants in agricultural products, foods and plants. **Antioxidants**, v. 4, n. 3, p. 482–497, 2015.

DE BEI, R. et al. Rapid measurement of total non-structural carbohydrate concentration in grapevine trunk and leaf tissues using near infrared spectroscopy. **Computers and Electronics in Agriculture**, v. 136, p. 176–183, 2017.

DECRUYENAERE, V. et al. Development of near-infrared spectroscopy calibrations to quantify starch and soluble sugar content in the roots of Rumex obtusifolius. **Weed Research**, v. 52, n. 1, p. 1–5, 2012.

DING, N. et al. Effects of crop load on distribution and utilization of 13 C and 15 N and fruit quality for dwarf apple trees. **Scientific Reports**, v. 7:14172, n. November 2016, p. 1–9, 2017.

DISCHE, Z. **General color reactions**. In 'Carbohydrate chemistry'. Eds RL Whistler, ML Wolfram. Academic Press: New York. pp. 477–520. 1962.

FARRES, S. et al. Argan oil authentication using visible/near infrared spectroscopy combined to chemometrics tools. **Vibrational Spectroscopy**, v. 102, n. September 2018, p. 79–84, 2019.

FURZE, M. E. et al. Whole-tree nonstructural carbohydrate storage and seasonal dynamics in five temperate species. **New Phytologist**, v. 221, n. 3, p. 1466–1477, 2019.

HARBONE, J. B. **Phytochemical Methods. A guide to modern techniques of plant analysis**. Second Edi ed. London: [s.n.].

HARTMANN, H. et al. Identifying differences in carbohydrate dynamics of seedlings and mature trees to improve carbon allocation in models for trees and forests. **Environmental and Experimental Botany**, v. 152, n. September 2017, p. 7–18, 2018.

HARTMANN, H. et al. Plant carbon allocation in a changing world – challenges and progress: introduction to a Virtual Issue on carbon allocation: Introduction to a virtual issue on carbon allocation. **New Phytologist**, v. 227, n. 4, p. 981–988, 2020.

HARTMANN, H.; TRUMBORE, S. Understanding the roles of nonstructural carbohydrates in forest trees - from what we can measure to what we want to know. **The New phytologist**, v. 211, n. 2, p. 386–403, 2016.

HÄUSLER, R. E.; LUDEWIG, F.; KRUEGER, S. Amino acids - A life between metabolism and signaling. **Plant Science**, v. 229, p. 225–237, 2014.

HERRERA-RAMÍREZ, D. et al. Probability distributions of nonstructural carbon ages and transit times provide insights into carbon allocation dynamics of mature trees. **New Phytologist**, v. 226, n. 5, p. 1299–1311, 2020.

HILDEBRANDT, T. M. et al. **Amino Acid Catabolism in PlantsMolecular Plant**, 2015.

HOCH, G.; KÖRNER, C. Global patterns of mobile carbon stores in trees at the high-elevation tree line. **Global Ecology and Biogeography**, v. 21, n. 8, p. 861–871, 2012.

HOCH, G.; RICHTER, A.; KÖRNER, C. Non-structural carbon compounds in temperate forest trees. **Plant, Cell and Environment**, v. 26, n. 7, p. 1067–1081, 2003.

HUANG, J. et al. Winter wheat optimizes allocation in response to carbon limitation. v. 18, p. 2328, 2016.

KAUR, B.; SANGHA, M. K.; KAUR, G. Development of Near-Infrared Reflectance Spectroscopy (NIRS) Calibration Model for Estimation of Oil Content in Brassica juncea and Brassica napus. **Food Analytical Methods**, v. 10, n. 1, p. 227–233, 2017.

KÖRNER, C. Carbon limitation in trees. **Journal of Ecology**, v. 91, n. 1, p. 4–17, 2003.

KÖRNER, C. Paradigm shift in plant growth control. **Current Opinion in Plant Biology**, v. 25, p. 107–114, 2015.

KOZLOWSKI, T. T.; PALLARDY, S. G. Acclimation and adaptive responses of woody plants to environmental stresses. **Botanical Review**, v. 68, n. 2, p. 270–334, 2002.

KUMAR, V. et al. Differential distribution of amino acids in plants. **Amino Acids**, v. 49, n. 5, p. 821–869, 2017.

LOHR, D. et al. Non-destructive determination of carbohydrate reserves in leaves of ornamental cuttings by near-infrared spectroscopy (NIRS) as a key indicator for quality assessments. **Biosystems Engineering**, v. 158, p. 51–63, 2017.

MAGEL, E.; EINIG, W.; HAMPP, R. Carbohydrates in trees. **Developments in Crop Science**, v. 26, n. C, p. 317–336, 2000.

MARRUBINI, G. et al. Determination of the Sugar Content in Commercial Plant Milks by Near

Infrared Spectroscopy and Luff-Schoorl Total Glucose Titration. **Food Analytical Methods**, v. 10, n. 5, p. 1556–1567, 2017.

MARTÍNEZ-VILALTA, J. et al. Dynamics of non-structural carbohydrates in terrestrial plants: A global synthesis. **Ecological Monographs**, v. 86, n. 4, p. 495–516, 2016.

MILLER, G. L. Use of DinitrosaIicyIic Acid Reagent for Determination of Reducing Sugar. **Analytical Chemistry**, v. 31, n. 3, p. 426–428, 1959.

NGAO, J. et al. Spatial variability in carbon and nitrogen related traits in apple trees: the effecs of the light environment and crop load. **Journal of Experimental Botany.**, 2020.

PASQUINI, C. Near infrared spectroscopy: A mature analytical technique with new perspectives – A review. **Analytica Chimica Acta**, v. 1026, p. 8–36, 2018.

PEAT, S. Plant Carbohydrates. **Annu. Rev. Biochem.**, v. 15, p. 75–92, 1946.

PREISS, J. Regulation of the biosynthesis and degradation of starch. **Annual Review of Plant Physiology**, v. 33, p. 431–454, 1982.

QUENTIN, A. G. et al. Application of near-infrared spectroscopy for estimation of non-structural carbohydrates in foliar samples of Eucalyptus globulus Labilladière. **Tree Physiology**, v. 37, n. 1, p. 131–141, 2017.

RAI, V. K. **Role of Amino Acids in Plant Responses to Stresses**, 2002. Disponível em: <internal-pdf://0892970347/RAI et al 2002 Role of Amino Acids in Plant R.pdf>

RAMIREZ, J. A. et al. Near-infrared spectroscopy (NIRS) predicts non-structural carbohydrate concentrations in different tissue types of a broad range of tree species. **Methods in Ecology and Evolution**, v. 6, n. 9, p. 1018–1025, 2015.

RICHARDSON, A. D. et al. Seasonal dynamics and age of stemwood nonstructural carbohydrates in temperate forest trees. **New Phytologist**, v. 197, n. 3, p. 850–861, 2013.

RICHARDSON, A. D. et al. Distribution and mixing of old and new nonstructural carbon in two temperate trees. **New Phytologist**, v. 206, n. 2, p. 590–597, 2015.

RÍOS-REINA, R. et al. NIR spectroscopy and chemometrics for the typification of Spanish wine vinegars with a protected designation of origin. **Food Control**, v. 89, p. 108–116, 2018.

SALA, A.; WOODRUFF, D. R.; MEINZER, F. C. Carbon dynamics in trees: Feast or famine? **Tree Physiology**, v. 32, n. 6, p. 764–775, 2012.

SILVA, E. A. et al. Seasonal changes in vegetative growth and photosynthesis of Arabica coffee trees. **Field Crops Research**, v. 89, n. 2–3, p. 349–357, 2004.

STICK, R.; WILLIAMS, S. **Carbohydrates: The Essential Molecules of Life**. 2nd Edition. Elsevier Academic Press. 496p. 2009.

THARANATHAN, R. N. et al. Plant carbohydrates--An overview. **Proc. Indian Acad. Sci.**, v. 97, n. 2, p. 81–155, 1987.

TIXIER, A. et al. Comparison of phenological traits, growth patterns, and seasonal dynamics of non-structural carbohydrate in Mediterranean tree crop species. **Scientific Reports**, v. 10, n. 1, p.

1–11, 2020.

TSUCHIKAWA, S.; KOBORI, H. A review of recent application of near infrared spectroscopy to wood science and technology. **Journal of Wood Science**, v. 61, n. 3, p. 213–220, 2015.

TÜRKER-KAYA, S.; HUCK, C. W. A review of mid-infrared and near-infrared imaging: Principles, concepts and applications in plant tissue analysis. **Molecules**, v. 22, n. 1, 2017.

WÜRTH, M. K. R. et al. Non-structural carbohydrate pools in a tropical forest. **Oecologia**, v. 143, n. 1, p. 11–24, 2005.

YEMM, E. W.; COCKING, E. C.; RICKETTS, R. E. The determination of amino-acids with ninhydrin. **The Analyst**, v. 80, n. 948, p. 209–214, 1955.

YEMM, E. W.; WILLIS, A. J. The estimation of carbohydrates in plant extracts by anthrone. **The Biochemical journal**, v. 57, n. 3, p. 508–514, 1954.

ZANANDREA, I. et al. Tolerance of Sesbania virgata plants to flooding. **Australian Journal of Botany**, v. 57, n. 8, p. 661–669, 2009.

ZOECKLEIN, B. W. et al. **Production Wine Analysis**. [s.l: s.n.].

FINAL CONSIDERATIONS

Brazil, especially the state of Minas Gerais, is the main coffee producer and exporter in the world. Physiological aspects such as the differential carbon investment between the different organs of the plant as a function of phenology, in temporal and spatial scales, was the main focus of this doctoral work, due to the importance and relevance of the subject for management, agroecological and socioeconomic issues.

With the aim of identify in detail the spatio-temporal patterns of the source-sink relationship in coffee trees under field conditions in response to climate, three analytical methods were approached: primary and secondary growth analysis, stable isotopic analysis, and biochemical analysis to quantify the non-structural carbohydrate profile validated by near infrared spectroscopy (NIRS).

Through growth analysis we identified patterns of biomass allocation for leaves, stems, and fruits as a function of plant phenology, corroborating the bienniality dynamic that exist in the region for arabica coffee. This dynamic is closely linked to the negative correlation that exists between growth and reproduction. We identified the most dynamic regions of the tree in terms of growth and the high capacity of the fruits to import carbohydrates, constituting strong sinks in relation to vegetative and storage structures. We also identified the possibility of using dimensional parameters of the tree's growth rings (width and area) to indirectly determine, through modeling tools, the allocation of biomass to the different organs of the plant and the dynamics of the primary growth of the tree.

Through stable isotopic analysis, we quantified the isotopic ratios of carbon and nitrogen ($\delta^{13}C$ and $\delta^{15}N$) of different plant organs over time. A non-significant temporal variation of the C isotopic ratio was found, since it is an inherent characteristic of the carboxylative metabolism of the plant, with characteristic values of a C3 plant. In turn, the N isotopic ratio changed in time, apparently as a function of the fertilization of the experimental plot. In terms of spatial variation, heterotrophic tissues such as stems and fruits showed more C13 in relation to leaves, and the lower third of the trees was more depleted in relation to the other thirds. This spatial pattern may be due to the fact that only the distal section of the entire tree was analyzed, without considering

the intermediate and proximal sections. Again, the fruits comprised a strong drain with a high capacity to import resources from other source structures of the trees.

Through biochemical analysis and the carbohydrate profile we identified the patterns of NSC accumulation in different parts of the plant over time. Differences were found in the accumulation of immediate use compounds such as total soluble sugars and the accumulation of storage compounds such as starch, as a function of phenology, growth rates, seasonality, and climate. From the values determined in the laboratory, we evaluated the ability to accurately estimate six biochemical properties from NIR spectra, identifying the main regions of the spectrum that are important for the correct prediction of these properties, as well as the main models with the best statistical performance for each combination of organ and NSC.

Through this long-term study and with a systematic and thorough sampling, we were able to use these three methods to get closer to the "metabolic flux" approach initially proposed. We had an **integrative view** of the physiological processes and climate controls involved in the allocation and investment of carbon and nitrogen for growth, reproduction, and storage in the different portions of the tree canopy throughout the experimental period.

SUPPLEMENTARY MATERIAL

ANNEX A – Climatic information database

SM Table 1 - Database with the climatic information obtained after the data quality control process and after the determination of the calculated variables

Year	Tmin	Tmed	Tmax	SL	RH	WindS	Prec	Evap	ETo	Max Tmax	Min Tmin
2011											
Jan	18.77	22.74	28.91	5.57	79.87	1.38	437.77	75.50	136.50	33.90	15.60
Feb	18.15	23.42	30.82	7.15	71.36	1.31	124.90	97.93	135.50	33.40	14.80
Mar	18.20	21.80	27.49	3.66	81.12	1.18	271.23	61.50	109.60	32.00	13.80
Apr	15.74	20.61	27.84	6.78	77.27	1.07	81.57	72.63	97.70	31.30	10.00
May	12.18	17.29	25.03	6.91	76.58	1.02	19.07	70.13	78.20	28.40	5.40
Jun	8.95	14.81	23.37	6.71	76.68	1.06	34.43	67.73	65.40	27.10	0.70
Jul	9.53	16.31	25.20	7.16	70.97	1.11	0.00	88.23	79.50	29.10	-0.30
Aug	11.42	18.74	27.85	7.94	62.97	1.37	8.27	134.43	109.60	32.60	0.50
Sep	11.79	19.72	28.82	7.84	53.67	1.65	2.53	152.87	139.00	34.60	2.60
Oct	15.60	20.92	27.53	5.82	68.42	1.62	148.00	117.13	137.00	35.00	9.20
Nov	15.22	20.42	27.03	6.48	71.18	1.48	136.37	92.73	135.80	32.10	9.20
Dec	17.44	21.75	28.03	5.38	79.12	1.27	321.80	76.93	138.00	32.40	12.60
2012											
Jan	17.34	21.29	27.38	4.75	80.35	1.24	391.77	67.70	130.70	31.40	13.20
Feb	17.48	22.86	29.66	7.66	71.45	1.16	89.17	102.77	134.40	33.70	13.40
Mar	16.92	21.91	29.03	6.51	74.87	1.17	121.70	89.10	126.10	33.80	13.00
Apr	16.23	20.87	27.53	6.22	78.41	1.03	56.43	73.20	95.30	31.50	10.60
May	11.56	16.77	24.01	6.34	78.82	1.00	61.93	61.97	74.70	28.10	5.40
Jun	12.26	17.02	23.89	5.11	82.88	0.81	100.23	49.67	60.00	27.80	4.00
Jul	9.19	15.71	24.59	7.53	72.47	0.97	18.57	84.40	75.40	28.70	2.00

Aug	10.02	17.14	25.35	8.23	64.93	1.45	2.53	109.90	102.80	28.40	4.60
Sep	12.40	19.77	28.55	7.81	59.59	1.52	42.57	134.17	130.30	34.70	4.20
Oct	15.91	22.55	30.39	7.76	60.93	1.45	71.63	147.60	156.10	35.90	8.80
Nov	17.05	21.68	28.12	5.85	74.15	1.51	152.37	95.17	135.20	33.60	11.40
Dec	19.01	23.64	30.52	6.48	76.71	1.21	282.23	94.47	151.10	33.20	16.40
2013											
Jan	18.05	21.98	28.17	4.65	80.75	1.40	469.30	69.37	134.80	32.20	13.00
Feb	18.23	22.88	29.85	6.41	75.80	1.02	162.27	78.33	125.20	32.60	13.60
Mar	17.96	21.82	27.83	4.65	81.25	1.13	182.50	65.97	113.40	32.30	11.80
Apr	14.63	19.34	26.00	5.74	78.94	1.13	59.80	63.27	90.10	31.00	8.60
May	12.22	17.54	24.88	6.15	78.15	1.01	53.90	69.80	76.90	29.50	4.80
Jun	12.64	17.21	24.28	5.06	83.11	0.88	27.20	53.17	61.50	27.40	6.80
Jul	9.96	15.91	24.16	6.97	75.72	1.18	45.77	75.33	74.90	29.20	-1.00
Aug	9.67	17.03	26.15	8.19	65.97	1.33	6.10	109.30	103.20	29.90	1.40
Sep	12.85	19.56	27.65	6.97	66.88	1.36	62.53	109.80	122.00	33.80	6.60
Oct	14.71	20.09	26.97	5.80	72.45	1.44	108.53	94.90	132.80	34.40	8.60
Nov	16.51	21.36	27.55	5.94	75.03	1.37	251.63	85.73	132.70	35.00	12.00
Dec	18.30	22.72	29.10	5.86	77.74	1.45	167.83	79.63	143.90	33.20	13.60
2014											
Jan	17.59	23.98	31.65	9.60	66.58	1.41	117.93	127.17	169.40	34.50	12.40
Feb	17.27	23.91	31.41	8.94	61.71	1.47	55.00	126.60	148.80	34.80	13.60
Mar	17.25	22.49	29.41	7.04	71.14	1.38	106.87	97.80	131.70	32.40	12.00
Apr	15.59	20.70	27.93	6.83	73.75	1.36	94.20	76.20	102.90	32.60	4.20
May	11.51	17.58	25.54	7.05	73.21	1.18	18.63	80.67	84.00	28.90	5.00
Jun	10.99	16.93	25.16	6.26	74.89	1.11	6.50	67.20	70.80	28.00	4.20
Jul	10.13	16.06	23.70	6.10	72.66	1.23	43.27	77.07	74.90	28.60	3.60
Aug	10.28	17.75	27.26	8.22	61.65	1.43	8.10	117.80	110.20	31.70	1.40
Sep	13.44	20.55	28.70	7.22	58.47	1.67	30.90	104.23	135.10	33.60	6.20
Oct	14.93	21.88	30.26	7.81	57.76	1.62	43.77	158.13	161.50	37.00	5.80
Nov	17.47	22.23	28.98	6.06	71.64	1.50	192.73	99.73	141.10	33.20	11.80

Dec	17.77	22.83	29.32	6.21	73.20	1.37	191.57	91.13	149.70	33.80	14.00
					2015						
Jan	18.27	24.35	31.99	8.16	67.01	1.30	78.13	125.17	167.70	36.40	14.40
Feb	18.07	22.48	29.10	5.80	78.01	1.44	225.10	71.67	123.00	32.60	14.80
Mar	17.59	21.60	27.53	4.21	82.77	1.23	198.53	60.83	111.10	31.60	12.20
Apr	16.15	20.78	27.60	6.80	76.68	1.18	35.30	68.53	97.50	31.30	10.40
May	13.22	17.79	24.34	5.52	80.35	1.15	46.33	59.07	74.00	29.60	7.40
Jun	11.29	16.65	23.95	6.13	78.42	1.13	26.90	59.07	65.20	27.80	2.80
Jul	11.74	17.33	24.90	5.66	74.62	1.07	8.17	79.47	74.70	28.50	6.80
Aug	10.84	18.21	27.25	8.27	64.10	1.18	26.73	111.40	104.80	31.20	6.20
Sep	15.00	20.81	28.01	5.83	69.41	1.15	150.00	107.33	114.70	35.80	9.40
Oct	17.11	23.37	31.36	7.73	63.53	1.29	56.30	87.13	155.60	36.20	12.40
Nov	18.71	22.97	29.55	5.09	79.26	1.21	220.07	75.67	136.40	34.20	16.20
Dec	18.90	23.00	29.68	4.91	79.78	1.22	209.43	71.93	143.70	33.50	16.60
					2016						
Jan	18.78	22.63	28.40	4.58	81.05	1.21	409.13	68.17	131.10	32.60	15.40
Feb	18.81	23.48	30.64	6.39	77.66	1.05	154.63	84.23	132.20	34.30	14.80
Mar	18.19	22.56	29.05	5.54	79.83	1.00	192.43	72.90	118.60	32.50	14.80
Apr	15.90	21.73	29.62	8.29	74.14	0.90	14.07	98.33	105.60	33.10	12.00
May	12.79	17.86	25.19	6.00	79.45	0.99	31.37	54.40	77.60	28.30	5.00
Jun	10.31	15.74	23.50	6.21	78.48	0.76	86.17	59.93	61.40	28.00	-0.80
Jul	9.49	16.49	25.81	7.74	69.30	0.95	0.00	93.50	80.60	29.70	1.50
Aug	10.96	17.99	26.93	7.82	65.73	1.02	28.97	110.03	99.50	31.70	3.40
Sep	14.08	21.02	29.86	8.08	60.20	1.39	18.97	132.27	134.80	34.30	7.40
Oct	16.42	21.66	29.03	6.56	70.90	1.35	182.47	105.60	139.90	35.70	10.00
Nov	16.70	21.60	28.08	5.89	75.35	1.25	179.07	83.83	134.10	32.60	8.60
Dec	17.59	23.02	30.22	6.81	73.30	1.33	108.97	100.63	154.80	36.10	12.40
					2017						
Jan	18.75	23.12	30.26	5.68	77.91	1.07	208.33	86.87	147.30	35.70	16.20
Feb	18.17	23.33	30.30	7.83	71.27	1.28	75.00	95.53	133.60	33.80	15.20

Mar	16.79	22.00	29.27	6.80	74.31	1.23	125.07	86.53	128.70	32.80	10.60
Apr	15.54	20.60	27.49	6.15	77.56	1.11	73.10	70.80	97.50	31.00	10.00
May	13.34	18.12	25.11	5.35	80.47	1.06	72.73	60.53	75.60	29.50	9.00
Jun	10.70	16.69	24.90	6.67	76.98	1.17	20.90	69.93	70.10	28.80	3.30
Jul	8.58	15.03	23.28	7.31	68.95	1.48	0.00	87.97	80.80	26.60	1.60
Aug	10.61	17.61	26.41	7.46	65.61	1.37	14.73	103.90	103.00	32.30	3.80
Sep	11.55	20.24	29.36	8.78	51.80	1.43	46.67	167.80	140.20	33.20	6.20
Oct	16.23	22.00	29.16	6.37	66.81	3.05	136.17	115.73	141.40	35.10	10.80
Nov	16.78	21.38	27.33	4.64	74.53	1.22	141.23	83.07	128.10	32.00	9.60
Dec	17.91	22.53	29.07	5.43	77.18	1.22	212.97	85.47	144.40	33.60	14.20
2018											
Jan	18.36	22.62	29.26	5.13	78.08	1.03	238.93	78.00	0.00	32.80	14.80
Feb	18.04	22.40	28.79	5.42	77.34	1.30	110.07	72.83	0.00	32.90	13.40
Mar	18.28	23.07	30.24	7.04	77.32	1.03	115.77	81.17	0.00	33.20	13.80
Apr	14.92	20.38	27.61	6.66	75.46	1.17	14.07	79.70	0.00	30.40	7.60
May	11.48	17.72	26.09	7.47	71.81	1.05	42.07	85.90	0.00	30.10	1.80
Jun	12.14	17.56	24.97	5.44	76.19	0.83	30.10	67.23	0.00	29.30	6.20
Jul	9.22	16.41	25.73	7.43	69.15	0.94	7.60	90.13	0.00	28.60	1.70
Aug	11.68	17.36	24.93	5.84	71.55	1.07	67.40	84.00	0.00	29.60	3.60
Sep	13.91	20.18	27.95	6.88	66.78	1.33	69.47	107.90	0.00	33.90	5.80
Oct	17.17	21.49	27.64	4.54	78.90	1.18	204.10	71.87	0.00	33.20	7.80
Nov	17.45	21.39	26.92	4.38	79.79	1.27	203.57	41.73	0.00	32.70	13.60
Dec	17.70	22.81	30.04	7.23	73.79	1.11	254.57	62.63	0.00	34.60	8.80

Source: from the author (2022).

ANNEX B - Calibration and validation of prediction models

All statistical analyzes were conducted using the RStudio statistical software (Version 1.2.5033 © 2009-2019 RStudio, Inc.). The main open-source packages used were “caret”, “pls”, “plsdepot”, “mlbench” and “randomForest”. NIR spectra are subject to interference from several factors and, therefore, pre-treatment of the data collected in the spectrum is necessary to reduce noise and improve the calibration adjustment of the created models. Thus, in order to evaluate the spectral range that best fits and generates the best prediction values, the general database was filtered/reorganized, evaluating three different spectral ranges: 12,500 to 4000, 9,000 to 4,000 and 12,500 to 5,500 cm^{-1}.

We utilized a modeling approach to predict the biochemical properties of the three coffee organs from spectral information using three different models: (1) Partial least squares regression – PLSR, (2) Principal components regression – PCR, and (3) Random Forest regression - RFR. Multivariate regression methods like PCR and PLSR are standard statistical approaches used in chemometric analyzes that have been designed to confront the situation that there are many, possibly correlated, predictor variables, and relatively few samples, reducing the large predictor matrix (i.e., spectral reflectance data) down to a relatively few, noncorrelated latent components (Mevik and Wehrens, 2020; Serbin et al., 2014). On the other hand, RFR builds multiple decision trees which are known as forest and glue them together to urge a more accurate and stable prediction. In this approach, multiple trees are generated by bootstrap samples from training data and then the correlation between the trees is reduced (Breiman, 2001; Breiman and Cutler, 2018).

In a general way, these regressions models were applied to associate the variations in the spectra (Matrix X) with the variations in the NSC (Matrix Y). For each combination of biochemical property and organ type, the three models were calibrated in the three spectral ranges for a total of 162 models tested (6 biochemical traits x 3 models x 3 ranges x 3 organs). For example, the three regression models (PLSR, PCR and RFR) were calibrated in the three spectral ranges mentioned above for the leaf-protein, stem-protein, and fruit-protein combination, and so on for the other biochemical properties evaluated in the laboratory. In all cases, 75% of the matrix was used for the "training" process and the remaining 25% for the "testing" process. The selection of the best regression models for each combination was based on the coefficient of determination (R^2) and the root mean square error (RMSE), resulting from the testing step.

After the model calibration and validation step, in which the best range and regression model was obtained for each organ-NSC pair, the model was run on a set of data disposed for the prediction process. This dataset consists of the reflectance spectra measurements of the 11 remaining samplings in which no laboratory measurements were made to determine the NSC (Figure 3). The database totals 3264 samples (1350 leaf, 1282 stem and 632 fruit), and in the same way, for each sample, two readings were taken. From this data set, when running the model, the same number of samples were obtained with the predicted values of the 6 biochemical properties. With this, it was possible to count on the complete database with the temporal and spatial variation of the NSCs for its subsequent analysis and correlation with the climatic characteristics of the region. The quality of the prediction was established by comparing against the measured values, considering minimum and maximum values, the mean, number of NAs and negative values for each biochemical variable.

Results

Regarding the best results found in terms of spectral range and models (SM Table 2), for leaf and stems, the main regression model which had the best performance was the PCR, in the spectral range of 9000-4000 cm^{-1}. In the case of fruits, each type of NSC performed better with a different model and spectral range. Based on R^2, in general, the PCR model efficiently predicted ($R^2 > 0.5$) the values of the biochemical properties, showing a good agreement between the predicted and observed values (SM Table 2). The properties that presented models with the best performance were amino acids and starch, while protein and sucrose presented the lowest performance. The RMSE of the models varied for each property as follows: 2,008.00 to 5218.00 µg protein g^{-1} MS, 15.18 to 60.90 µmol RS g^{-1} MS, 17.24 to 32.95 µmol aa g^{-1} MS, 30.82 to 98.78 µmol of glucose g^{-1} MS for TSS, 17.59 to 34.13 µmol of glucose g^{-1} MS for starch and 27.16 to 37.19 µmol of glucose g^{-1} MS for sucrose. These values correspond to 16-43%, 8-34%, 18-35%, 11-36%, 12-25% and 28-39% of the average value observed, for each property respectively.

SM Table 2 - Spectral range and model combinations that showed the best performance for each plant organ and biochemical property

Organ		Protein	RS	AA	TSS	Starch	Sucrose
Leaves	SR	9000-4000	9000-4000	9000-4000	9000-4000	9000-4000	9000-4000
	RM	PCR	PCR	PCR	PCR	PCR	PCR
	R^2	0.331	0.388	0.649	0.421	0.544	0.155
	RMSE	3591.00	32.92	17.24	58.13	30.83	37.19
Stems	SR	9000-4000	12500-4000	9000-4000	9000-4000	9000-4000	9000-4000
	RM	PCR	RF	PCR	PCR	PCR	PCR
	R^2	0.560	0.526	0.782	0.663	0.606	0.548
	RMSE	2008.00	15.18	47.08	30.82	17.59	27.16
Fruits	SR	12500-5500	12500-4000	12500-4000	9000-4000	12500-5500	12500-5500
	RM	PCR	PLSR	RF	PLSR	RF	PCR
	R^2	0.152	0.694	0.765	0.572	0.726	0.4435
	RMSE	5218.00	60.90	32.95	98.78	34.13	36.94

Note. SR, spectral range; RM, regression model; R^2, coefficient of determination; RMSE, root mean square error. RS, reducing sugars; AA, amino acids; TSS, total soluble sugars. PCR, principal components regression model; PLSR, partial least squares regression model; RF, Random Forest regression model. Source: From the author (2022).

After running all models, predicted values were generated. SM Table 3 shows the summary of the prediction and its quality, based on the count of total, NAs and negative values and the calculation of the mean, minimum and maximum for both measured and predicted values. In none of the cases missing values/NAs were generated, but the models executed for the fruits predicted a good number of negative values, which would have no biological sense. In this case, the greatest number of negative values generated was for the protein and sucrose properties, in which 50 and 68 negative values were presented, respectively, which corresponds to 8 and 10% of the total predicted data value for the fruits.

SM Figure 1- Regression models performance for datasets. Observed vs. predicted plots are shown for each biochemical property and the three plant organs: (a) leaves, (b) stems, (c) fruits. The black lines indicate 1:1 relation and the blue line represents the best fit for linear regression between the observations and predictions made for datasets. RS, reducing sugars; AA, amino acids; TSS, total soluble sugars.

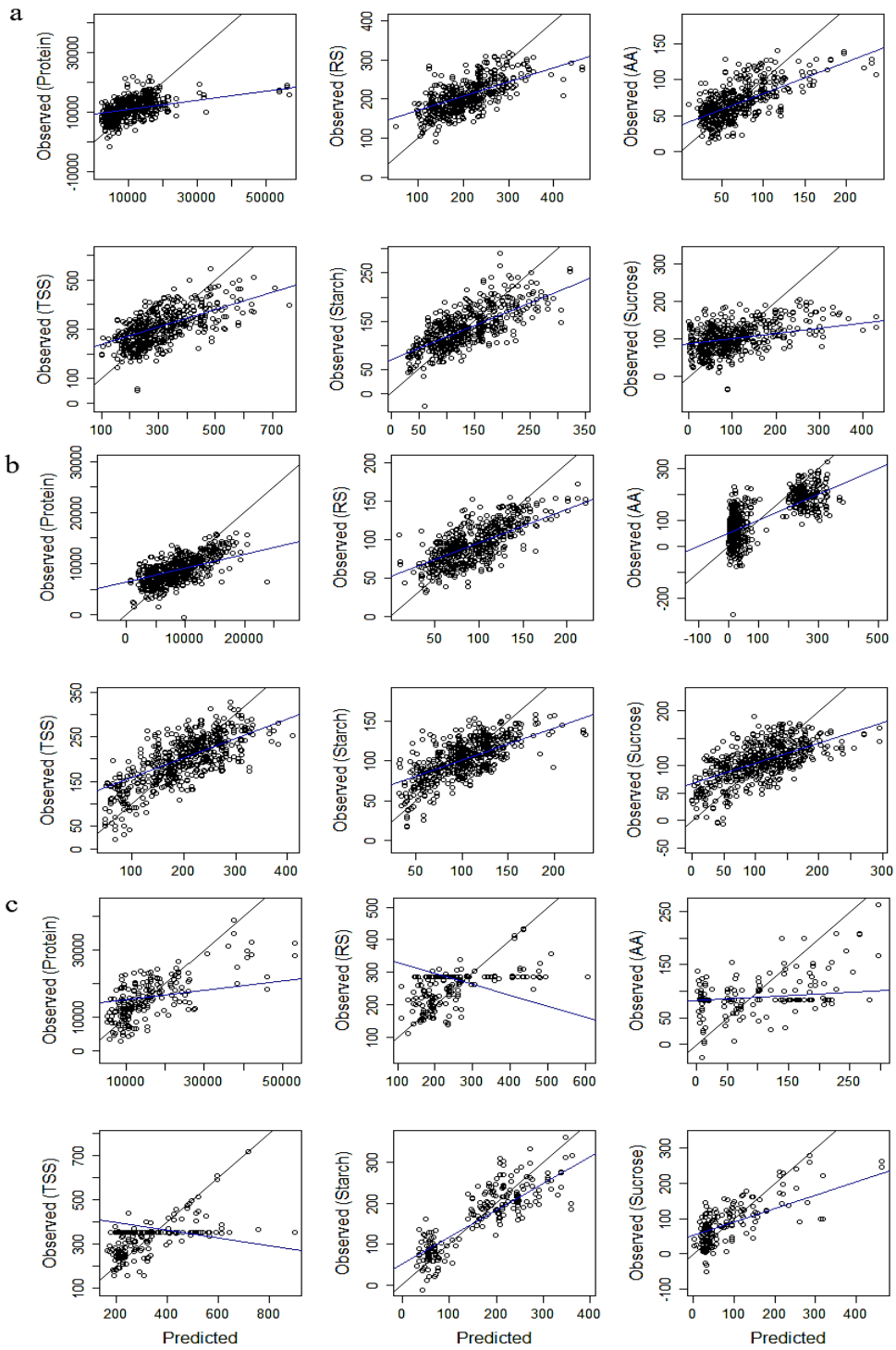

In all cases where there were no negative values, the predicted minimum and maximum values were within the range of measured minimum and maximum values. And even with negative minimum values, the maximum predicted value was below the maximum measured value, for most variables. Likewise, the average values were similar between the measured and predicted data, with the exception of the TSS model for fruit, in which some very high predicted values were presented, above the maximum measured values, pulling the average upwards.

SM Table 3 - Comparison between measured and predicted values for each plant organ and biochemical property. The table presents the number of measured and predicted samples (NS), the maximum and minimum values presented (MaxV and MinV, respectively), the average value (AV) and the number of negative values (NV).

Organ	NSC	Measured values				Predicted values				
		NS	MaxV	MinV	AV	NS	MaxV	MinV	AV	NV
Leaves	Protein	363	56818.54	2250.42	11217.40	1350	21150.99	-9016.56	14262.36	2
	RS	363	463.77	50.25	203.14	1350	305.90	-9.73	212.98	1
	AA	363	235.73	10.29	69.68	1350	115.74	-1.67	76.02	1
	TSS	363	759.05	94.64	299.21	1350	472.85	-49.22	331.43	2
	Starch	363	322.21	19.42	135.07	1350	228.13	-26.26	151.00	2
	Sucrose	363	430.12	-133.26	96.08	1350	189.04	-41.14	118.22	2
Stems	Protein	750	23833.84	661.80	8784.00	1282	17032.16	4139.50	11226.82	0
	RS	750	221.30	9.46	92.11	1282	153.43	41.95	96.69	0
	AA	750	382.74	1.40	106.08	1282	356.28	36.27	212.42	0
	TSS	750	409.72	47.73	199.63	1282	344.40	123.87	234.96	0
	Starch	750	234.39	31.36	104.38	1282	176.37	79.22	127.06	0
	Sucrose	750	295.61	0.43	107.52	1282	196.31	81.29	138.27	0
Fruits	Protein	270	53111.19	5152.62	15537.09	632	26849.14	-3632.79	13449.64	50
	RS	270	608.11	108.61	253.41	632	44495.56	-124.34	250.64	27
	AA	270	297.01	1.88	88.15	632	224.01	7.14	55.19	0
	TSS	270	898.76	164.24	335.24	632	961392.54	-197.96	1793.41	36
	Starch	270	360.43	32.29	161.85	632	304.23	47.83	211.09	0
	Sucrose	270	463.23	2.66	81.83	632	211.96	-92.36	69.33	68

Note. NCS, non-structural carbohydrates; RS, reducing sugars; AA, amino acids; TSS, total soluble sugars. Source: from the author (2022).

ANNEX C - NSC values for the complete time series

SM Table 4 - Protein, reducing sugars (RS), amino acids (AA), total soluble sugars (TSS), starch and sucrose contents quantified in each of the sampled divisions of the coffee trees (as an individual factors). The values correspond to 6 measured and 11 predicted samplings. Source: From the author (2022).

Factor	PROTEIN	RS	AA	TSS	STARCH	SUCROSE
Sampling (S)						
S1	12076.02	146.48	129.63	267.08	141.52	109.48
S2	11779.01	150.89	97.02	195.34	64.52	44.45
S3	11738.61	135.91	82.96	228.61	143.71	83.09
S4	13232.54	171.77	99.92	272.90	159.24	101.40
S5	13663.67	167.23	87.52	293.32	171.13	121.61
S6	9705.71	207.19	39.21	318.46	157.29	111.27
S7	13321.65	169.06	148.47	312.52	156.31	143.38
S8	11787.68	151.51	74.00	219.14	114.90	80.31
S9	12885.79	166.99	152.10	302.04	149.14	134.81
S10	12985.32	151.82	159.39	279.29	138.64	127.44
S11	8206.20	158.44	139.76	263.08	156.22	108.01
S12	12804.98	165.13	163.18	293.03	137.54	120.63
S13	12894.65	163.53	137.53	291.93	153.62	118.48
S14	13617.15	167.27	103.62	289.86	171.51	119.27
S15	12021.55	177.34	46.32	324.79	164.44	147.45
S16	15243.55	187.34	153.56	340.58	160.58	150.16
S17	14179.07	142.17	154.86	265.29	134.91	123.12
Plant organs (O)						
Leaves	13217.68	209.74	73.80	320.51	145.59	112.58
Stems	10340.96	95.54	174.90	222.41	118.73	126.86
Fruits	15215.26	209.68	68.47	306.05	198.51	82.22
Third (Th)						
LT	11724.60	152.58	109.09	259.37	131.66	106.64
MT	12505.79	169.68	111.05	285.68	149.44	114.24
UT	13125.85	168.66	121.41	290.22	154.95	117.05
Section (Se)						
D	12649.00	175.82	113.08	289.79	145.97	112.71
I	12550.47	165.15	112.36	281.44	146.19	113.72
P	11990.99	147.61	115.27	260.29	142.44	110.65

SM Table 5 - Protein, reducing sugars (RS), amino acids (AA), total soluble sugars (TSS), starch and sucrose contents quantified in each of the plant organs and samplings. The values correspond to 6 measured and 11 predicted samplings. Source: From the author (2022).

Factor		PROTEIN	RS	AA	TSS	STARCH	SUCROSE
Organ x Sampling (O x S)							
F	S01	781.98	84.40	114.67	139.77	169.53	50.83
F	S02	13177.94	210.84	179.61	245.45	63.67	34.61
F	S03	12175.37	161.15	42.35	239.25	209.46	50.47
F	S04	14720.54	213.60	39.86	282.20	214.85	69.74
F	S05	18132.10	207.08	25.62	349.09	254.96	128.78
F	S06	16905.66	315.47	10.67	427.47	220.86	112.00
F	S11	10950.36	171.41	69.58	237.95	239.59	79.13
F	S12	13054.63	177.72	149.19	278.32	96.93	61.19
F	S13	14126.70	163.53	55.68	295.34	207.32	68.75
F	S14	15532.74	172.21	19.68	271.90	255.04	87.04
F	S15	33037.24	252.61	80.09	439.90	304.87	187.28
F	S16	23564.54	476.07	56.67	700.25	255.63	185.23
L	S01	14653.50	207.78	76.40	319.29	138.86	111.29
L	S02	16393.32	179.04	91.81	248.02	68.39	68.98
L	S03	13561.90	161.18	79.36	243.32	111.83	81.71
L	S04	14315.38	207.71	76.13	314.93	140.64	106.82
L	S05	13547.83	210.48	66.64	319.17	142.71	108.46
L	S06	6520.22	210.61	57.87	293.85	141.97	83.24
L	S07	15352.62	233.67	69.69	372.76	174.98	138.95
L	S08	12793.02	185.37	114.72	227.90	125.97	66.00
L	S09	13978.77	227.78	77.98	359.21	166.07	130.98
L	S10	13839.34	198.55	89.49	311.21	144.22	112.60
L	S11	6529.38	206.49	70.24	311.89	148.89	105.39
L	S12	13360.79	218.80	76.37	337.42	153.69	118.65
L	S13	13904.51	228.97	80.06	351.14	161.19	122.20
L	S14	14357.69	221.93	71.77	349.01	158.46	126.85
L	S15	9061.83	242.76	49.50	370.84	167.21	128.09
L	S16	16221.27	224.18	71.32	364.23	166.71	139.55
L	S17	14985.83	193.00	38.72	327.01	151.59	134.01
S	S01	11237.01	104.23	192.80	243.99	128.90	139.76
S	S02	6082.54	63.12	16.65	95.10	61.82	31.98
S	S03	9565.34	86.29	127.67	203.85	107.04	117.56
S	S04	10723.04	96.16	182.84	224.71	119.89	128.55
S	S05	9381.68	86.22	168.92	213.48	116.19	127.26

S	S06	4076.72	76.34	56.08	211.97	96.07	135.62
S	S07	10909.88	92.34	242.03	240.99	134.13	148.65
S	S08	10888.97	121.24	37.60	211.32	105.00	90.07
S	S09	11586.59	94.72	240.19	234.09	129.03	139.37
S	S10	11991.56	97.45	240.73	242.15	132.16	144.70
S	S11	8356.27	105.63	243.36	229.72	119.10	124.09
S	S12	12096.53	102.11	262.14	252.65	139.35	150.54
S	S13	11362.02	94.82	229.25	228.45	125.09	133.63
S	S14	11301.06	98.65	204.39	233.10	124.36	134.45
S	S15	8896.94	96.47	34.01	250.59	122.89	154.12
S	S16	13017.97	107.32	247.33	262.21	139.99	154.89
S	S17	13405.93	93.45	266.15	206.14	118.92	112.69

SM Table 6 - Protein, reducing sugars (RS), amino acids (AA), total soluble sugars (TSS), starch and sucrose contents quantified in each of the plant organs and tree sampled divisions. The values correspond to 6 measured and 11 predicted samplings. Source: From the author (2022).

Factor			PROTEIN	RS	AA	TSS	STARCH	SUCROSE
Organ x Third x Section (O x Th x Se)								
F	LT	D	14609.64	207.81	67.10	288.43	186.99	74.13
F	LT	I	15040.31	202.40	80.82	299.82	175.00	86.74
F	LT	P	13499.09	188.15	76.69	257.55	186.66	64.98
F	MT	D	13290.36	206.04	60.74	286.98	193.33	64.00
F	MT	I	15851.48	231.89	61.75	329.32	205.20	84.95
F	MT	P	16920.42	228.56	67.63	328.50	209.72	89.64
F	UT	D	13929.35	178.57	71.73	269.85	187.14	75.06
F	UT	I	15788.94	214.01	67.30	324.48	206.95	89.52
F	UT	P	18956.65	220.87	60.84	385.79	240.04	118.22
L	LT	D	12909.93	199.27	71.28	309.30	136.32	110.85
L	LT	I	12127.81	187.79	70.30	286.83	123.90	101.89
L	LT	P	12612.73	182.44	65.58	278.11	119.29	97.57
L	MT	D	13119.04	223.44	77.09	342.28	155.81	122.71
L	MT	I	13496.39	219.45	73.94	340.13	155.13	122.64
L	MT	P	12330.90	205.13	73.54	309.72	147.69	105.62
L	UT	D	14236.82	224.87	82.47	333.37	154.56	110.46
L	UT	I	14570.83	235.51	76.66	363.36	171.25	127.64
L	UT	P	14790.62	219.42	72.55	340.03	167.78	120.34
S	LT	D	10040.24	115.64	142.07	237.42	121.43	121.78

S	LT	I	9851.08	88.20	180.12	211.86	114.42	123.66
S	LT	P	9323.01	78.50	174.83	203.22	115.18	124.72
S	MT	D	11478.98	117.16	168.77	245.22	121.27	128.06
S	MT	I	10224.20	92.13	171.58	216.27	115.80	124.15
S	MT	P	9946.18	83.31	171.00	213.05	117.44	129.74
S	UT	D	11437.36	116.25	207.51	247.18	126.85	130.93
S	UT	I	10554.19	91.85	169.36	218.45	115.07	126.61
S	UT	P	10211.33	84.62	172.39	217.83	127.34	133.21

REFERENCES

BREIMAN, L. Random Forests. **Machine Learning**, v. 45, p. 5–32, 2001.

BREIMAN, L.; CUTLER, A. Package 'randomFores' Version 4,6-14. **The Comprehensive R Archive Network**, p. 1–29, 2018.

MEVIK, B.-H.; WEHRENS, R. Introduction to the pls Package. **Help section of the "pls" package of RStudio software**, p. 1–24, 2020.

SERBIN, S. P. et al. Spectroscopic determination of leaf morphological and biochemical traits for northern temperate and boreal tree species. **Ecological Applications**, v. 24, n. 7, p. 1651–1669, 2014.